

NOTE TO USERS

This reproduction is the best copy available.

UMI[®]

EFFECT OF SODIUM ALKYL SULFATES
ON POLAROGRAPHIC WAVES

A dissertation submitted to the
Division of Graduate Studies
of the University of Cincinnati
in partial fulfillment of the
requirements for the degree of
Doctor of Philosophy

1970

by

Vinay Kumar

B.Sc.(Hons.), University of Delhi, Delhi (India), 1958.

M.S., University of Delhi, Delhi (India), 1960.

M.S., State University College, Oswego, N.Y., 1967.

UNIVERSITY OF CINCINNATI LIBRARY

UMI Number: DP16175

INFORMATION TO USERS

The quality of this reproduction is dependent upon the quality of the copy submitted. Broken or indistinct print, colored or poor quality illustrations and photographs, print bleed-through, substandard margins, and improper alignment can adversely affect reproduction.

In the unlikely event that the author did not send a complete manuscript and there are missing pages, these will be noted. Also, if unauthorized copyright material had to be removed, a note will indicate the deletion.

UMI®

UMI Microform DP16175

Copyright 2009 by ProQuest LLC.

All rights reserved. This microform edition is protected against unauthorized copying under Title 17, United States Code.

ProQuest LLC
789 E. Eisenhower Parkway
PO Box 1346
Ann Arbor, MI 48106-1346

UNIVERSITY OF CINCINNATI

July 31, 1970

I hereby recommend that the thesis prepared under my supervision by VINAY KUMAR

entitled "Effect of Sodium Alkyl Sulfates on Polarographic Waves"

be accepted as fulfilling this part of the requirements for the degree of Doctor of Philosophy

Approved by:

T.W. Gilbert
George Lohman
Rept R. Meyer
Joseph E. Curran

ACKNOWLEDGMENTS

The author wishes to express his gratitude to Dr. L.A.Knecht for suggesting the problem and for his guidance in the initial stages of the work. The author is grateful to Dr. T.W.Gilbert for agreeing to guide the rest of the work and for providing many helpful discussions which proved fruitful in furthering the research.

The author is indebted to Dr. George Dahlgren and Dr. Joseph Caruso, members of his graduate committee, for their help, interest and cordiality.

The author would like to thank Ed. Graf, who constructed the Faraday cage, which was used to cut down the "noise" in the oscilloscopic signals.

The author also wishes to thank the Department of Chemistry for providing the financial support during the course of this study.

Finally, special thanks to my wife, Sunila, for typing this thesis.

NOV 30 1970

TO MY PARENTS

TABLE OF CONTENTS

<u>Chapter</u>	<u>Page</u>
LIST OF TABLES -----	(i)
LIST OF FIGURES -----	(ii)
I. INTRODUCTION -----	1
II. POLAROGRAPHIC MAXIMA -----	3
III. EXPERIMENTAL -----	19
(i) C-V plots	19
(ii) Procedure for determining MSP	20
(iii) E-C curve measurements	21
(iv) CMC determination	21
(v) Current-time curves	22
(vi) Reagents	23
IV. CRITICAL MICELLE CONCENTRATION OF SODIUM ALKYL SULFATES -----	26
V. ELECTROCAPILLARY CURVES IN PRESENCE OF SODIUM ALKYL SULFATES -----	34
VI. DETERMINATION OF MAXIMUM SUPPRESSION POINTS -- Results and discussion	57 57
VII. EFFECTS OF SODIUM ALKYL SULFATES ON POLAROGRAMS OF COMPLEXES -----	76
(i) Results	77
(ii) Discussion	99
VIII. CURRENT-TIME CURVES (Results and Discussion)--	102
IX. CONCLUSIONS AND SUMMARY -----	137

continued on next page.

<u>Chapter</u>		<u>Page</u>
	APPENDIX I -----	143
	APPENDIX II -----	144
X.	BIBLIOGRAPHY -----	147

LIST OF TABLES

<u>Number</u>		<u>Page</u>
1.	Critical micelle concentrations of sodium alkyl sulfates.	29
2.	Electrocapillary curve in presence of various concentrations of sodium dodecyl sulfate.	39
3.	Electrocapillary curve in 0.2M acetate buffer.	50
4.	Maximum suppression points of sodium alkyl sulfates in case of lead, oxygen and nickel maxima.	58
5.	Maximum suppression points of sodium alkyl sulfates in presence of Tl^+ , Se(IV), and CdI_4^{2-} .	71
6.	t^0 (sec.) and $C(\text{moles/l}) \times 10^{+4}$ values.	116
7.	$C \times 10^{+6} M$, t^0 , $C \times t^0 \times 10^{+6}$, and $10^{-6}/C$ values.	129
8.	$C \times 10^{+6} M$, t^0 , $C \times t^0 \times 10^{+6}$, $10^{-6}/C$ values.	135

LIST OF FIGURES

<u>Number</u>		<u>Page</u>
1.	Current-voltage curve.	3
2.	Polarographic Maxima.	9
3.	Direction of streaming with maxima of the first kind.	10
4.	Motion in the mercury drop caused by the flow from the capillary.	14
5.	Electrocapillary curve.	34
6.	Electrocapillary curve in presence of dodecyl sulfate.	38
7.	Electrocapillary curve in presence of sodium octyl and decyl sulfate.	40
8.	Electrocapillary curve in presence of tetradecyl sulfate.	41
9.	Electrocapillary curve in presence of sodium hexadecyl and octadecyl sulfate.	42
10.	Electrocapillary curve in 0.1M NaCl.	45
11.	Electrocapillary curve in 0.2M acetate buffer.	47
12.	Electrocapillary curve in 0.2M acetate buffer.	49
13.	Electrocapillary curve in 0.25M EDTA.	51
14.	Droptime vs. Log(SAS conc.) plot in case of C ₁₀ .	54
15.	Droptime vs. Log(SAS conc.) plot in case of C ₈ .	54
16.	Droptime vs. Log(SAS conc.) plot in case of C ₁₂ .	55

<u>Number</u>		<u>Page</u>
17.	Droptime vs. Log (SAS conc.) plot in case of C ₁₄ .	55
18.	Droptime vs. Log(SAS conc.)plot in case of C ₁₆ .	56
19.	Droptime vs. Log(SAS conc.) plot in case of C ₁₈ .	56
20.	Oxygen Maximum.	59
21.	Effect of octadecyl sulfate on Lead maximum.	62
22.	Effect of sodium tetradecyl sulfate on Lead maximum.	64
23.	Effect of sodium octyl sulfate on UO ₂ ²⁺ maximum.	67
24.	Effect of Sod. dodecyl sulfate on Ni ²⁺ Maximum.	69
25.	Effect of Sod. octyl sulfate on Cu(tetren) ²⁺ reduction wave.	79
26.	Effect of Sod. hexadecyl sulfate on Cu(tetren) ²⁺ wave.	81
27.	Effect of Sod. dodecyl sulfate on Cu(trien) ²⁺ wave.	83
28.	Effect of sodium octyl sulfate on Cu-EDTA wave.	88
29.	Effect of sodium decyl sulfate on Cu-EDTA wave.	89
30.	Effect of sodium dodecyl sulfate on Cu-EDTA wave.	91
31.	Effect of sodium tetradecyl sulfate on Cu-EDTA wave.	92
32.	Cu(Tart) ⁰ Maximum.	94
33.	Effect of sodium octyl sulfate on Cu(tart) ⁰ wave.	95

<u>Number</u>		<u>Page</u>
34.	Effect of sodium tetradecyl sulfate on Cu(tart) ^o wave.	98
35.	Inhibition of electrode rxn.	105
36.	Surface coverage controlled by adsorption equili- brium.	105
37.	i-t curves for a solution containing $1 \times 10^{-3} \underline{\text{M}}$ Cu(II), $0.25 \underline{\text{M}}$ EDTA and sodium decyl sulfate.	111
38.	i-t curves for a soln. containing $1 \times 10^{-3} \underline{\text{M}}$ Cu(II), $0.25 \underline{\text{M}}$ EDTA and sodium tetradecyl sulfate.	113
39.	i-t curves for a solution containing $1 \times 10^{-3} \underline{\text{M}}$ Cu(II), $0.25 \underline{\text{M}}$ EDTA and sodium hexadecyl sulfate.	114
40.	i-t curves for a solution containing $1 \times 10^{-3} \underline{\text{M}}$ Cu(II), $0.25 \underline{\text{M}}$ EDTA and sodium octadecyl sulfate.	115
41.	Plot of data in table 6.	117
42.	i-t curves in case of Cu-Tetren system containi- ng sodium octyl sulfate.	119
43.	i-t curves in case of Cu-Tetren system containi- ng sodium decyl sulfate.	119
44.	i-t curves for a solution containing $1 \times 10^{-3} \underline{\text{M}}$ Cu(II), $1 \times 10^{-2} \underline{\text{M}}$ tetren in $0.16 \underline{\text{M}}$ acetate buffer and sodium tetradecyl sulfate.	120
45.	i-t curves in case of Cu-Tetren system containing sodium hexadecyl sulfate.	120

<u>Number</u>		<u>Page</u>
46.	i-t curves in case of Cu-Tetren system containing sodium octadecyl sulfate.	121
47.	i-t curves in case of 0.01M KCl containing sodium octyl sulfate.	121
48.	i-t curves in case of 0.01M KCl containing sodium decyl sulfate.	124
49.	i-t curves in case of 0.01M KCl containing sodium dodecyl sulfate.	124
50.	i-t curves in case of 0.01M KCl containing sodium tetradecyl sulfate.	125
51.	i-t curves in case of 0.01M KCl containing sodium hexadecyl sulfate.	125
52.	i-t curves in case of 0.01M KCl containing sodium octadecyl sulfate.	126
53.	Plot of data in table 7.	128
54.	i-t curves for a solution containing $1 \times 10^{-3} \text{M}$ Cu(II) in 0.1M Tartrate buffer and sodium decyl sulfate.	132
55.	i-t curves for a solution containing $1 \times 10^{-3} \text{M}$ Cu(II) in 0.1M tartrate buffer (A) sodium hexadecyl sulfate and (B) sodium octadecyl sulfate.	133
56.	Plot of data in table 8.	134

I. INTRODUCTION

Synthetic detergents for household use make up over 80% of the world's production and almost all of those produced in Western countries are of the anionic alkyl sulfate and alkyl aryl sulfonate type. These days, even in sewage and effluent analysis, one is mainly concerned with these two types of detergents. Likewise, in natural water, most surface active materials resulting from pollution are of anionic type.

Sodium alkyl sulfates, or, the paraffin-chain salts as they are called, are anionic surfactants and display a remarkable tendency to concentrate at interfaces, because they contain groups which differ greatly in polarity. This is demonstrated in a striking manner by their surface activity in water. In addition to being wetting agents, many of them are detergents and emulsifying agents, properties which suggest that these substances are capable not only of collecting in a 2 - dimensional film as at a surface, but also of forming 3 - dimensional aggregates even in fairly dilute solutions.

Among the sodium alkyl sulfates, the one which has been investigated the most is sodium dodecyl sulfate. Its behavior as a surfactant has been studied by a great number of investigators. Frequently, sodium dodecyl sulfate is used as a maximum suppressor in polarographic work (4,30,55). But only rarely have the other members of the homologous series (sodium hexyl, octyl, decyl, tetradecyl, hexadecyl and

octadecyl sulfates) been employed for suppressing polarographic maxima.

The effect of surface active substances on polarographic current-voltage curves is of great importance from both theoretical and practical standpoints. As the electrode process generally takes place at the interface between two separate phases, it is very much affected by surface phenomena like adsorption of surface active substances. In order to investigate the physico-chemical properties of sodium alkyl sulfates completely as a group and in order to compare their behavior, it was decided to study their effect on polarographic waves both in the presence and absence of maxima. The studies were carried out on polarographic waves of simple and complex metal ions.

To understand the mechanism by which the anionic surfactants suppress various kinds of maxima, both current-voltage plots (called "polarograms" or "voltammograms") and current-time curves were studied. In some cases, the effect of these surfactants on electrocapillary curves was also investigated.

The studies were further extended to apply the electrocapillary method for determining critical micelle concentration (CMC) of these compounds in presence of foreign (supporting) electrolyte. CMC's of sodium alkyl sulfates in water and in presence of electrolytes were also determined by the spectral dye method.

II. POLAROGRAPHIC MAXIMA

Polarography involves the electrolysis of solutions containing electro-oxidizable or electro-reducible materials between a dropping mercury electrode (DME) and some reference electrode, usually a saturated calomel electrode (SCE). The potential applied between the two electrodes is varied and consequent changes in the current are measured. The relationship between voltage and current (the current-voltage curve) is automatically recorded with a recording polarograph. The main features of a normal current-voltage curve are shown in the figure 1.

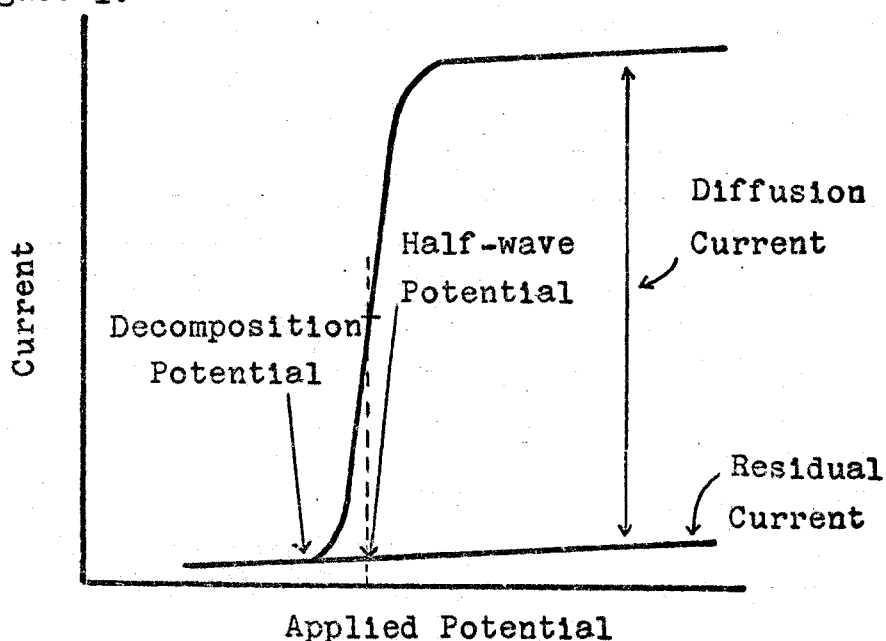


FIGURE 1

As the applied potential is increased from zero, an

extremely low charging current flows through the polarographic cell. This behavior continues until the decomposition potential of the metal ion in question is reached. At this point, the reduction process begins and the current rises. As the applied potential is increased further, a potential region is reached in which the current becomes constant because of the establishment of complete concentration polarization (58) at the surface of the DME. This current, called the diffusion current, is proportional to the concentration of the material undergoing electrolysis at the mercury drop. The slowly increasing current at the foot of the wave is known as the residual current, which, unlike the diffusion current, is non-faradaic in nature. The potential at the mid-point of the curve (or wave), where the current is exactly half of its limiting value (corrected for the residual current), is known as the half-wave potential $E_{\frac{1}{2}}$. This quantity is characteristic of a particular species under fixed solution conditions and thus serves for the qualitative identification of that species.

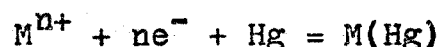
The theory of a dropping mercury electrode was developed by Ilkovic (19). He derived the following equation for the average diffusion current, i_d :

$$i_d = 607 n D^{\frac{1}{2}} m^{\frac{2}{3}} t^{\frac{1}{6}} C,$$

Where n is the number of electrons taking part in the

electrochemical reaction, D is the diffusion coefficient of the electroactive substance ($\text{cm}^2/\text{sec.}$), C is its concentration (millimoles/l) in the bulk of the solution, m is the mass of mercury flowing in mg per second and t represents the life-time (drop-time) in seconds of a drop. The terms m and t are called "capillary characteristics" and are constant and reproducible at a fixed height of the mercury column and applied potential. Similarly, if n and D are constant for a particular solute species, then i_d is proportional to C , that is, a linear relationship between diffusion current and concentration is obtained.

In order to derive an equation which describes the relation between current and potential, the following reversible process is considered:



The above equation describes the reduction of a simple metal ion, M^{n+} , to give metal atoms, which dissolve in mercury to form the amalgam, $M(\text{Hg})$. If thermodynamic equilibrium is very rapidly attained, the concentrations of the metal ions and the metal atoms at the drop surface will conform to the Nernst equation:

$$E_{d.e.} = E^{\circ} - \frac{RT}{nF} \ln \frac{f_a C_a^{\circ}}{a_{\text{Hg}}^{\circ} f_s C_s^{\circ}}$$

Where E° is the standard potential of the half-reaction,

C_s^0 and C_a^0 are the molar concentrations of the dissolved ion and of the metal in the amalgam at the mercury surface, f_s and f_a are the corresponding activity coefficients, and a_{Hg}^0 is the activity of the mercury in the amalgam at the drop surface. Since in the amalgam there is excess of mercury, its activity is taken as unity. "It is assumed that the rate of diffusion of the metal ion M^{n+} to the drop surface, and hence the current i , is proportional to the difference between the concentrations of M^{n+} in the bulk of the solution and at the electrode surface:

$$i = k_s(C_s - C_s^0)$$

----- At any potential on the plateau of the wave, C_s^0 is virtually zero because the ions are reduced as rapidly as they reach the electrode surface, while the current is equal by definition to the diffusion current i_d . Hence, $i_d = k_s C_s$, so that, according to the Ilkovic equation, k_s is equal to $607 n_s D_s^{1/2} m^{2/3} t^{1/6}$. ----- Meanwhile, the concentration of the metal atoms in the amalgam at the drop surface is also proportional to the current: $i = -k_a C_a^0$, where k_a has the same form as k_s but involves the diffusion coefficient of the metal atoms in the amalgam instead of that of the metal ions in the solution. On combining the above equations, the following equation is obtained:

$$E_{d.e.} = E^0 - \frac{RT}{nF} \ln \frac{f_a k_s}{f_s k_a} - \frac{RT}{nF} \ln \frac{1}{i_d - i} \quad \text{-----(1)}$$

When the potential of the dropping electrode is equal to

the half-wave potential $E_{\frac{1}{2}}$, $i = i_d/2$ by definition, and since the last term of equation (1) then becomes zero one has

$$E_{d.e.} = E_{\frac{1}{2}} = E_s^0 - \frac{RT}{nF} \ln \left(- \frac{f_a k_s}{i_s k_a} \right)$$

which may also be written as

$$E_{\frac{1}{2}} = E_s^0 - \frac{RT}{nF} \ln \left(- \frac{k_s}{k_a} \right)$$

where E_s^0 is the formal potential of the half-reaction under the experimental conditions (ionic strength, temperature, etc.) employed" (70). Equation (1) can be re-written as

$$E_{d.e.} = E_{\frac{1}{2}} - \frac{RT}{nF} \ln \frac{1}{i_d - i}$$

or, at 25°,

$$E_{d.e.} = E_{\frac{1}{2}} - \frac{0.059}{n} \log \frac{1}{i_d - i}$$

The above equations are applicable to reduction processes, in which i is the cathodic current resulting from the reduction of metal ions.

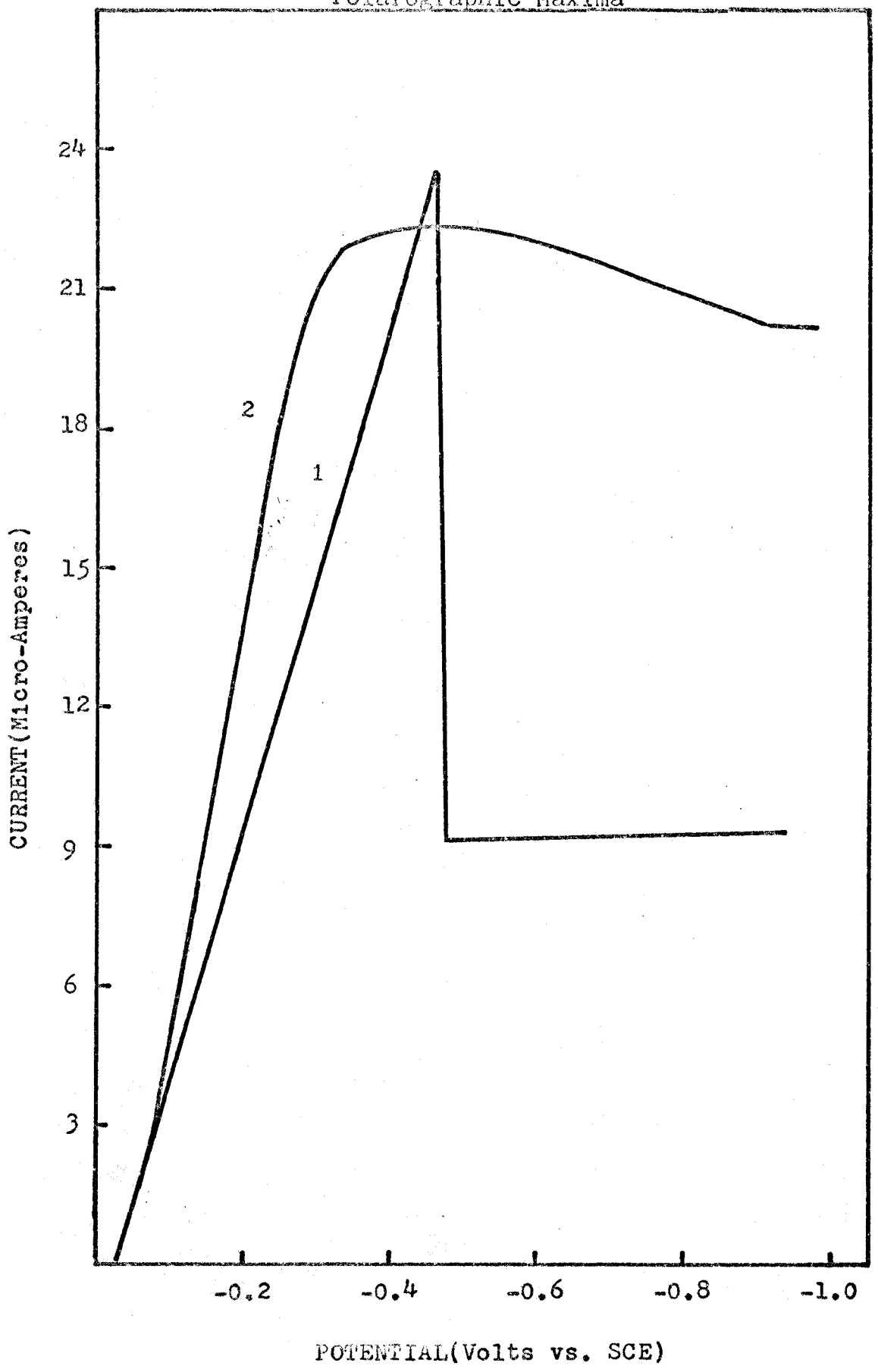
However, in many instances the current-voltage curves sharply deviate from the shape predicted by equation (1). In all such cases, the current-voltage curves show a sharp increase in current up to a certain voltage, followed by a sharp or sometimes

smooth decrease in the current to values predicted by the Ilkovic equation. This phenomenon is designated as a polarographic maximum. These maxima which vary in shape from sharp peaks to rounded humps (fig. 2) were first described in detail by Heyrovský and his collaborators (8,9). In some cases the origin of the current maximum is related to the mechanism of the electrode process (e.g. as in the catalytic discharge of hydrogen ions), but mostly, the maxima are caused by increased transport of the depolarizer towards the electrode surface by a streaming motion of the solution. The streaming or tangential motion is of two kinds and consequently gives rise to two kinds of maxima e.g. (a) Maxima of the first kind (curve 1 in fig. 2) and (b) Maxima of the second kind (curve 2 in fig. 2).

Maxima of the first kind: These maxima appear on the rising portion of the polarographic curves and usually occur in dilute solutions of supporting electrolytes. Maxima of the first kind tend to be more prominent when they occur on waves whose half-wave potentials are more positive than the electrocapillary maximum potential than when they occur on waves at more negative potentials. If the half-wave potential of the depolarizer lies on the positive side of the E-C curve, the maximum is described as a positive maximum and if during the formation of the maximum, the electrode is

Figure 2

Polarographic Maxima



negatively charged with regard to the solution, the term negative maximum is employed. Lead and thallos ions yield positive maxima, whereas, nickel and cobalt ions give rise to negative maxima. Antweiler (59), who studied the streaming motion at the surface of a dropping mercury electrode proved that maxima of the first kind are caused by streaming. Due to the streaming motion, far more depolarizer is transported to the electrode than is possible by diffusion alone. "In (60) the case of positive maxima, the solution streams from the neck of the mercury drop to its bottom (i.e. from the capillary orifice past the drop surface into the body of the solution (fig. 3A); for negative

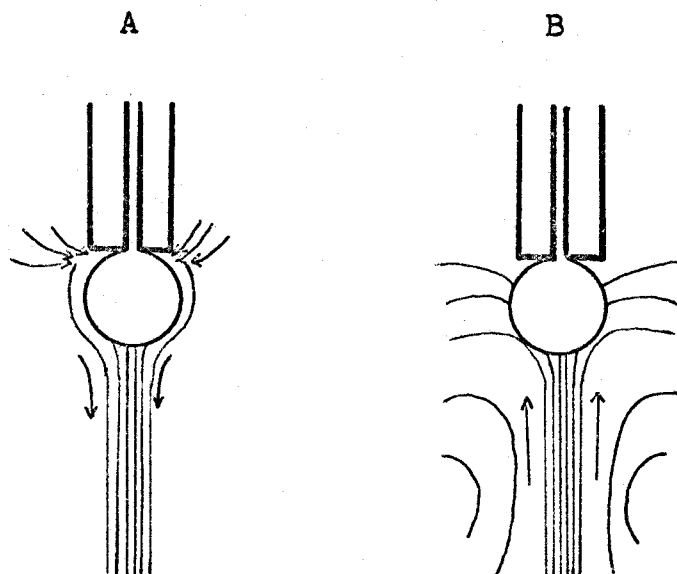


Figure 3: Direction of streaming with maxima of the first kind: (A) Positive Maxima (B) Negative Maxima.

maxima, the streaming takes place from the bulk of the solution towards the bottom of the mercury drop, on past its surface to the neck of the drop and then sideways just underneath the tip of the capillary." (fig. 3B). Thus, during streaming conditions, the normal diffusion effects are not operative and instead, there are convection effects and these cause the rapid rise in the current. According to Heyrovsky (9), streaming is an electro-kinetic effect, which arises due to differences of surface charge between the upper and lower parts of the drop (61).

Frumkin and his co-workers (10,14,15) have put forward a theory of the maxima of first kind. This theory, which explains the origin of streaming, is also supported by Stackelberg et al. (16,17). In dilute supporting electrolytes solutions, the DME is not homogeneously polarized when current passes and a potential difference arises on the surface of the drop. This is attributed to different current densities at different places of the drop. Due to differences in potentials on the surface of the mercury electrode, (which is screened by the tip of the capillary), differences in surface tension are caused. This then leads to the motion of the mercury and the surface contracts to the places where the surface tension is high. The contraction or motion of the surface causes the inner layer of the mercury and

the adhering layers of solution to move. The rate of motion of the solution decreases with the increase in distance from the electrode surface. Due to the convective motion and the diffusion, the depolarizer is transported to the electrode in greater amounts and so the current rises above the limiting diffusion current. In the case of the positive maximum, the bottom of the drop has a greater surface tension than the neck (62) and the mercury surface streams from the neck to the bottom; this motion causes the solution to flow in the same direction. This way, due to the streaming of the solution, fresh particles of the depolarizer are transported to the neck of the drop, while the partially exhausted layers of solution flow to the bottom. This process increases still further the potential difference between the neck and the bottom of the drop. When the mean potential of the electrode nears the potential at the E-C maximum, the differences in surface tension are minimized and the motion of the mercury and the solution stops. For negative maxima, the surface tension is greater at the neck of the drop and so in this case, the mercury surface moves from the bottom to the neck and the fresh particles of the depolarizer are brought to the bottom of the drop. Since the solution near the neck is partially exhausted, the neck is more strongly polarized and the potential difference on the drop surface

decreases. When the depolarizer concentration at the electrode surface becomes zero (i.e. as concentration polarization occurs), the surface tension becomes uniform over the whole drop surface and the motion of the drop stops causing the current to drop to value predicted by Ilkovic equation.

Heyrovský, who originally regarded the adsorption of the depolarizer as the process responsible for the occurrence of maxima (a), later accepted and modified (18) a theory of Ilkovic (64), according to which the observed motions of the mercury surface and the maxima are caused by strong electrolyte streamings. Thus, we see that the maxima of first kind are caused due to the non-uniform distribution of current over the drop surface during polarization. The consequent differences of potential between various parts of the drop surface lead to differences in surface tension and hence to the tangential motion of the surface of mercury drop.

It follows from the above discussion that both the electrochemical and the hydrodynamic factors of the dropping mercury electrode-solution system take part in the formation of the maxima of first kind. Due to the complexity of the process, it is difficult to describe the maxima accurately by mathematical equations.

Maxima of the second kind: These maxima, which are observed

usually in concentrated (greater than $0.2F$) solutions (13) of supporting electrolyte, are caused by the vortex motion of the mercury in the drop as a result of the flow of mercury from the capillary into the growing drop, as shown by Kryukova (11,12). The flow of mercury from the capillary is shown in fig. 4 . "The stream (63) is reflected back from the bottom of the drop causing vortex motion within the drop. The surface moves upward and carries the surrounding liquid with it". This way a stirring action starts, that

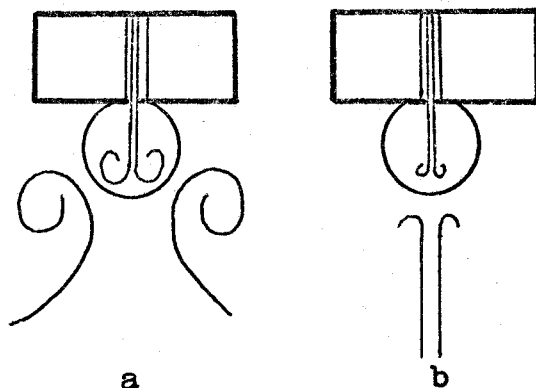


Figure 4: Motion in the mercury drop caused by the flow from the capillary, and motion of the solution around the drop. (a) In $0.1N$ KCl at the E-C maximum potential (b) in the same solution at a potential of $-1.6v$. (vs. NCE)

transports larger amounts of depolarizer to the electrode

and thus causes an increase of current (or a maximum). Thus, the maxima of second kind have a purely hydrodynamic origin and are not caused by any processes at the electrode. The tangential motion causing the maxima of second kind is most pronounced when the mercury surface is uncharged, i.e.; at the potential of the E-C maximum. (At this potential maxima of the first kind do not occur). The motion of the surface occurs at all concentrations of the supporting electrolyte. At other potentials, the rate of motion depends on the concentration of the supporting electrolyte, namely, potassium chloride (63).

As shown in figure 2, the current for maxima of the second kind does not fall abruptly to the limiting current, but decreases slowly, and the greater the distance from the electrocapillary zero, the slower the decrease. The rate of flow of mercury influences the occurrence of maxima of this kind. For example, the maxima appear as soon as the linear flow exceeds 2 cm/sec. (65); this corresponds to $m = 2.14$ mg/sec. for a capillary with a diameter of 0.1 mm. As the flow-rate is increased further, the height of the maximum increases approximately linearly and this continues till the flow rate is 8 cm/sec; after which the growth of the maximum is decreased. Maxima of the second kind can be suppressed by reducing the flow-rate, i.e., by lowering the

height of the mercury column. Unlike the maxima of first kind, maxima of second kind can also be suppressed by lowering the concentration (and the conductivity) of the electrolyte solution. A quantitative treatment of these maxima has been worked out by Levich (66).

SUPPRESSION OF MAXIMA BY SURFACE-ACTIVE SUBSTANCES:

The suppression of polarographic maxima is important, because, in the presence of maxima, it is difficult to measure accurately either the diffusion current or the half-wave potential. And since maxima prevent the analysis of polarographic waves, it becomes impossible even to distinguish between irreversible and reversible processes.

There are a large number of substances known which suppress maxima. Such substances, often known simply as "maximum suppressors" have surface-active properties and are usually of moderately high molecular weight. These are preferentially adsorbed onto the surface of the mercury drop and thus retard or prevent the motion of the mercury surface which is the cause of streaming, and, hence, the maximum formation. The suppression mechanism operates as follows: The surface-active substance present in the solution is adsorbed at the electrode surface, and the motion of the mercury and the solution transports it to the neck of the

drop where it gathers. This causes the surface tension at the neck to decrease more than at the bottom. The difference in surface tension thus gives rise to a force opposing the direction of the motion and the streaming.

Among the most common substances which have been employed for this purpose are gelatin, agar-agar, organic dyes like methylene blue, methyl red, methyl orange, methyl violet and fuchsine, Triton X-100 (a non-ionic detergent which is a polyethyleneglycol ether of monoisooctyl phenol), cationic and anionic soaps like dodecyltrimethylammonium and hexadecyltrimethylammonium bromides, and the sodium salts of lauric and myristic acids, and dodecyl sulfonic acid (13,63). As indicated earlier, among the sodium alkyl sulfates, only sodium dodecyl sulfate has been used as a polarographic maximum suppressor (4,30,55). Since the other members of the series are readily available and have not been explored as maximum suppressors, it was decided to study these as a group and to compare and contrast their behavior with that of sodium dodecyl sulfate.

The ability of surface-active substances to suppress a maximum can be conveniently examined by measuring their maximum suppression point (MSP) as shown by Colichman (1). The MSP is defined as the minimum concentration of the surface active substance which is necessary to make the

maximum current, i_m , equal to the diffusion current, i_d ; and as indicated earlier, it is determined graphically by plotting i_m/i_d against the log of the concentration of the surface active substance. The MSP's of sodium octyl, decyl, dodecyl, tetradecyl, hexadecyl and octadecyl sulfates for various reducible ions were measured and are tabulated in tables 4 and 5.

In addition to suppressing maxima, maximum suppressors affect the polarograms in a number of other ways (21). For example, they can distort a wave, shift the half-wave potential, split the wave or even eliminate the wave completely and inhibit or accelerate the electrode reaction. To study these effects in case of sodium alkyl sulfates, current-voltage and current-time studies were carried out (chapters 7 and 8) on the reduction waves of $\text{Cu}(\text{EDTA})^{2-}$, $\text{Cu}(\text{tetren})^{2+}$, $\text{Cu}(\text{trien})^{2+}$ and $\text{Cu}(\text{tart})^0$ complexes. The data thus obtained enables us to understand the part played by the sodium alkyl sulfates in connection with the electrode processes.

III. EXPERIMENTAL

All polarograms were recorded with a Sargent POLAROGRAPH Model XV. The capillary used in the dropping mercury electrode (DME) had the following characteristics: $m = 1.21 \text{ mg. sec.}^{-1}$ and $t = 4.93 \text{ sec.}$ in $0.1M$ KCL solution at a height of the mercury reservoir of 70 cm. (closed circuit). An H-shaped cell, fitted with a stop-cock for passing nitrogen gas was used in all measurements. An external saturated calomel electrode (SCE) with an agar bridge served as a reference electrode. One compartment of the H-cell in which the agar bridge was immersed contained only supporting electrolyte. This intermediate compartment was necessary to insure that no agar, which contains some surface active substances, entered the test solution. All potentials reported are referred to the SCE. For a run, 20 ml. of the test solution was placed in the cell and 0.005 to 1.0 ml. of solution of the surface active agent were added from a micrometer buret. In this way the dilution did not exceed 5% and its effect on polarograms was considered negligible. Except in the case of studies involving the oxygen maximum, pure, dry nitrogen gas was bubbled for 10-15 minutes through the solution to expel the oxygen. During the run, the nitrogen gas was allowed to flow over the surface of the solution. All polarograms were recorded at ambient temperature, which was maintained at $25.0 \pm 1^{\circ}C$.

PROCEDURE FOR DETERMINING MSP

Polarographic measurements were carried out after taking a known volume of the metal salt or complex metal ion solution in the cell, adding the supporting electrolyte and making up the total volume to 20 ml. The polarogram was taken and then the process was repeated in the presence of the surface-active agent whose maximum suppression point (MSP) was to be determined (1). Increasing amounts of the surfactant were added until the maximum was completely eliminated. Except in the case of the oxygen maximum, after each addition of the surfactant, the solution was stirred by bubbling nitrogen gas for about half a minute. A graph was constructed of i_m/i_d (ratio of current at the maximum and the diffusion current when the maximum was suppressed) vs. the log of the concentration of surface active agent. The MSP was found by extrapolation of the straight line which was obtained to the point where i_m/i_d is unity (corresponding to complete suppression of the maximum). For most of the MSP work, the solutions of the surfactants used were 0.01 - 0.1% w/v.

ELECTROCAPILLARY CURVE MEASUREMENTS

In order to investigate the effect of sodium alkyl sulfates on the electrocapillary maximum (or E-C maximum), the procedure followed was the same as described by Malik, Chand and Saleem (5).

Twenty ml. of air-free 0.1M KCl was taken in the cell and increasing potentials were applied from 0 to -1.2 volts vs. SCE. This was done manually, and at each potential the time for 10 drops to fall was noted with a precision stopwatch. The height of the mercury column was kept constant during all the measurements. Later on, increments of suppressors were added to the KCl solution and droptime measurements were repeated at each new concentration of the suppressor. Freshly prepared 1% solutions of the suppressors were employed. Solutions of tetradecyl, hexadecyl and octadecyl sulfates were heated to 50-60° C. This was done because these materials are too insoluble at room temperature (57).

The electrocapillary curve measurements in presence of 0.1M NaCl, EDTA and acetate buffer were also carried out by following the above procedure.

CMC DETERMINATION USING PINACYANOL CHLORIDE

The procedure employed for determining the critical micelle concentration of sodium alkyl sulfates was essentially

the same as the one followed by Nichols and Kindt (2) in case of sodium dodecyl sulfate. Stock solutions of the detergents were made and these were diluted with a $2 \times 10^{-5} \text{ M}$ solution of pinacyanol chloride (F. Wt. = 388.5) in such a way that in each case at the start of the photometric titration the concentration of the detergent was higher than its reported CMC (3). The total volume of the solution to be titrated was kept at 25 ml. This way the starting dye concentration was $1 \times 10^{-5} \text{ M}$. The titration was carried out in a 50-ml. beaker at 610 nm (slit width = 0.29 mm), the wavelength of maximum absorption for the dye. The titrant, a $1 \times 10^{-5} \text{ M}$ solution of pinacyanol chloride was added from a 10 ml. buret in increments of 0.5 to 1 ml. After adding each increment, the solution was stirred with a magnetic stirrer for 30 sec. Next, the absorbance of the solution was noted on a Model B Spectrophotometer (Beckman Instruments, Inc; Fullerton, Calif.). To get the CMC, the plot between absorbance and volume of titrant was extrapolated.

CURRENT-TIME CURVES OF SINGLE DROPS

The current-time curves were measured osciloscopically using the circuit shown schematically in Appendix II. A manual polarograph was used to provide a constant potential. External read out was accomplished by passing the cell current through a 174-ohm resistor (connected in series with the polarographic

cell) and displaying the resulting IR drop on a Tektronix Type 502 A double-beam oscilloscope. The oscilloscopic trace was then photographed using a Polaroid Camera and type 107 (speed 3000) Polaroid Land film pack (black and white). Even though shielded leads were used to make the various connections, there was pickup of 60-cycle as well as radio frequency signals by the assembled apparatus. It became apparent that the mercury column of the DME served as an excellent antenna. In order to eliminate this "noise" from the oscilloscopic signals, the manual polarograph, dropping mercury electrode, and the H-Cell were all enclosed in a Faraday cage shielded with copper screening and aluminum foil.

REAGENTS

1. The sodium alkyl sulfates [octyl (C_8), decyl (C_{10}), dodecyl (C_{12}), tetradecyl (C_{14}), hexadecyl (C_{16}), and octadecyl (C_{18})] were obtained through the courtesy of Dr. Wharton of the Proctor and Gamble Company, Cincinnati, Ohio. These were pure white crystalline compounds and were used without further purification. To prevent biodegradation and hydrolysis freshly prepared solutions of these surfactants were used throughout.

2. Potassium Chloride, Sodium Acetate (anhydrous powder), Sodium Tartrate, Potassium Iodide, Triethylenetetramine Disulfate,

Copper Sulfate (hydrated), Nickel Sulfate (hydrated) were all Baker Analyzed (J. T. Baker Chemical Co; Phillipsburg, N. J.) reagents and were used without purification.

3. Cadmium Chloride, Agar, Ammonium Thiocyanate, Lead Nitrate, Barium Chloride were all reagent grade and were obtained from Matheson Coleman and Bell Chemical Co., Norwood, Ohio.

4. Tetraethylenepentamine (technical grade) was from Eastman Organic Chemicals. It was purified according to the procedure described by Jonassen et al. (28). (Ethylene dinitrilo) tetra-acetic acid, disodium salt and Pinacyanol Chloride were also Eastman Organic Chemicals.

5. P-Dimethylaminoazobenzene, and Thallous Nitrate were from Fischer Scientific Company.

6. Potassium Nitrate (analytical reagent grade) was from Mallinckrodt Chemical Works, N. Y.

7. Tartaric Acid and Manganous Nitrate (50% solution) were products of Allied Chemical Co; New York, N. Y.

8. Rhodamine 6G dye was obtained from National Aniline Division of Allied Chemical and Dye Corporation, New York, N.Y.

9. Purified $(\text{UO}_2)(\text{NO}_3)_2 \cdot 6\text{H}_2\text{O}$ was obtained from Eimer and Amend Co. of New York.

10. Phenosafranin, Pinaverdol, Orthochrom-T and Pinachrome were products of Hoechst Company of Germany.

11. Double distilled water with the second distillation

made from alkaline permanganate in an all-glass still was used throughout.

12. Triple-distilled mercury was used for the DME.

13. The polarographic H-cell was cleaned between each run by washing, rinsing with distilled water, and then steaming it upside down for 20-30 minutes so that the condensate continually dripped from the vessel.

IV. CRITICAL MICELLE CONCENTRATION OF SODIUM ALKYL SULFATES

The sodium alkyl sulfates which have the general formula $C_n H_{2n+1} SO_4^- Na^+$ can be classified as association colloids, because their solutions, if sufficiently dilute, contain only simple ions, while at higher concentrations they undergo aggregation. This aggregation of ions, or micelle formation, was postulated by McBain (31) from studies of the electrical conductivity and other properties of aqueous solutions of soaps. One of the consequences of aggregation in paraffin-chain electrolytes like sodium alkyl sulfates is a marked decrease in the equivalent conductance of solutions at a characteristic "critical concentration for micelles." Thus the existence of such a break in the conductivity curves of the colloidal electrolytes can be construed as evidence of micelle formation. The critical micelle concentration (CMC) is defined as the concentration at which the presence of micelles becomes perceptible. Most physical properties of colloidal electrolyte solutions show a change of slope with respect to concentration at the CMC and thus many of these serve to determine the critical micelle concentration. For example, the following methods have been proposed for CMC determination: Dye solubilization, (32,36), Spectral Dye (2,33), Diffusion (34), Osmotic Coefficient (35),

Conductivity (36), Density (37), Viscosity (38), Surface Tension (39), Light Scattering (36), X-rays (40), Membrane Potential (41) and Flow Birefringence (42). The methods listed above differ greatly in sensitivity, reliability and also degree of experimental difficulty.

Goette (3) listed various physical methods, which have been employed by different workers for the determination of CMC of sodium alkyl sulfates. However, the CMC values reported by Goette were mostly for the aqueous solution of these detergents at low ionic strengths. As all of this author's work was performed in the presence of supporting electrolytes like potassium chloride, sodium chloride and potassium nitrate, and since salts are known to have a significant effect upon the aggregation and hence the CMC of paraffin chain salts in aqueous solution (43,44), it was essential to know the CMC of sodium alkyl sulfates in presence of salts. A survey of the literature (2,29,45,46) revealed that many researchers had studied the effect of salts on the critical micelle concentration of sodium dodecyl sulfate. However, since the CMC values of other members of the homologous series in the presence of salts are not available, it was decided to carry out their determination in the presence of 0.1M NaCl by using spectral dye method (2,33). This method was chosen because it is very simple and

easy to perform. According to Corrin and Harkins(33), "the suitability of a dye as an indicator in the determination of critical concentration for the formation of micelles in soap solutions is related to the existence of an equilibrium mixture of the dye in aqueous solution from which one form is preferentially solubilized by the soap micelle. In addition, the charge on the dye ion must be opposite to that on the micelle." Accordingly, the following cationic dyes were tried: Pinacyanol chloride, Rhodamine 6G, Pheno-safranin, Pinaverdol, and Pinachrom (see Appendix I for their structural formulae). However, the color of the solutions of only the first two dyes were affected by the addition of sodium alkyl sulfates (33) and thus these two (Pinacyanol chloride and Rhodamine 6G) were selected for the determination of CMC by the spectral dye method. The method was also utilized to confirm the CMC values of sodium alkyl sulfates in water and salt solutions as reported by Goette (3) and other workers (29,46). The experimentally determined and the literature values of the CMC's are listed in table 1.

The effect of salts upon the critical concentration for the formation of micelles in solutions of long-chain electrolytes can be considered by applying the mass law to the equilibrium between the unassociated long-chain ions, counter (or "gegen") ions and the aggregates. For example,

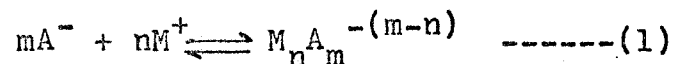
TABLE 1

CRITICAL MICELLE CONCENTRATIONS OF SODIUM ALKYL SULFATES

Sod. Alkyl Sulfate	Experimental Values			Literature Values(3)	
	In water $\times 10^{+3} \underline{M}$	In 0.1M Nacl $\times 10^{+3} \underline{M}$	In 0.1M Kcl $\times 10^{+3} \underline{M}$	In water $\times 10^{+3} \underline{M}$	In 0.1M Nacl $\times 10^{+3} \underline{M}$
C ₈	98.6(23°)*	33.8(23°)*	33.3(23°)%	130(25°)**	-
C ₁₀	29.15(24°)*	13.04(24°)*	12.77(23°)%	31(25°)**	-
C ₁₂	6.18(24°)#	1.2(24°)#	1.05(23°)%	8.1(25°)** 6.9(21°)@	1.35(25°) 1.45(29)
C ₁₄	0.98(23°)* 0.97(23°)#	0.35(23°)# 0.43(23°)#	0.47(23°)%	1.6(40°)@ 2.5(60°)@	-
C ₁₆	0.21(24°)* 0.25(24°)#	0.145(24°)* 0.162(24°)#	0.155(23°)%	0.4(40°)@ 0.6(60°)@	-
C ₁₈	0.083(23°)* 0.103(23°)#	0.077(23°)#	0.070(23°)%	0.30(60°)@ 0.17(60°)!(22)	-

Legend: *Spectral dye method (Pinacyanol Chloride); #Spectral dye method (Rhodamine 6G); **Conductivity method; @Osmotic pressure method; !Surface tension method; %Electrocapillary curve method.

the formation of micelles in case of anionic detergents can be represented by the following equation:



where A^- represents the long-chain anion and M^+ , the counter ion, which might be any cation. m and n are the number of paraffin-chain and counter ions respectively, entering into one micelle. The activity product relation for (1) can be written as

$$K = \frac{(a_{A^-})^m (a_{M^+})^n}{(a_{M_n A_m})}$$

Based on their experimental studies, Corrin and Harkins (46) reported that "if this formulation is correct the activity coefficient of the aggregate cannot be a function of the ionic strength of the solution, since the behavior of neutral long chain electrolytes at concentrations lower than the critical concentration is similar to that of strong electrolytes.

In aqueous solutions of ordinary electrolytes the charge on any ion is always insufficient to produce enough repulsion between the ions of like charge to keep them apart at very large distances. At the interionic distances exhibited in dilute solutions (mean thickness of the ionic atmosphere about 30 Å. for a uni-univalent electrolyte at an ionic strength of 0.01) the repulsion between ions of

like charge is increased as the charge per ion increases in such a way as to give the relations expressed by the principle of ionic strength and the related Debye-Hückel theory.

In the case of a colloidal electrolyte the relations are different. The charge on the surface of the aggregated colloid ion is relatively large and may be considered as distributed in a sheet, with distances between charges in the sheet on the order of 4.5 Å. for an ordinary soap. The repulsion between the ions in this sheet and the adjacent salt ions of like charge is here sufficiently great to produce a greater separation than that considered above for simple salt ions of like charge. The result of this increased interionic distance is that the magnitude of the charge on each ion becomes much less significant and the effect is determined by the total charge. As a result those principles which indicate a large variation with the charges of individual ions now become invalid."

Thus it is shown that the behavior of the colloidal aggregates of long chain electrolytes cannot be described in terms of principle of ionic strength or the related Debye-Hückel relationships.

Corrin and Harkins (46) also reported that addition of salts results in lowering of the CMC of colloidal

electrolytes. They pointed out that depression of the critical concentration is related only to the concentration of that ion of an added salt which bears a charge opposite to that on the colloidal aggregate and the nature of the other ion is without effect. It was proved that the logarithm of the CMC of a colloidal electrolyte is a linear function of the logarithm of the total concentration of the ion opposite in charge to that on the aggregate.

Later, Goddard and coworkers (45) proved that the effect of univalent cations on micelle formation in case of anionic surfactants, depends not only on the concentration of the gegenions, but also on the structure of the ion and how closely it approaches the charged head groups of the detergent anions. According to them "the smaller the screening action on the charges of the micelle, the greater the depression of the critical concentration."

Stigter and Mysels (71) have indicated that on adding a salt, both the size and charge of the micelle increase, but the degree of ionization remains constant within the uncertainty of the determination. However, the addition of salts still caused lowering of the CMC.

The effects of salt addition on experimentally determined CMCs in the present work are indicated in table 1. Also as can be seen, the CMC values by the spectral dye

method came out to be lower than those determined by other methods. This observation was also made by Klevens (67), who said that the spectral change method yields lower CMC values because the use of a dye involves a degree of solubilization, which, like the effects of added hydrocarbons (68), decreases the CMC. Or alternatively, the dye acts like a salt and thus causes a decrease in the CMC values. Another reason for the slight decrease in the author's experimentally determined CMC values is the lower temperature at which the measurements were carried out. According to Flockhart and Ubbelohde (69), a rise of temperature usually increases the CMC.

Later, during the course of this study, CMC values of sodium alkyl sulfates were determined using the electrocapillary curve data (page 39). And as can be seen, the values obtained by the spectral dye method and the droptime method based on the shift of electrocapillary curves, as given on page 29, agree reasonably well.

V. ELECTROCAPILLARY CURVES IN PRESENCE OF SODIUM ALKYL SULFATES

The curves representing the variation of surface (or interfacial) tension of mercury in an ideal polarized electrode with the potential difference imposed across the interface are called electrocapillary curves (6) and are often almost parabolic in shape as shown in figure 5.

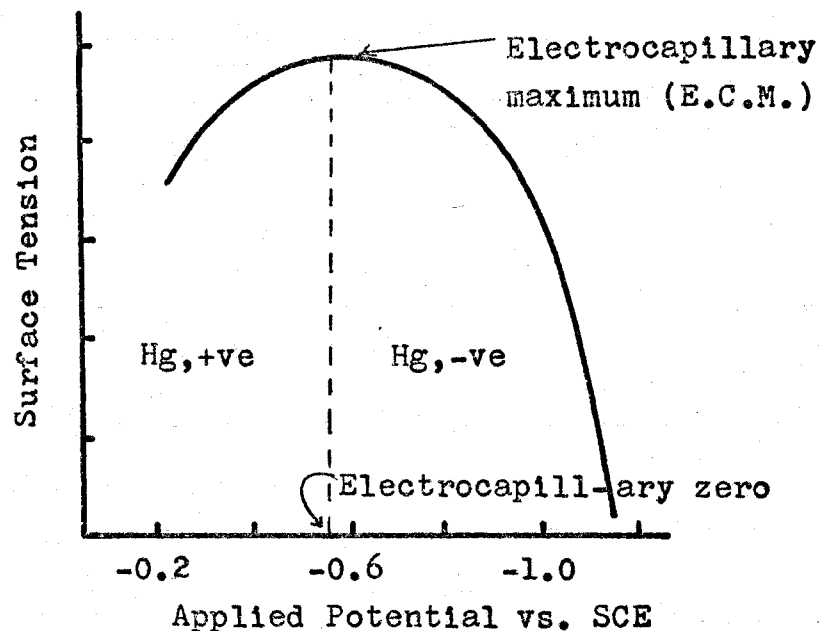


FIGURE 5

In all the electrocapillary curve studies which are done using a dropping mercury electrode (DME), the surface tension is substituted by the droptime, the time taken by each mercury drop to form. The droptime (which is proportional to the surface tension), varies with the height of the mercury column. The peak on the electrocapillary parabola, which is called the potential at

the electrocapillary maximum (E-C maximum) corresponds to the uncharged mercury surface. Thus, the E-C maximum, which lies at -0.56v (vs. SCE.) in 1N KCl may be regarded as approximately absolute zero (7), i.e. the potential at which the charge on the electrode is zero. However, the electrocapillary zero for mercury is not a universal constant and varies upon adding surface-active substances. The shape of the curve is explained as follows: The original positive charge on the mercury is neutralized by cathodic polarization and the surface tension increases (the positive, rising part of the curve). At the maximum, the positive charge is just neutralized, and the electrode bears zero charge. Beyond the electrocapillary maximum, the mercury is negatively charged and its surface tension, consequently, decreases.

The deformable anions (Br^- , I^- , CNS^- , S^- etc.), acid dyes and negative colloids cause a change in the shape of the positive part of the curve and shift the E-C maximum to more negative potentials. This is because, when these ions approach the electrode, they decrease the thickness of the electrical double layer and thus its capacity is increased. For the same applied voltage, the charge on the electrode is increased, and this in turn causes a decrease in the surface tension. At the potential at which the electrocapillary curve shows a maximum for weakly adsorptive electrolytes, adsorptive anions are still strongly

adsorbed and thus the maximum is shifted to a more negative potential. On the descending part of the E-C curve, the anions are repulsed and thus they do not effect the shape of this part of the curve. Likewise, adsorptive cations deform the negative part of the curve and shift the E-C maximum to more positive potentials. Neutral substances that are strongly adsorbed do not effect the shape of the curve, but decrease the surface tension in the neighborhood of the peak on the curve.

Since the electrocapillary curves give valuable information, especially about adsorption phenomena, the effect of surface-active substances on the electrode surface can be studied by electrocapillary measurements. Tamamushi and Yamanaka (4) studied the effect of sodium dodecyl sulfate on electrocapillary curves resulting from a 0.1N KCl solution.

In this work, to compare the behavior of sodium dodecyl sulfate with other members of the series, electrocapillary measurements were carried out in the presence of sodium octyl, decyl, tetradecyl, hexadecyl and octadecyl sulfates. Also, the work with sodium dodecyl sulfate (SDS) was repeated and the results obtained were found to be in complete agreement with those reported by Tamamushi and Yamanaka (4). For example, it was noticed that the addition of sodium dodecyl sulfate (SDS) more than $8.6 \times 10^{-5} M$ in its concentration flattened the E-C curve and shifted the maximum

to a more negative potential as shown in fig. 6. This clearly confirms the evidence that SDS is strongly adsorbed and is, therefore, potentially a good maximum suppressor. On increasing the concentration of sodium dodecyl sulfate, a further decrease in the interfacial tension (droptime) was noticed. This continued up to the suppressor concentration of $1.05 \times 10^{-3} \text{ M}$. After this a further increase in the concentration of surfactant did not cause any appreciable change in the droptime. In fact at a concentration of $3.99 \times 10^{-3} \text{ M}$, the droptime at various applied potentials was more than that obtained in case of $1.05 \times 10^{-3} \text{ M}$ solution. (for data see table 2). This behavior is explained by saying that at a concentration of $1.05 \times 10^{-3} \text{ M}$ which is close to the CMC ($1.45 \times 10^{-3} \text{ M}$) of sodium dodecyl sulfate (29), the DME is completely covered by the surfactant and that is why a further increase in the concentration of suppressor did not produce any change in the interfacial tension at the mercury-solution interface. As shown in figures 7 and 9, a similar behavior was observed in case of sodium octyl, decyl, hexadecyl and octadecyl sulfates. Thus, in all these cases, on adding a small amount of suppressor to the potassium chloride solution, a decrease in the interfacial tension (droptime) was observed. This decrease was relatively greater in case of sodium decyl and dodecyl sulfates and clearly indicates that these two surfactant are stronger than the other members of the series. As in the case of SDS, on

FIGURE 6

Electrocapillary curve in presence of dodecyl sulfate

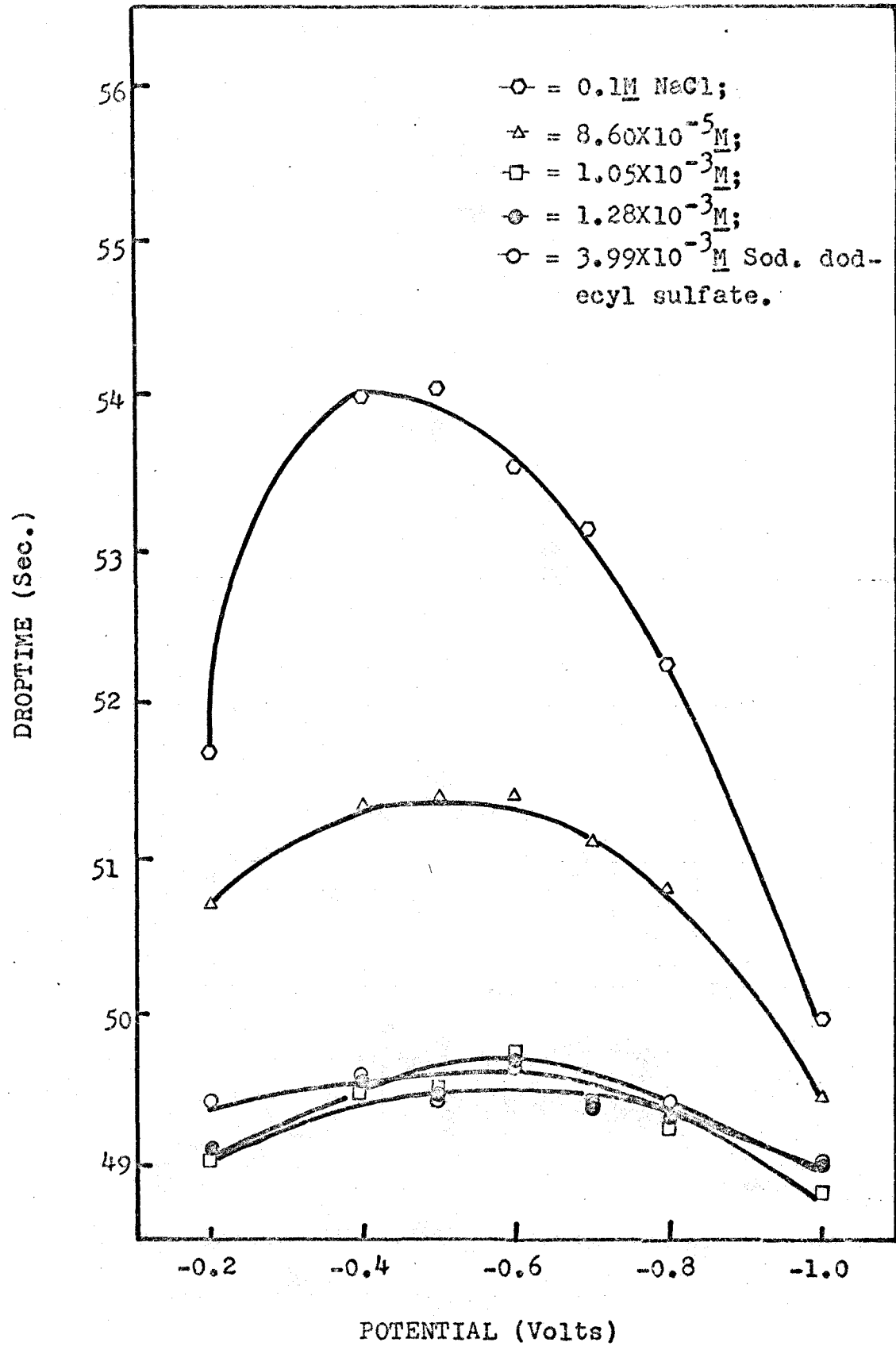


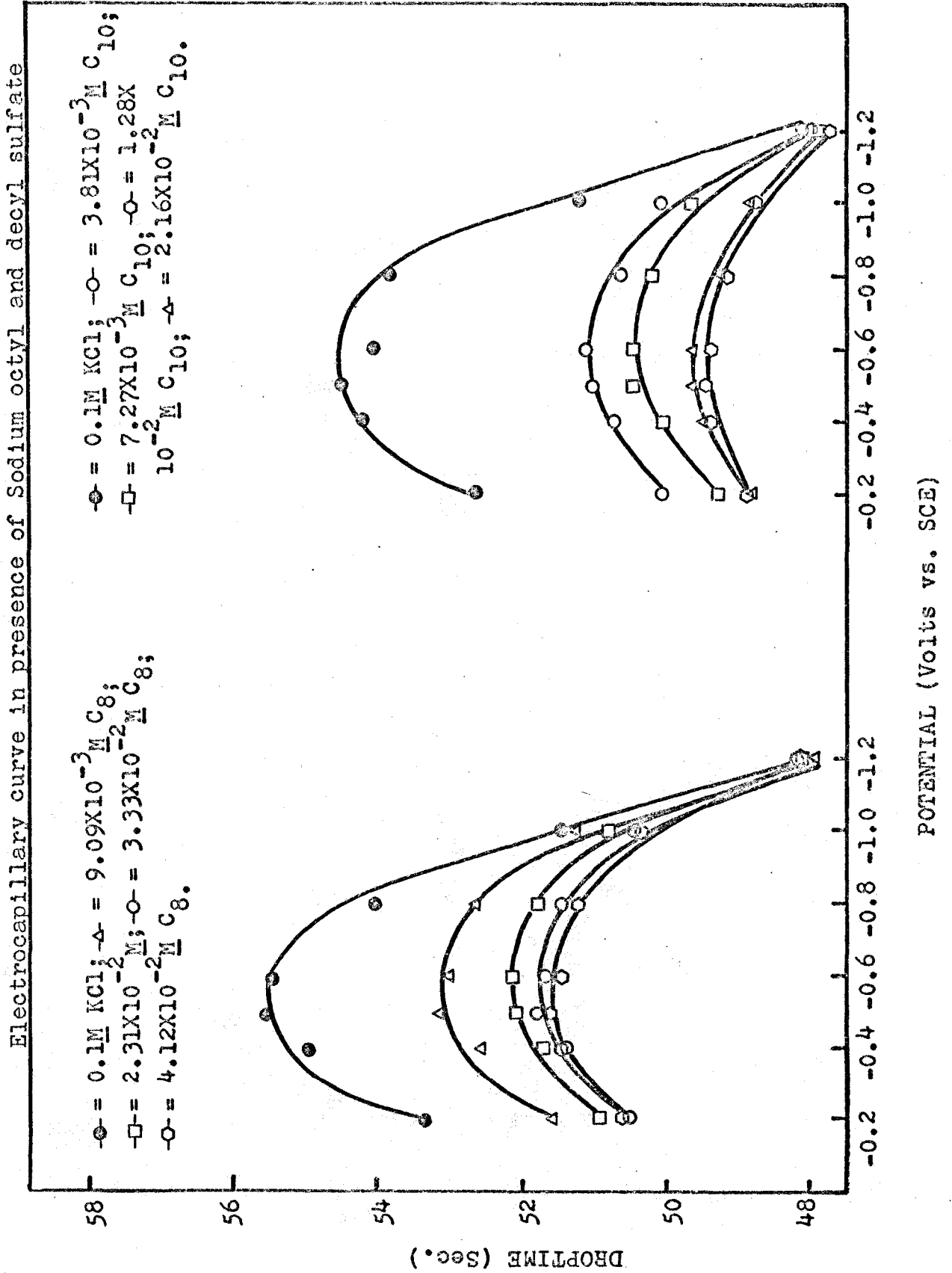
TABLE 2

ELECTROCAPILLARY CURVE IN PRESENCE OF VARIOUS CONCENTRATIONS OF SODIUM DODECYL SULFATE

Potential (volts)	Droptime in seconds* (for 10 drops) in presence of					
	0.1M Kcl	$8.60 \times 10^{-5} \text{M}$	$1.05 \times 10^{-3} \text{M}$	$1.28 \times 10^{-3} \text{M}$	$3.99 \times 10^{-3} \text{M}$	$4.94 \times 10^{-3} \text{M}$
-0.20	51.66	50.68	49.05	49.10	49.40	49.50
-0.40	53.97	51.32	49.48	49.52	49.53	49.71
-0.50	54.03	51.37	49.48	49.46	49.45	49.65
-0.60	53.50	51.38	49.72	49.65	49.65	49.76
-0.70	53.10	51.07	49.38	49.36	49.38	49.60
-0.80	52.22	50.78	49.25	49.26	49.36	49.49
-1.00	49.90	49.40	48.78	48.98	48.98	48.95

* The values shown in the table are an average of at least two measurements.

FIGURE 7



Electrocapillary curve in presence of tetradecyl sulfate

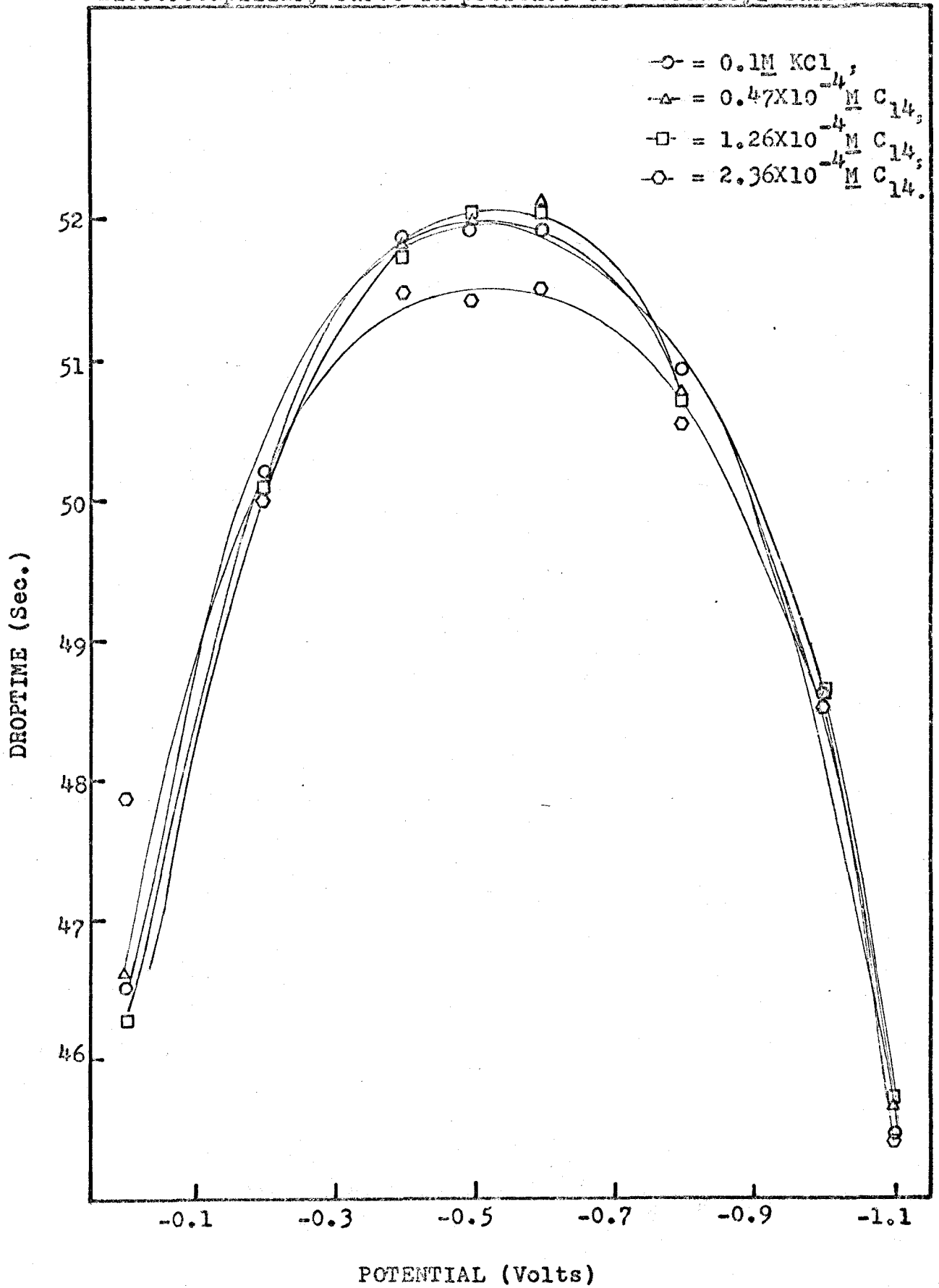
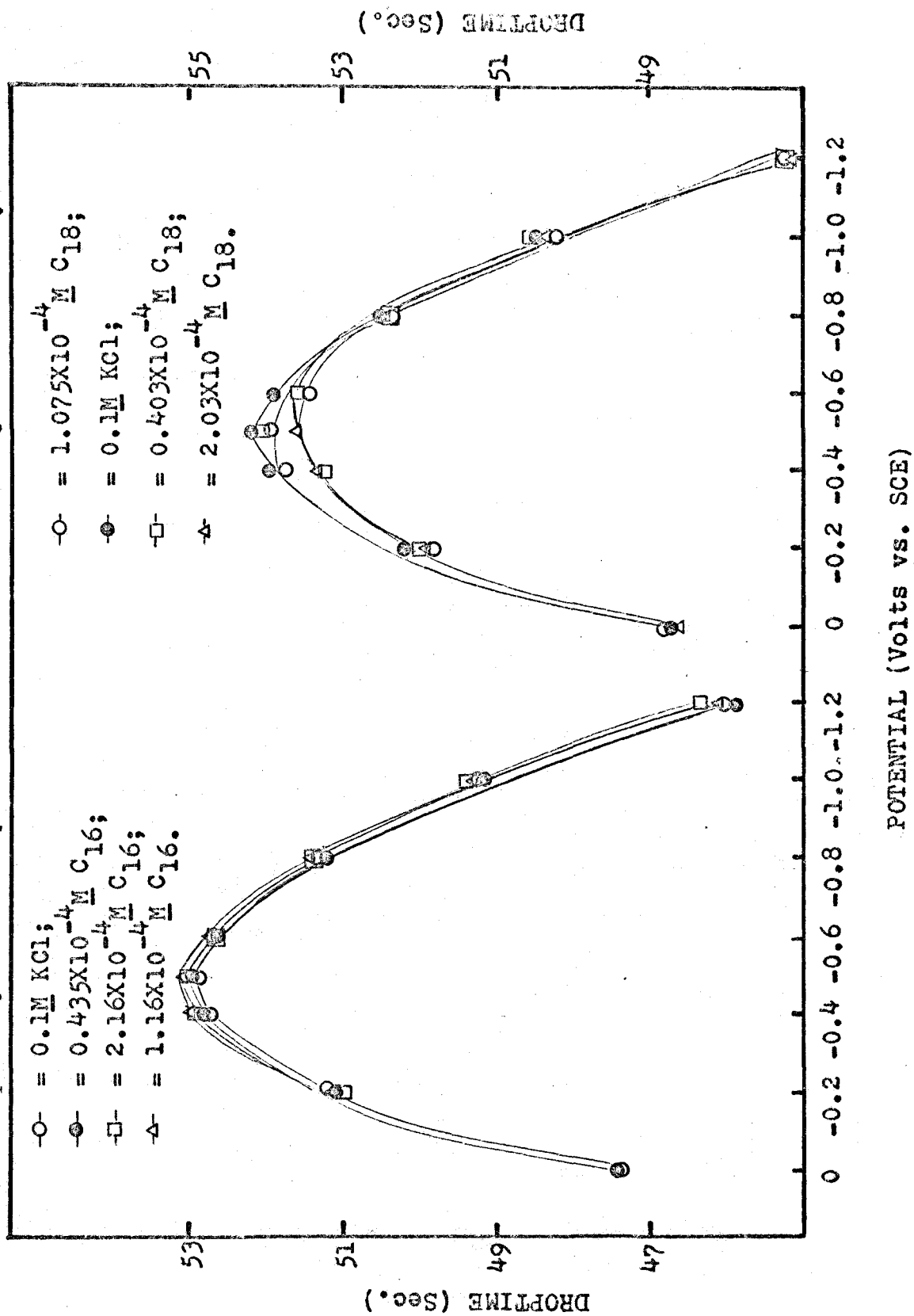


FIGURE 9

Electrocapillary curve in presence of sodium hexadecyl and octadecyl sulfate



raising the concentration of the surfactant beyond their CMC values, the interfacial tension did not change much and in fact a slight increase was observed. As explained earlier, when the concentration of a particular surfactant exceeds its CMC value, the mercury drop gets completely covered and a further increase in the surfactant concentration produces no change in the droptime or interfacial tension.

As can be seen in figures 8 and 9, addition of sodium tetradecyl, hexadecyl and octadecyl sulfates produces very little change (decrease) in the interfacial tension at the mercury-solution interface. From this, one concludes that they are only weakly adsorbed and, consequently, are likely to be poor suppressors. The chief reason for this weak behavior of long-chained alkyl sulfates is the turbidity or white precipitate which resulted on the addition of these surfactants to the electrolyte solution. Most probably, the precipitate appeared because of the formation of insoluble potassium salt. However, since the turbidity formation was observed when the suppressor concentrations were in the vicinity of their respective CMC values (table 1) it can be said that due to formation of micelles (aggregates) one observes the "streamy" white precipitate which settles down on standing. In order to further establish the true nature of the turbidity, electrocapillary measurements were carried out by using 0.1M NaCl solution.

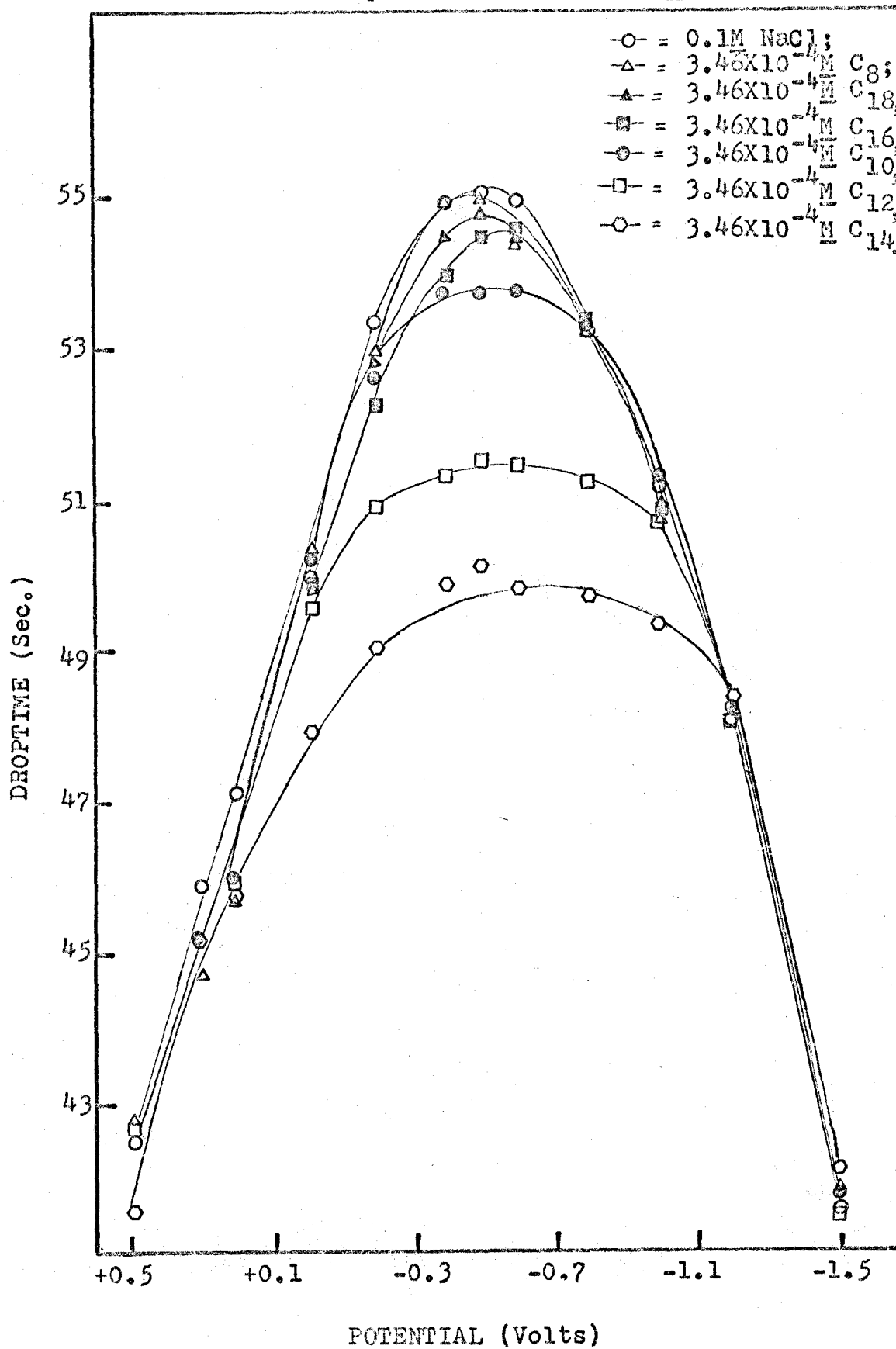
In this case, the addition of sodium tetradecyl sulfate to the sodium chloride solution did not result in any turbidity, however, some "cloudiness" was observed in case of hexadecyl and octadecyl sulfate. And as a result of this, sodium tetradecyl appeared to be more strongly adsorbed and it lowered the interfacial tension even more than the sodium dodecyl sulfate (fig. 10). The formation of slight turbidity in the form of "cloudiness" in case of hexadecyl and octadecyl sulfates indicates the presence of micelles.

Due to their anionic nature, the sodium alkyl sulfates, were more strongly adsorbed at less negative potentials and as a result, the positive leg of the E-C curve was the portion most affected by the increasing concentration of surfactants. This is understandable, because at potentials less negative than the isoelectric point (E-C zero), excess of positive charge on mercury surface promotes the adsorption of anionic polar groups in the surfactant molecules. And when the potential is made more negative, it becomes increasingly difficult for the anionic polar group to be adsorbed and the E-C curve begins to coincide with the normal curve.

Jacobsen and Kalland (30) had studied the electrocapillary curves in 0.2M acetate buffer (in the pH range 3-7.5) in the presence of sodium dodecyl sulfate (SDS), Triton X-100 and Armeen 12D, a cationic suppressor. They indicated that all of these were strongly adsorbed at the dropping mercury

FIGURE 10

Electrocapillary curve in 0.1M NaCl



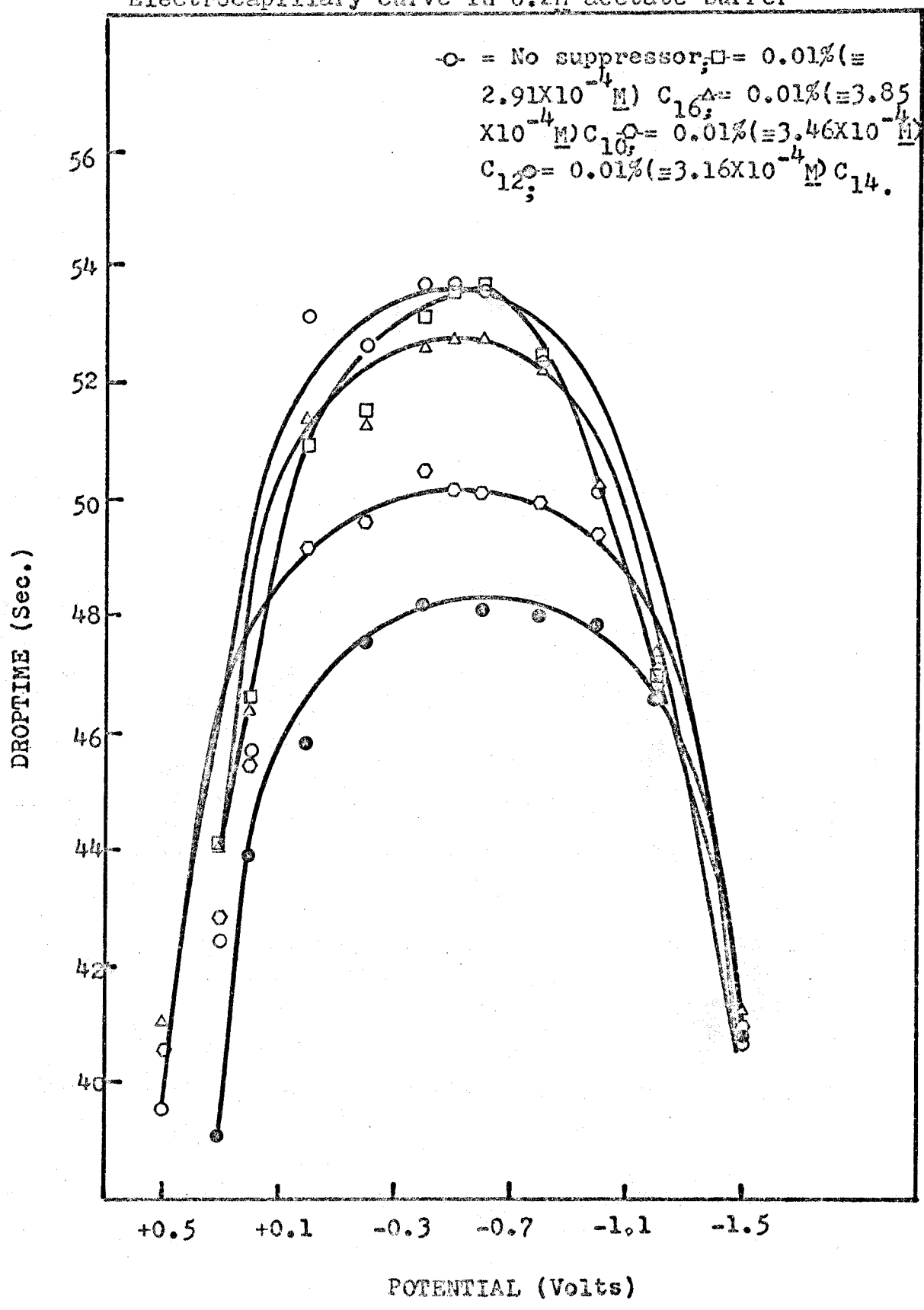
electrode. It was reported that a 0.01% ($= 3.46 \times 10^{-4} \text{ M}$) solution of SDS caused a large decrease in the droptime over a considerable potential range. In order to check the adsorption behavior of other homologs of the series, it was decided to repeat the experiment of Jacobsen and Kalland. An air-free solution of 0.2M acetate buffer at pH of 4.50 was employed and droptime for 10 drops was recorded in the absence and presence of all the surfactants at 25°C. The concentration of each suppressor in the solution was kept at 0.01%.

On plotting the droptime vs. the applied potential (fig.11), a behavior similar to that observed in the case of 0.1M NaCl was noticed. Since addition of sodium tetradecyl sulfate to the acetate buffer solution did not result in any turbidity, and although its molar concentration (3.16×10^{-4}) was lower than that of sodium dodecyl sulfate (whose concentration was $3.46 \times 10^{-4} \text{ M}$), it caused a larger decrease in the droptime in the potential range +0.20 -- -1.50 v. (vs. SCE). On mixing sodium hexadecyl or octadecyl sulfates with the buffer, once again turbidity of white precipitate was formed and this reduced their adsorptive ability considerably and as a result these two surfactants did not decrease the droptime much.

The electrocapillary measurements described above were

FIGURE 11

Electrocapillary curve in 0.2M acetate buffer



made in the presence of 0.01% solutions of surfactants and since the molecular weight of each suppressor is different, it was decided to compare their activity at the same molar concentration, viz. $3.46 \times 10^{-4} \text{ M}$, which corresponds to 0.01% SDS. The droptime vs. potential plot (fig.12) obtained in this case clearly showed that tetradecyl sulfate was much more strongly adsorbed than the decyl and dodecyl sulfates. (The droptime values are shown in table 3).

The study of electrocapillary curves was extended further and measurements were carried out in 0.25M EDTA, which too can act as a supporting electrolyte. As in the earlier three cases, once again the addition of hexadecyl and octadecyl sulfates lead to the formation of "streamy" or "wavy" precipitate and as a result these two surfactants were only weakly adsorbed as shown in the E-C plot (fig.13). Unlike in the case of supporting electrolytes 0.1M NaCl and acetate buffer, the addition of tetradecyl sulfate to EDTA solution did produce the turbidity and because of this it was less strongly adsorbed than the sodium dodecyl sulfate.

The electrocapillary data in the case of 0.1M NaCl, 0.2M acetate buffer and 0.25M EDTA were obtained at a surfactant concentration of $3.46 \times 10^{-4} \text{ M}$, a figure which is close to the critical micelle concentration of tetradecyl sulfate and exceeds those of hexadecyl and octadecyl sulfates.

FIGURE 12

Electrocapillary curve in 0.2M acetate buffer

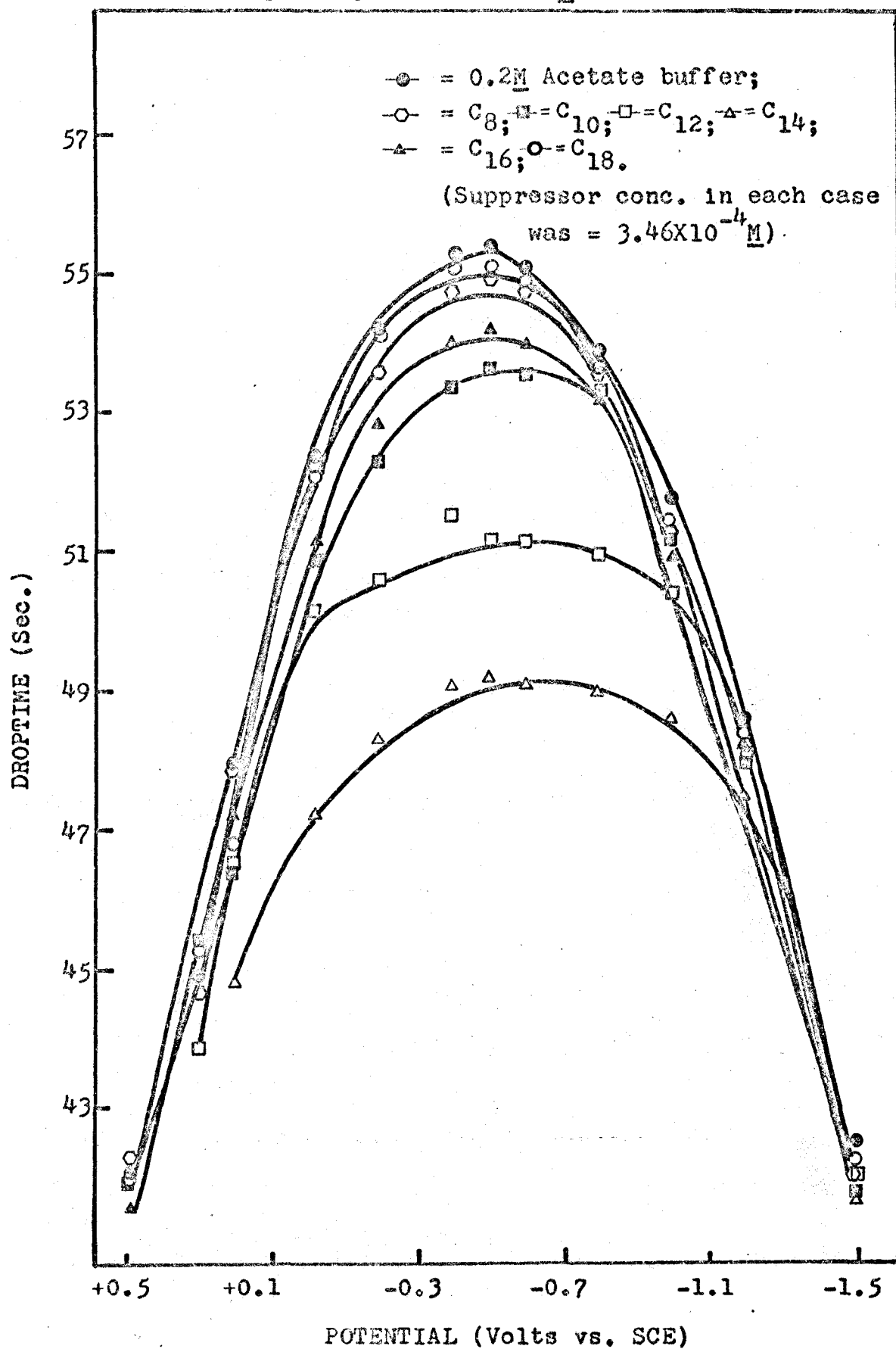


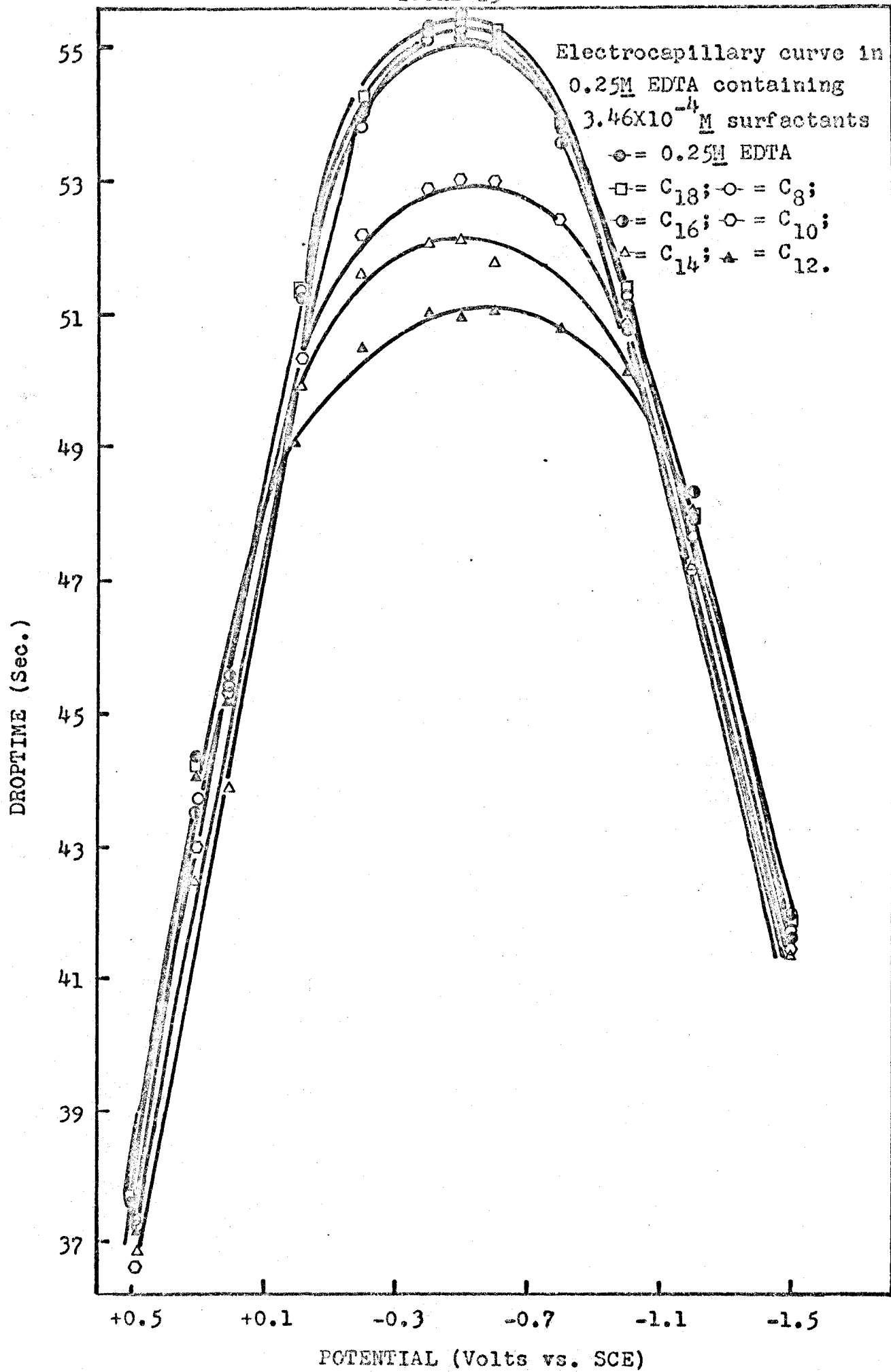
TABLE 3

ELECTROCAPILLARY CURVE IN 0.2M ACETATE BUFFER OF pH 4.5 AT 25° CENTIGRADE

Potential (volts) vs. SCE	Air-free 0.2M $\bar{A}c$ buffer	Droptime in seconds (for 10 drops)* in presence of					
		$3.46 \times 10^{-4} M$ C_8	$3.46 \times 10^{-4} M$ C_{10}	$3.46 \times 10^{-4} M$ C_{12}	$3.46 \times 10^{-4} M$ C_{14}	$3.46 \times 10^{-4} M$ C_{16}	$3.46 \times 10^{-4} M$ C_{18}
+0.49	42.00	42.25	42.06	41.55	39.85	41.50	42.02
+0.30	44.90	44.70	45.45	43.87	40.05	44.85	45.26
+0.20	47.95	47.85	46.40	46.50	44.80	47.20	46.75
-0.02	52.35	52.20	50.85	50.15	47.20	51.15	52.03
-0.20	54.20	53.58	52.25	50.60	48.30	52.80	54.10
-0.40	55.25	54.72	53.35	51.50	49.08	54.00	55.05
-0.50	55.33	54.90	53.60	51.18	49.20	54.15	55.05
-0.60	55.05	54.75	53.55	51.16	49.10	53.95	54.85
-0.80	53.90	53.55	53.25	50.95	49.00	53.15	53.55
-1.00	51.75	51.28	51.25	50.40	48.60	50.90	51.45
-1.20	48.60	48.10	48.12	48.10	47.50	48.20	48.38
-1.50	42.50	42.00	41.75	42.00	41.66	41.20	42.20

* The values reported represent an average of atleast two measurements.

FIGURE 13

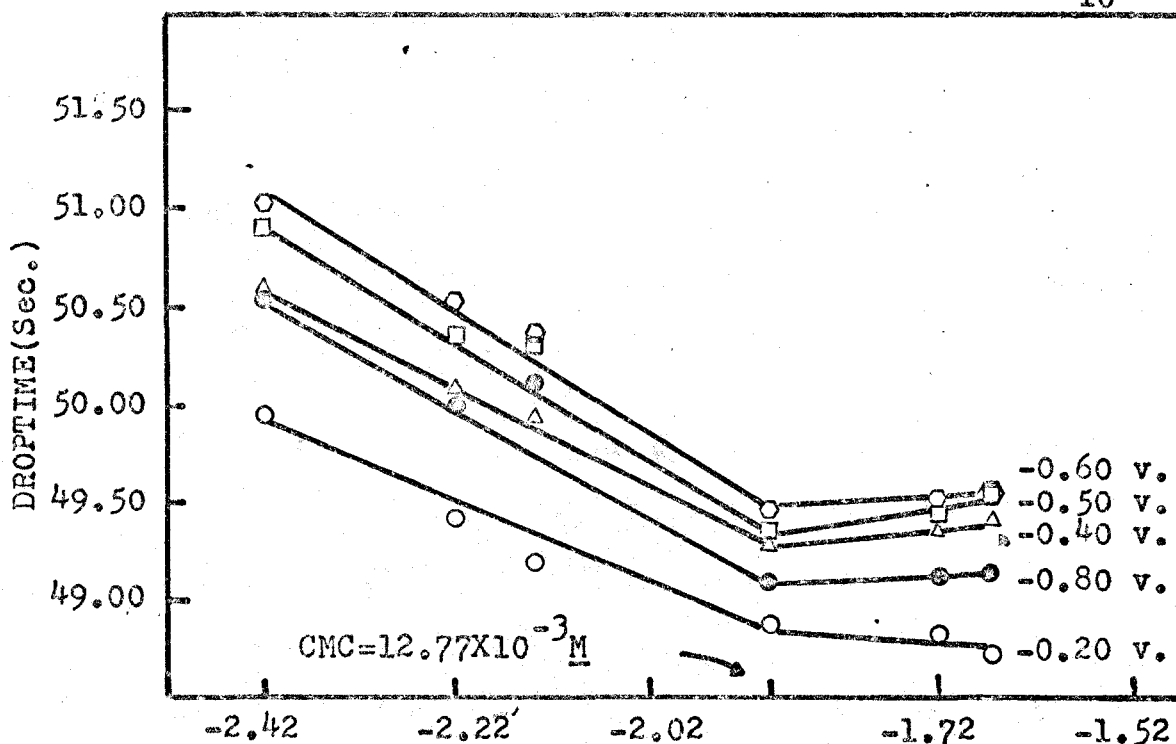


(see table 1 for experimentally determined values). And, since addition of these three surfactants resulted in turbidity formation, it can be said that formation of micelles in the presence of salt solutions causes the turbidity or the "wavy" precipitate and consequently affects their adsorbability. However, in the case of potassium chloride, the formation of an insoluble potassium salt of the alkyl sulfates also contributed to the formation of turbidity. This was proved by an independent experiment in which increasing concentrations of sodium dodecyl sulfate were added to a 0.1M KCl solution. Surprisingly enough, even in this case at a surfactant concentration of $0.25 \times 10^{-3} \text{M}$, turbidity was formed. Since this concentration figure is far less than the CMC ($1.45 \times 10^{-3} \text{M}$) of sodium dodecyl sulfate in presence of electrolytes, it is evident that precipitation of potassium salt of alkyl sulfates occurs especially when the surfactant concentration is very high.

Roe and Brass (29), who had carried out surface tension measurements on sodium dodecyl sulfate solutions had suggested that the CMC of the surfactant could be determined by plotting the surface tension against the log of the surfactant concentration. The point where the two branches of the curve intersected was taken as the critical micelle concentration. Later, Malik et al. (5) utilized the same technique and

measured the CMC of non-ionic surfactants by plotting the droptime measurements at various potentials against the log of the surfactant concentration. Following the procedure of Malik et al., the author obtained the CMC's of sodium alkyl sulfates by plotting the droptimes vs. log SAS conc. (figures 14-19). The CMC values thus obtained are listed in table 1 and as pointed out earlier, these values agreed well with those obtained by the spectral dye method.

Droptime vs. Log(SAS conc.) plot in case of C₁₀



LOG(Surfactant conc.), moles/l.

Droptime vs. Log(SAS conc.) plot in case of C₈

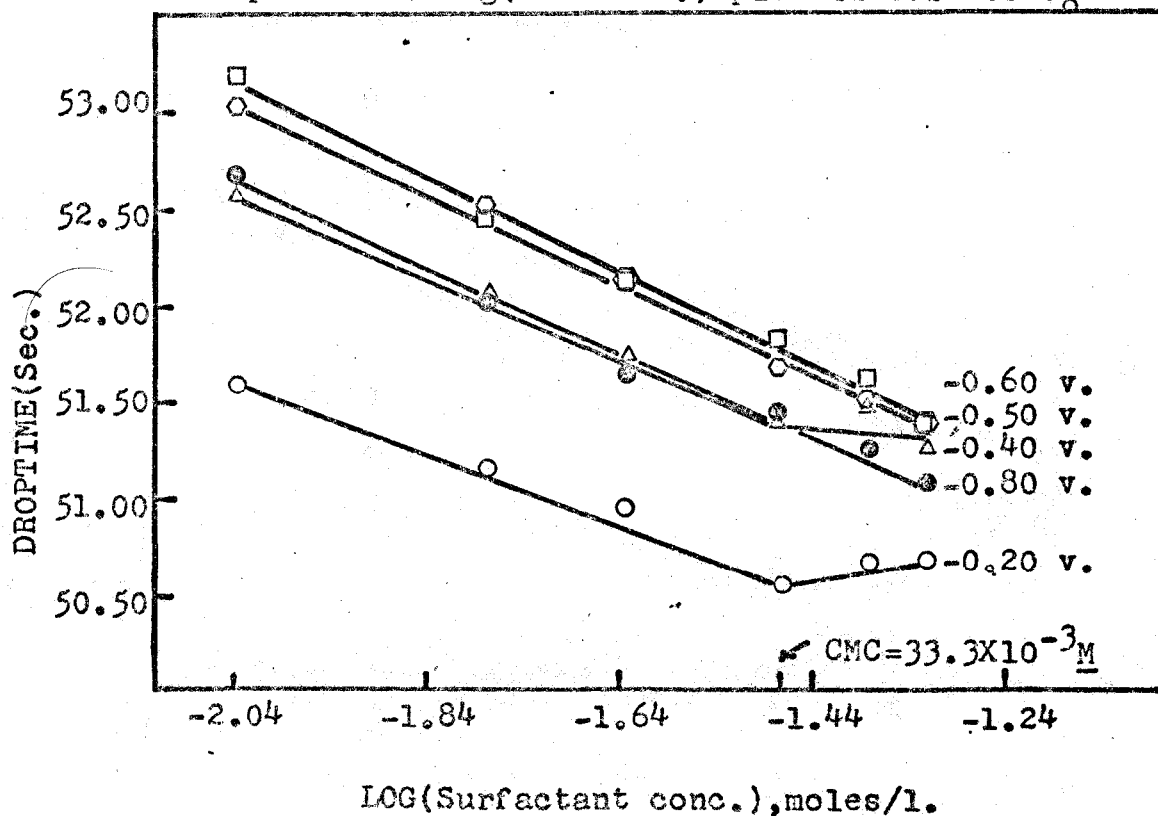


FIGURE 15

FIGURE 16

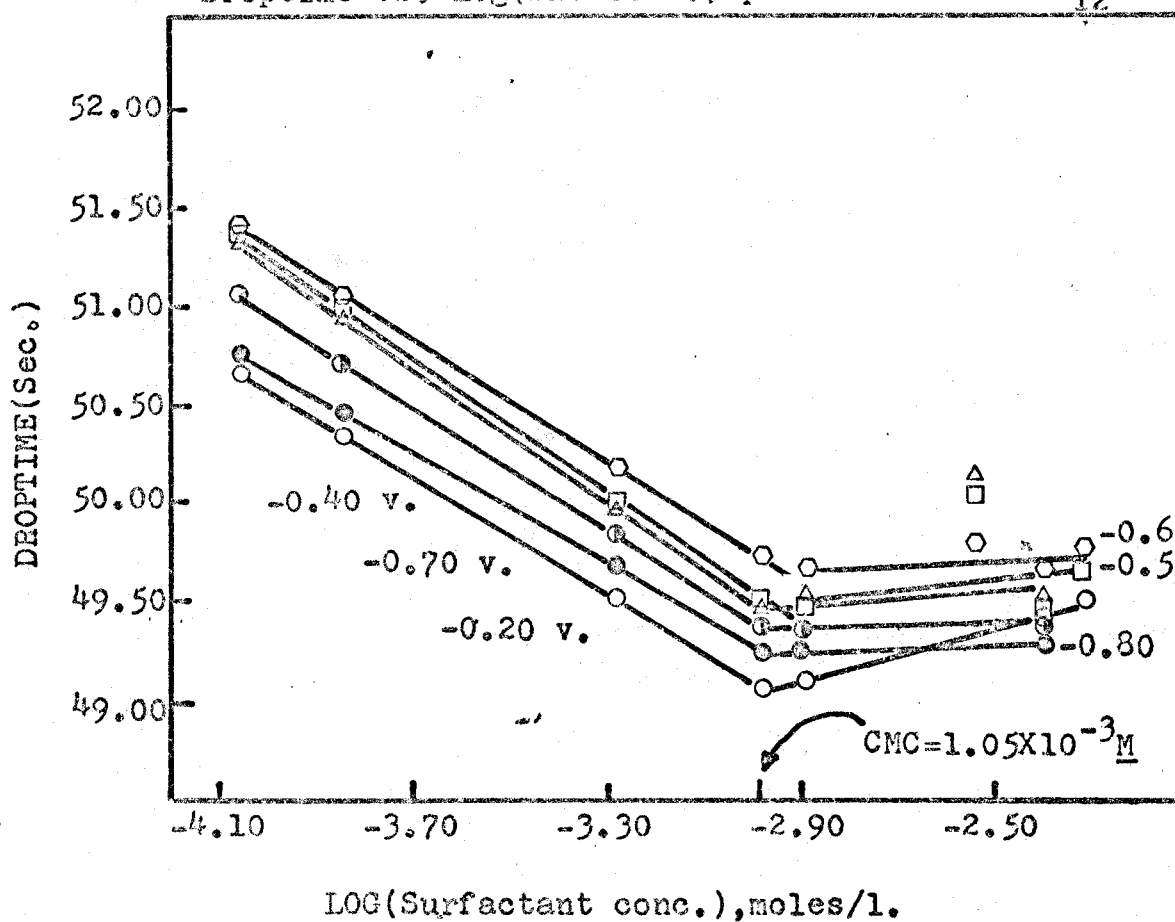
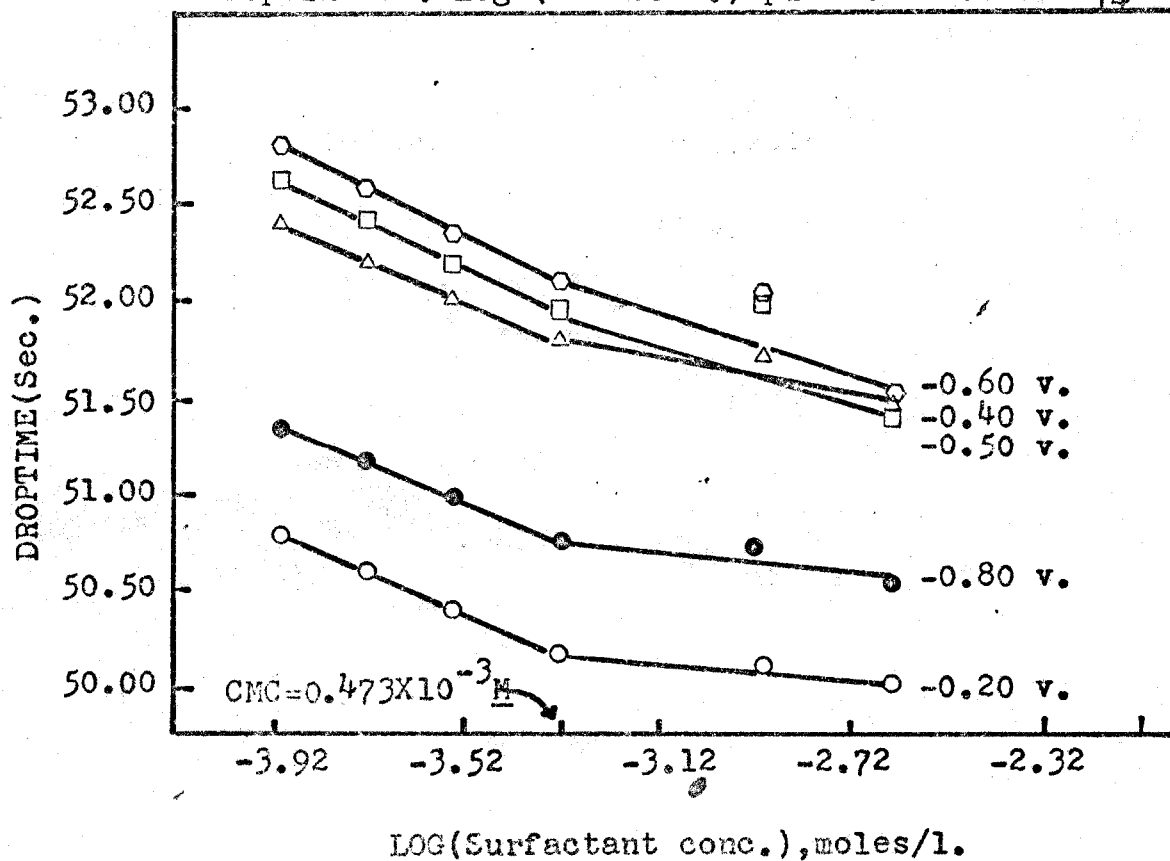
Droptime vs. Log(SAS conc.) plot in case of C_{12} 

FIGURE 17

Droptime vs. Log (SAS conc.) plot in case of C_{14} 

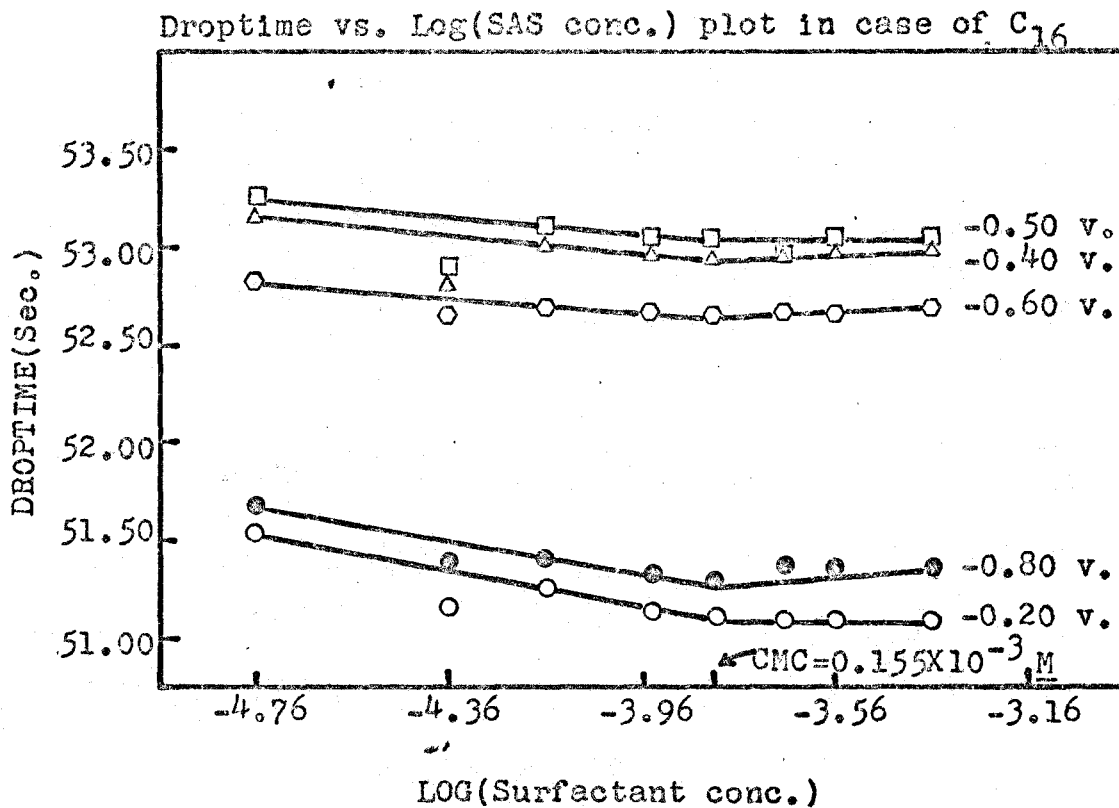
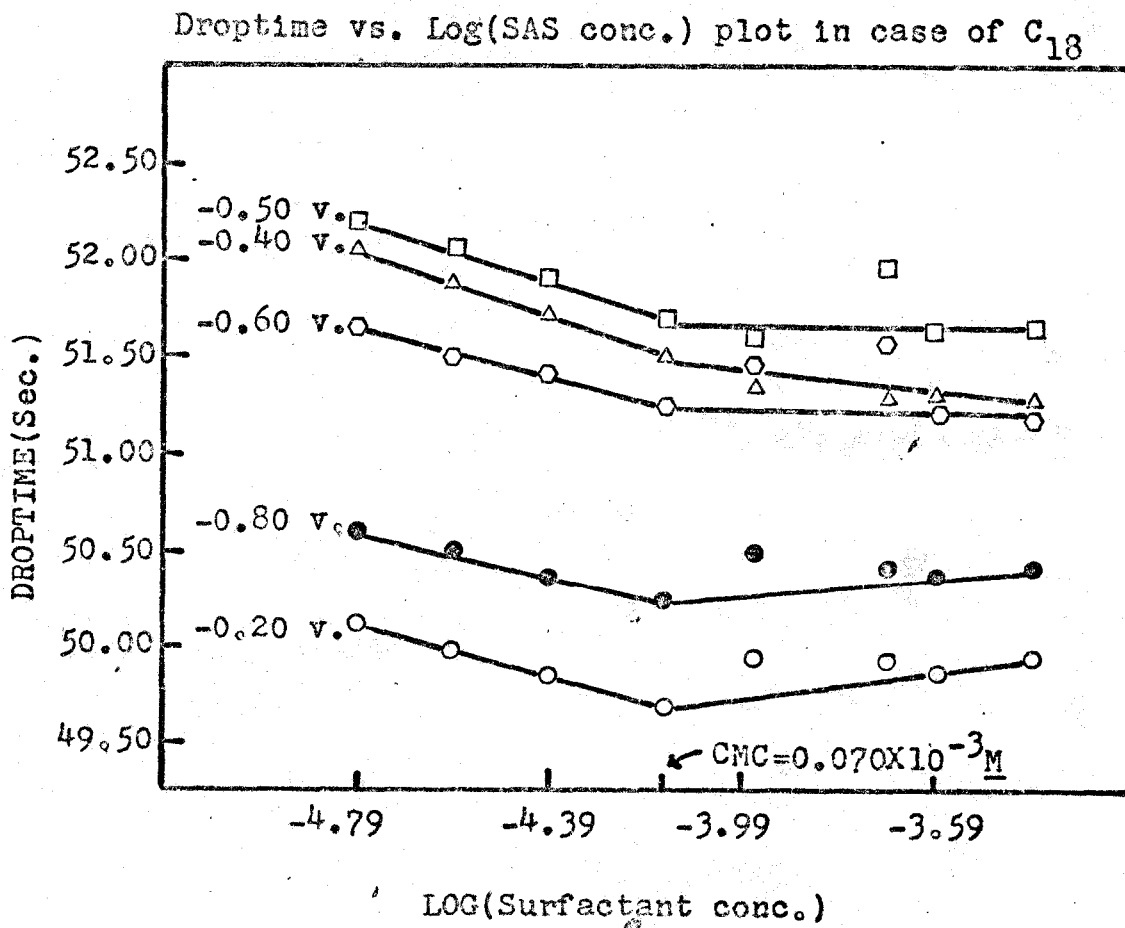


FIGURE 19



VI. DETERMINATION OF MAXIMUM SUPPRESSION POINTS

RESULTS AND DISCUSSION

OXYGEN MAXIMUM:

The oxygen maximum is obtained by employing air-saturated solutions of potassium or sodium chloride. The height of oxygen maximum depends on the amount (concentration) of oxygen present in the solution. In their study of the oxygen maximum by current-time curves, Barradas and Kimmerle (53), had employed 0.1M KCl solution and they obtained very large (of the order of about 120 microamp) current at the end of the drop life. On using an air-saturated 0.1M KCl solution, the author could not obtain the oxygen maximum and the limiting current did not exceed 10 microamp. Thus, it was decided to employ a 0.01M KCl solution. In order to study the dependence of the maximum on the concentration of dissolved oxygen, MSP determinations were also carried out with air-saturated 0.01M NaCl solution. The MSP values of various surfactants obtained in both cases are listed in table 4.

The formation of the oxygen maximum is explained as follows: The oxygen present in the solution is first adsorbed at the mercury-solution interface. As increasing negative potential is applied, reduction of the adsorbed oxygen takes place and the current rises sharply. The curve "a" in fig. 20 shows the first oxygen maximum in case of 0.01M KCl. When a maximum suppressor is introduced into the solution, it is

TABLE 4

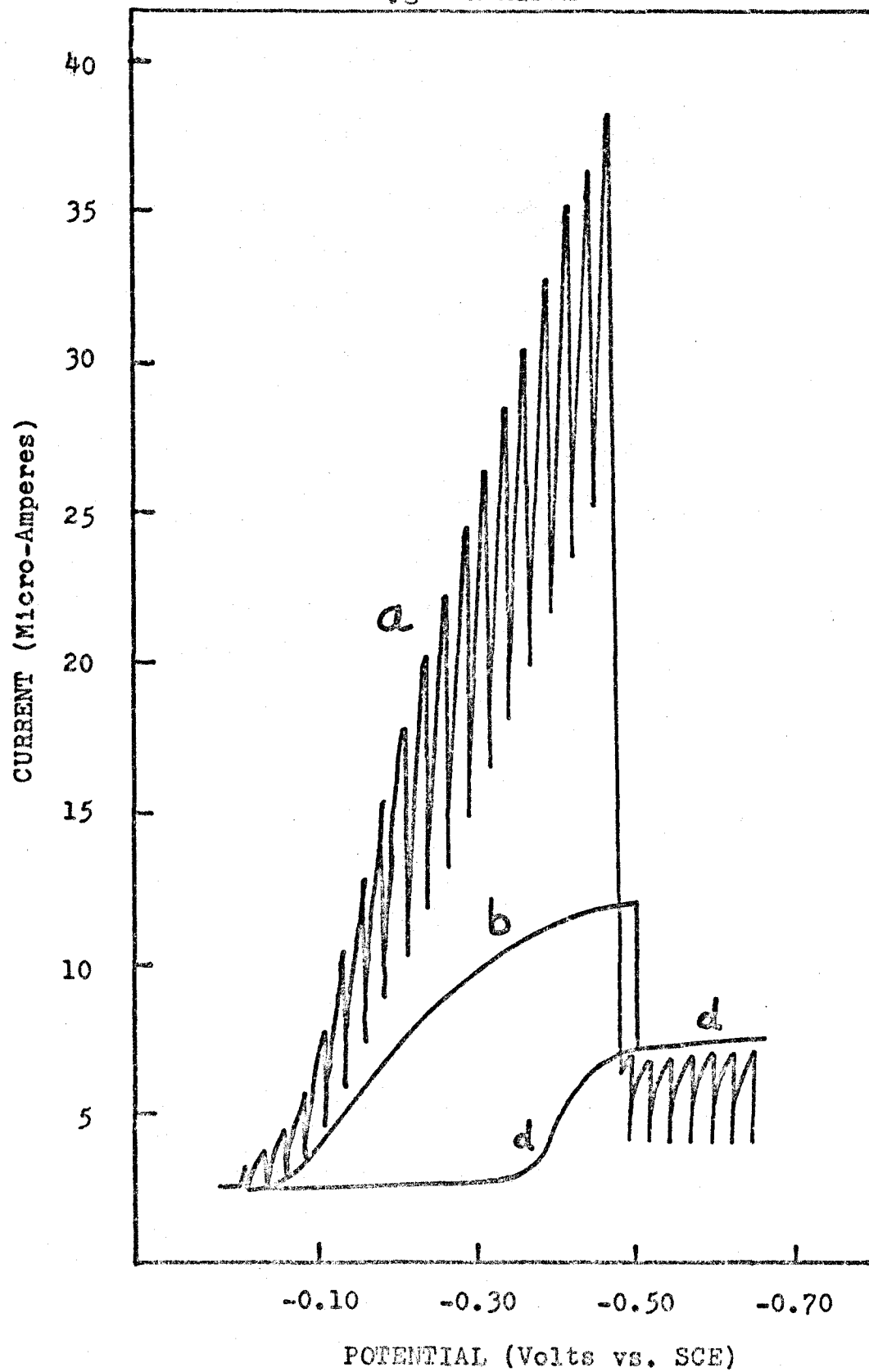
MAXIMUM SUPPRESSION POINTS OF SODIUM ALKYL SULFATES IN CASE OF Pb^{2+} , O_2 & Ni^{2+}
 MAXIMA USING DIFFERENT SUPPORTING ELECTROLYTES

Depolarizer and Supp. Electrolyte	MSP x 10 ⁺⁶ M at 25°C.					
	C ₈	C ₁₀	C ₁₂	C ₁₄	C ₁₆	C ₁₈
1) O ₂ in 0.01M NaCl	193	39.9	20.65	25.7	45.8	153.7
0.01M KCl	97.0	15.33	12.08	20.4	159.3	200.3
2) Pb ²⁺ in 0.1M LiCl	43.0	7.66	6.90	11.00	28.8	76.1
0.1M NaCl	53.8	8.71	6.90	9.44	28.8	36.0
0.1M KCl	42.7	9.58	6.03	11.15	34.5	-
3) UO ₂ ²⁺ in 0.1M HCl	10.5 (30-31°C)	0.77 (26°C)	0.52 (30-31°C)	0.79 (26°C)	5.08	6.16*
4) Ni ²⁺ in 0.1M KCl:	<u>MSP x 10⁺³ M</u>					
	8.32*	(1)3.20 (28°C)	(1)1.32*	1.82* (28°C)	5.25* (28°C)	10.33*
		(11)2.13	(11)0.944 (27°C)			
			(111)1.25 ^Δ			

* Extrapolated Values.

^Δ Value obtained by using a 2.5 x 10⁻³ M Ni (II) solution.

FIGURE 20
Oxygen Maximum



preferentially adsorbed and pushes out the oxygen from the interfacial film (the layer around the mercury drop) and thus causes a deficiency of oxygen in the adsorbed layer. This phenomenon is termed as "concentration polarization" and this results in rounding and suppression of the curve or the maximum as shown in curve "b" of figure 20. When the electrode surface is covered by a monolayer of the surfactant (53), the streaming phenomena associated with the oxygen maximum are halted and the maximum is completely suppressed. At this stage a small limiting diffusion current results (curve "d" in fig. 20); its value being determined by the Ilkovic equation.

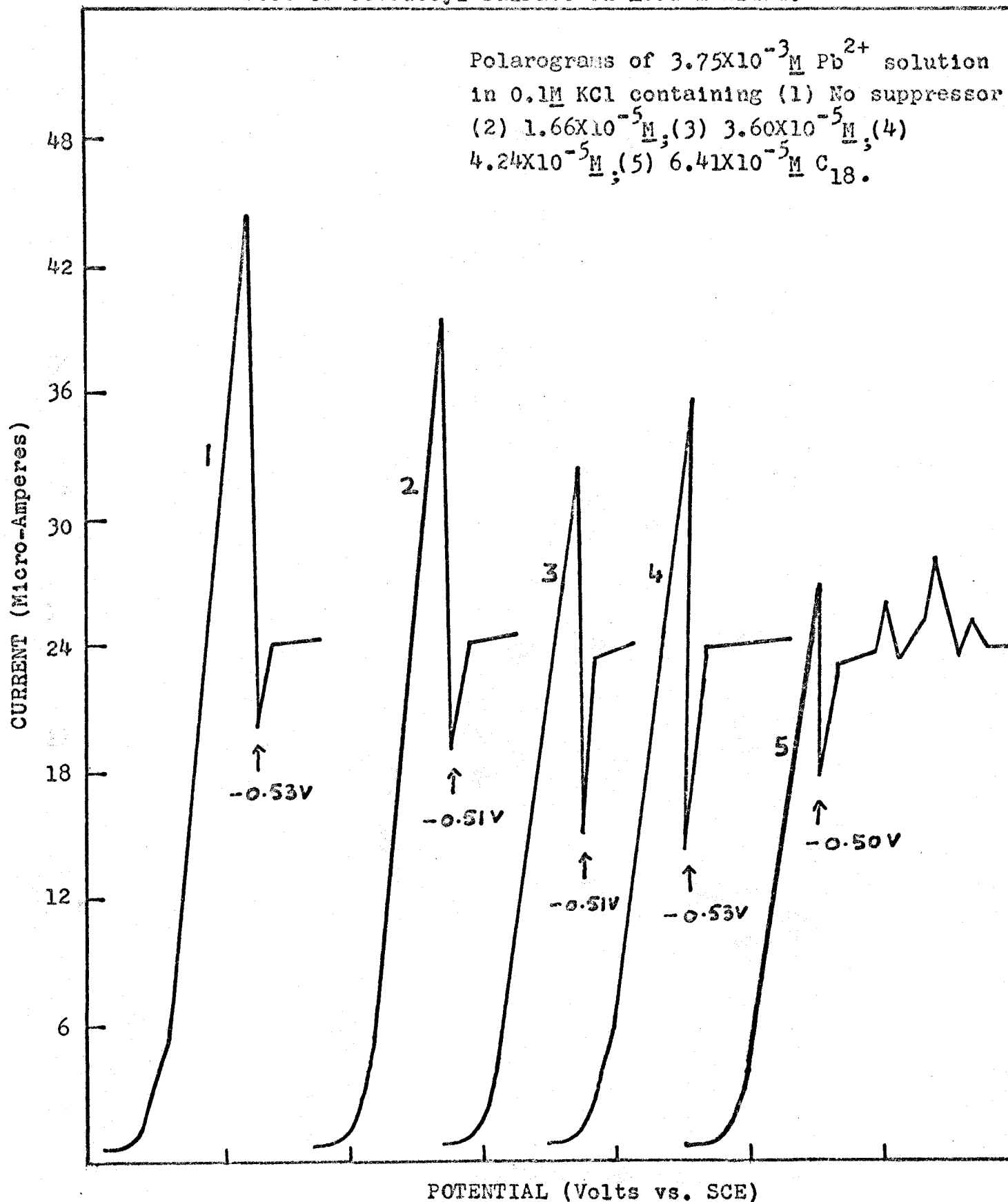
As shown in table 4, the MSP values of hexadecyl and octadecyl sulfates in case of potassium chloride solution were much higher than those obtained in case of sodium chloride solution. This is due to the turbidity or precipitate formation in case of potassium chloride. As a result of the precipitation, the effectiveness of the surfactants as maximum suppressors is reduced and thus one obtains very high MSP values for these surfactants.

The MSP values of other suppressors obtained in case of $0.01M$ KCl were considerably lower than those obtained in the case of $0.01M$ NaCl. Probably, these difference are due to different concentrations of oxygen in the two supporting electrolytes.

LEAD MAXIMUM:

A $3.75 \times 10^{-3} \text{ M Pb}^{2+}$ solution in 0.1 M KCl was employed to obtain the positive (break-off potential = $-0.52 \pm 0.01 \text{ v. vs. SCE}$) lead maximum. The maximum was easily suppressed on adding sodium octyl, decyl, dodecyl and tetradecyl sulfates. The MSP values obtained are shown in table 4. Contrary to expectations, the MSP value in the case of tetradecyl sulfate came out to be slightly higher than that of decyl sulfate. One reason for the higher MSP value of tetradecyl sulfate can be the slight turbidity which resulted on adding this surfactant to the solution containing lead ions in potassium chloride (supporting electrolyte). The turbidity, which probably was due to the formation of insoluble potassium or lead salt of the soap caused an erratic drop-time behavior. This led to distortion in the limiting current region of the current-voltage plot. Due to the erratic drop-time behavior, the limiting current rose sharply and sometimes it exceeded even the height of the maximum. The turbidity also resulted in case of hexadecyl and octadecyl sulfates; the distortions in case of octadecyl sulfate are depicted in figure 21. Due to greater distortions in case of hexadecyl and octadecyl sulfates, the maximum suppression points in these two cases could not be located precisely. In case of sodium hexadecyl sulfate, the MSP was estimated to be $3.45 \times 10^{-5} \text{ M}$ and in the case of octadecyl sulfate, due to the weak adsorbability

Effect of octadecyl sulfate on Lead maximum.

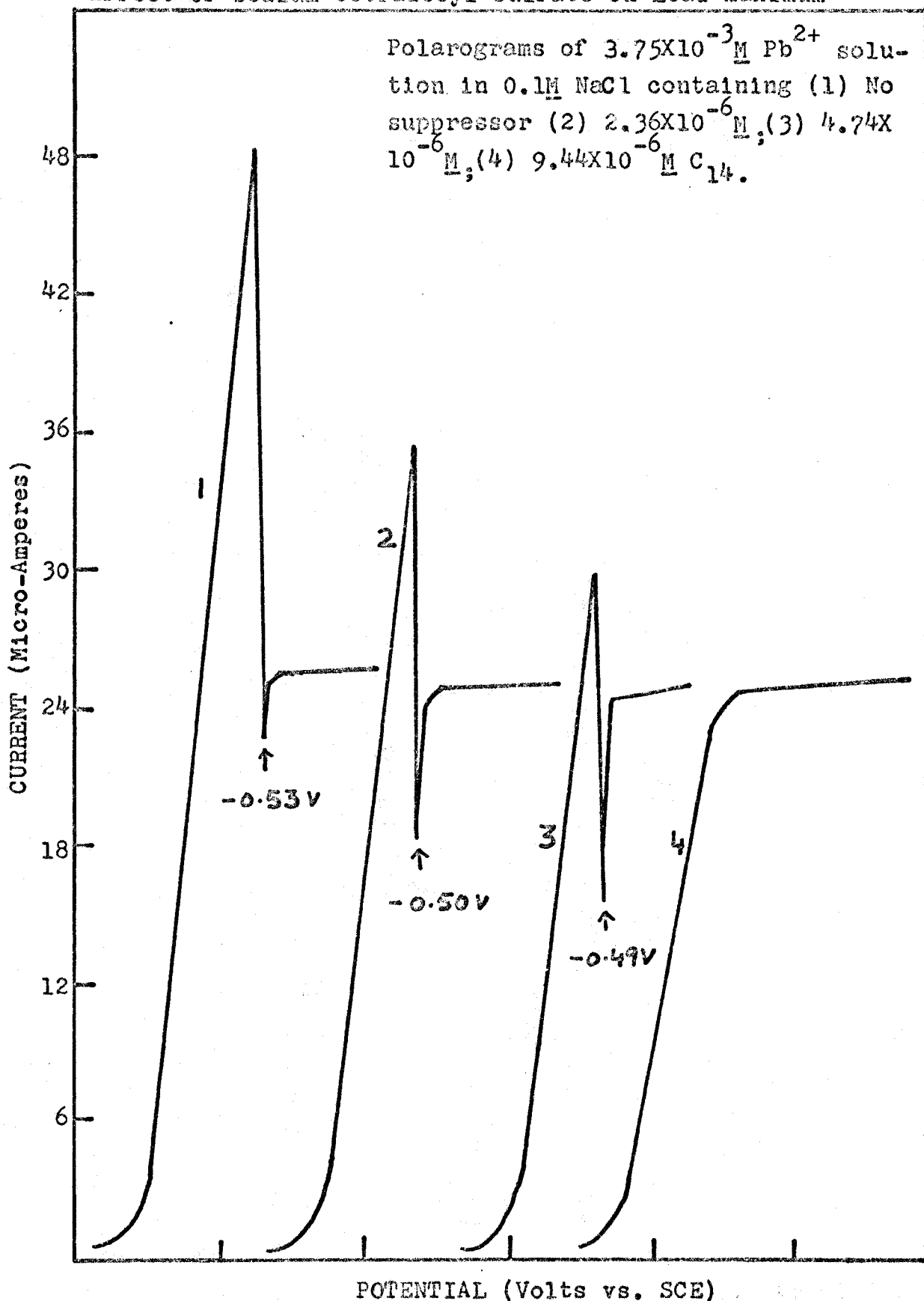


Each curve starts at -0.30 v .

of the surfactant, the maximum could not be eliminated completely even with the suppressor concentration of $6.41 \times 10^{-5} \text{M}$. Due to heavy distortions in the limiting current plateau, it was impossible to obtain even an approximate MSP value.

In order to avoid the effects of turbidity, MSP determination in case of lead maximum was also carried out using 0.1M solutions of NaCl and LiCl as supporting electrolytes. The MSP values obtained for sodium octyl, decyl, dodecyl and tetradecyl sulfates were almost the same as those obtained when KCl was used as supporting electrolyte. As expected, no turbidity resulted on the addition of sodium tetradecyl sulfate and thus no distortions in the C-V plot were observed (fig. 22). However, in case of hexadecyl and octadecyl sulfates, slight turbidity was observed and this led to slight distortion. Since the amount of distortion was not much, MSP values could be easily obtained. Whereas the MSP values for hexadecyl sulfate were the same in all three supporting electrolytes, octadecyl sulfate yielded different MSP values. The higher MSP values obtained in case of hexadecyl and octadecyl sulfates clearly show that these two are weak maximum suppressors. Besides, their MSP values tend to approach their experimentally determined CMC values in presence of sodium chloride (see table 1). Thus it can be said that before the maximum is completely suppressed, i.e., MSP value is reached, the CMC of C_{16} and C_{18} is reached and this causes the micelle

Effect of sodium tetradecyl sulfate on Lead maximum



Each curve starts at -0.30 volt.

formation, which we see in the form of "streamy" precipitate or white turbidity. The rest of the suppressors are strongly adsorbed and their MSP and CMC values are much different from each other.

The large difference between the MSP values of sodium alkyl sulfates and their CMC values clearly suggests that the suppression of the polarographic maximum concerns not only the change in the interfacial tension due to the presence of surface active substances but also the change in the structure of the electrical double layer.

Since the lead maximum occurs in the vicinity of electrocapillary zero, the resistance offered to the adsorption of the suppressors is very little, with the result that relatively small amounts of the surface-active agents are used to eliminate the maximum.

A common feature during the MSP determination was the shift of the break-off potential of the maximum to more positive potentials on addition of the surfactants to the depolarizer solution.

Finally, it was observed that the identity of the cations did not influence the shape of the maximum. In other words, by using LiCl, KCl or NaCl, no change in the shape of the curves or in the height of the maximum was noticed.

UO₂²⁺ MAXIMUM:

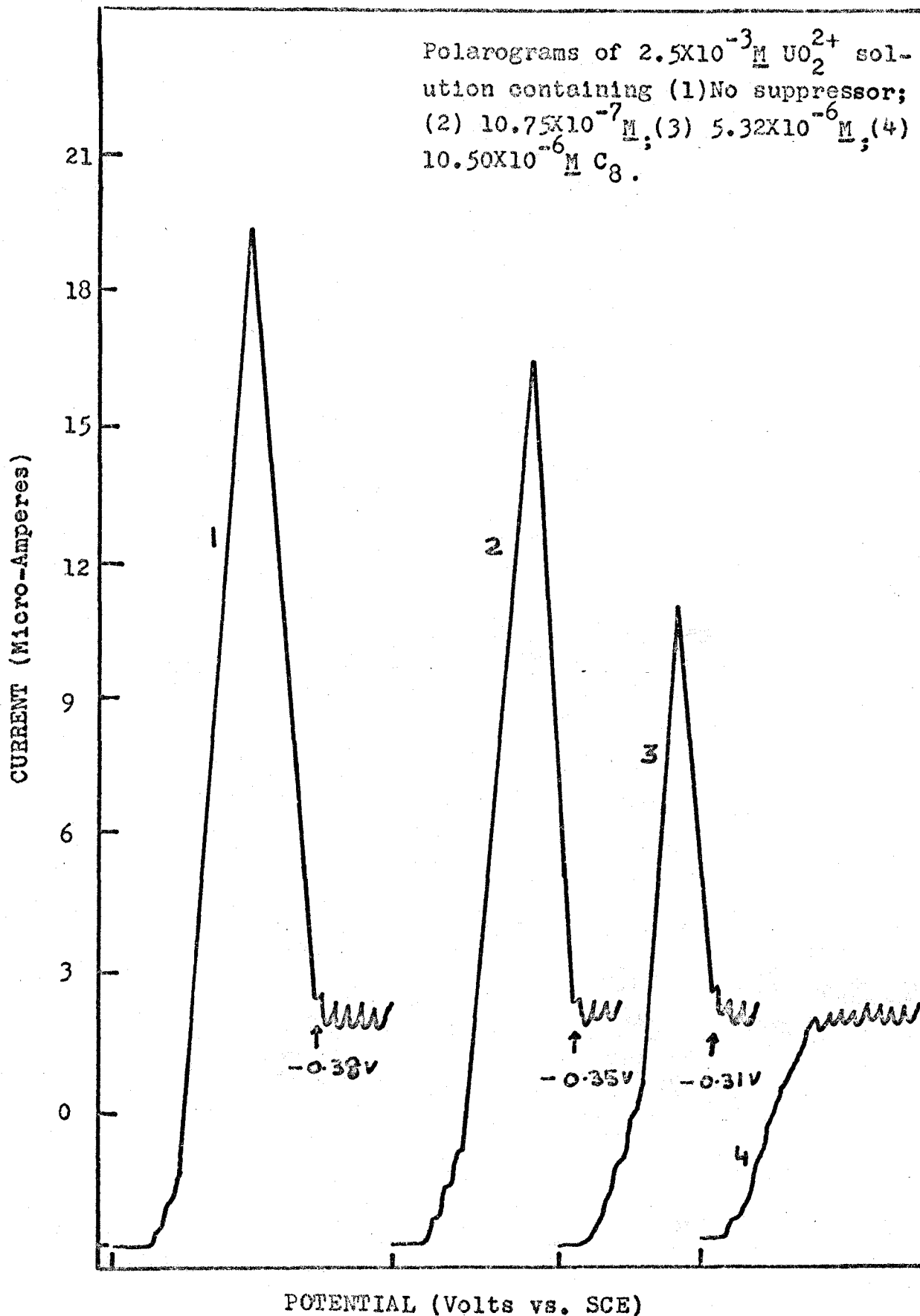
A $2.5 \times 10^{-3} \text{ M}$ solution of $(\text{UO}_2)(\text{NO}_3)_2 \cdot 6\text{H}_2\text{O}$ in 0.1 M HCl (supporting electrolyte) yields a large and sharp breaking (break-off potential = $-0.36 \pm 0.01 \text{ v. vs. SCE}$) maximum. Since the break-off potential in this case is more positive than that of the lead maximum, the MSP values for sodium alkyl sulfates in this case did come out much lower (table 4) than the corresponding values in case of the lead maximum. Except in the case of C_{18} , the maximum was suppressed very easily and completely by using small amounts of 0.01% suppressor solutions. The lower MSP values (as compared to those of lead maximum) clearly show that the anionic surfactants are adsorbed very strongly and efficiently at positive potentials. And due to adsorption of surfactants, the interfacial viscosity is enhanced and this hinders the passage of the electro-reducible ions, decreases the current, and thus contributes partially towards the elimination of the maximum.

As was observed during the suppression of lead maximum, the break-off potential in case of UO_2^{2+} maximum also shifted to more positive potentials on increasing the concentration of the suppressors. (fig. 23)

NICKEL MAXIMUM:

A $5 \times 10^{-3} \text{ M}$ Ni^{2+} solution in 0.1 M KCl yielded a negative

FIGURE 23

Effect of sodium octyl sulfate on UO_2^{2+} maximum

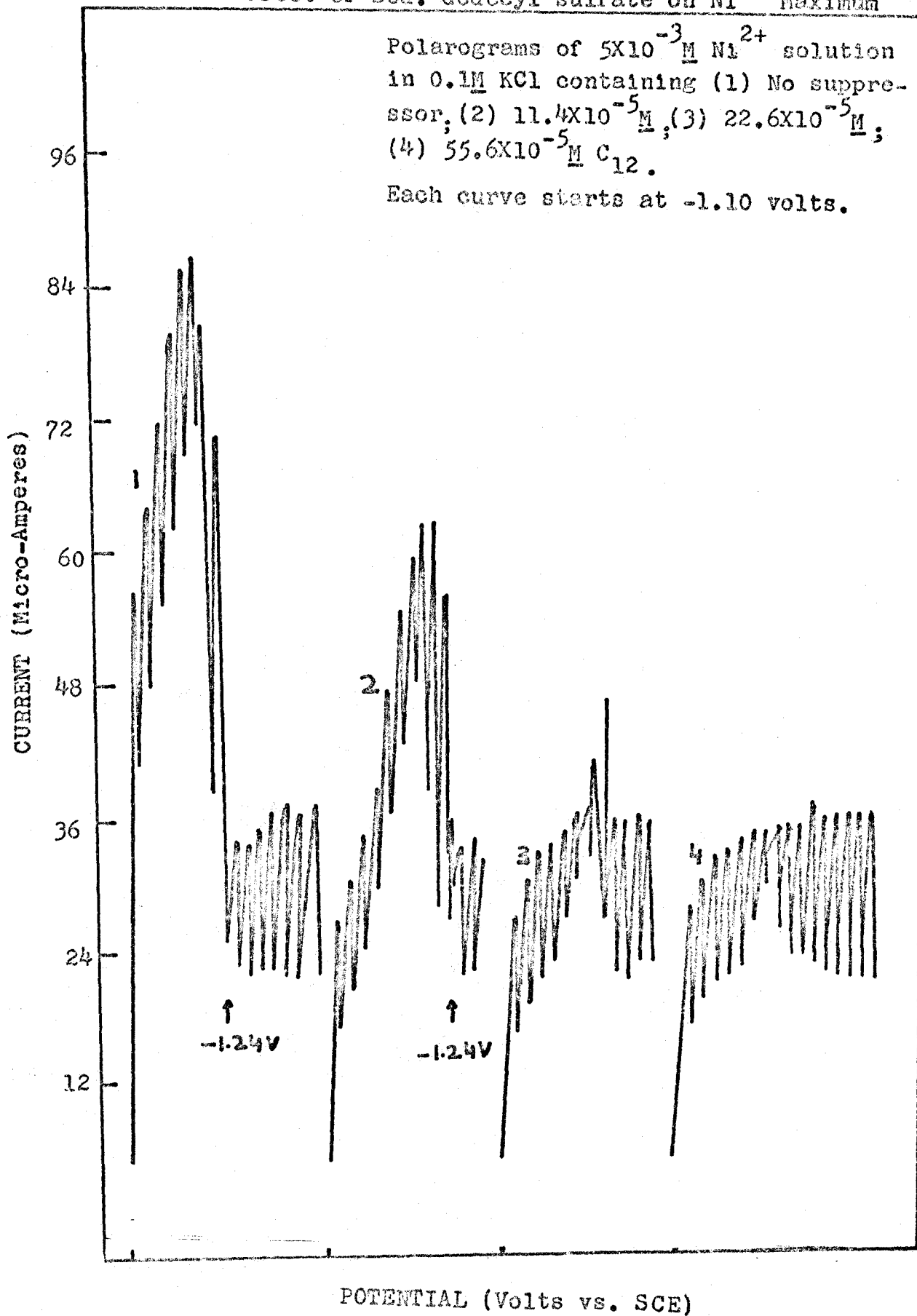
Each curve starts at -0.10 volt.

(break-off potential = -1.23 ± 0.03 v. vs. SCE) maximum (fig. 24). Unlike the positive maxima of O_2 , UO_2^{2+} , and Pb^{2+} ions, the nickel maximum was very hard to suppress. This is easy to explain because the charge on the mercury surface and the suppressors have the same (negative) sign. Even though 1% solutions of the suppressors were utilized, it was hard (except in the case of dodecyl sulfate) to suppress the maximum completely. As a result, the MSP values were obtained by extrapolation (1). Accordingly, the MSP values for various suppressors in table 4 are marked with an asterisk. (The MSP values for O_2 , UO_2^{2+} , and Pb^{2+} maxima are observed values and represent the minimum concentration of surfactants at which the maximum is completely suppressed---as observed from the current-voltage plot).

On comparing the MSP values in table 4 it can easily be seen that the values in case of the nickel maximum are greater than the values in case of the lead and oxygen maxima by an order of approximately 10^3 . This observation is in agreement with the MSP value for the nickel maximum reported by Tamamushi and Yamanaka (4). For dodecyl sulfate, they reported a MSP value of $1.1 \times 10^{-3} \text{ M}$ at 25°C . This compares well with our observed value of $0.944 \times 10^{-3} \text{ M}$ at 27°C and extrapolated value of $1.32 \times 10^{-3} \text{ M}$ at 25°C .

According to Tamamushi and Yamanaka, the higher MSP value of dodecyl sulfate is due to the fact that at large

FIGURE 24

Effect of Sod. dodecyl sulfate on Ni^{2+} Maximum

negative potentials, i.e; in the vicinity of the maximum, the suppressor is no longer adsorbed, but is desorbed. Alternatively, it can be said that the amount of the soap solutions required to suppress maximum of the same sign is greater than one possessing unlike charge. This is so because adsorption of the suppressor on the mercury drop is likely to be hindered due to similarity of charges.

Se(IV) MAXIMUM:

Selenious acid yields an acute negative maximum, which is reproducible (23). Lingane & Niedrach (24) investigated the polarographic characteristics of +4 oxidation state of selenium over a wide range of pH. They had carried out their studies in the presence of citrate, phosphate & borate-carbonate buffers, which served as supporting electrolytes.

In order to study further the effects of anionic surfactants on a negative maximum, MSP determinations were carried out by employing a $4 \times 10^{-3} \text{ M}$ solution of selenium dioxide in 0.3 M acetate buffer of pH 5. The resulting maximum had a break-off potential of $-0.93 \pm 0.01 \text{ v}$ (vs. SCE). Unlike the negative maximum due to nickel, the maximum due to Se(IV) could be suppressed completely. (See MSP values in table 5). Since the break-off potential of Se(IV) maximum is more positive than that of the nickel maximum, the MSP values in

TABLE 5

MAXIMUM SUPPRESSION POINTS OF SODIUM ALKYL SULFATES IN PRESENCE OF DIFFERENT IONS

ions	B. off pot. (volts)	Temp. ^o C	MSP X 10 ⁺⁶ <u>M</u>					
			C ₈	C ₁₀	C ₁₂	C ₁₄	C ₁₆	C ₁₈
1) Tl ⁺	-0.73	25-26	456*	19.12	11.2	1)18.85 11)14.17	570	-
		24	371					
2) Se (IV)	-0.93±0.01	23-24	101	21.0	6.92	18.8	~65.4	~140.5
			MSP X 10 ⁺³ <u>M</u>					
3) CaI ₄ ²⁻	-0.79±0.01	25-26	11.7*	1.33*	0.104*	4.79*	17.35*	-

*Extrapolated values.

the present case came out to be less than those for the nickel maximum.

The addition of hexadecyl and octadecyl sulfates resulted in white turbidity. In case of hexadecyl sulfate, the slight turbidity did not cause much distortion but in case of octadecyl sulfate, the distortion was too much and as a result the MSP value was hard to determine. Thus, the MSP values for these two suppressors are approximate.

A plausible mechanism for the removal of the maximum based on the considerations of the profile of the double layer can be easily given: The area or zone adjacent to the mercury drop is called the Helmholtz zone and consists of unsolvated ions which may be specifically adsorbed there. A little further from it exists a layer of solvated cations and anions. In other words, the Helmholtz layer is a duplex structure consisting of unsolvated ions and solvated ions. At the locus of the centers of the solvated ions, there is a diffuse layer called the Gouy or outer Helmholtz plane. On addition of surface-active substances the configuration of the double layer is altered. Unlike the nonionic surfactants like gelatin and Triton X-100, the long-chains of the anionic sodium alkyl sulfates bearing the polar head groups cannot penetrate deep into the Helmholtz zone. This is partly due to the orientation of the negative water-seeking

head groups and partly due to the repelling action of the negative mercury surface on these groups. However, because of the electrostatic attraction between solvated ions and the negative polar heads, some penetration is possible. In such a case the ions of the depolarizer do get a passage through the pores of the surfactant and the normal conditions of concentration polarization are achieved and these thus eliminate the maximum.

CdI_4^{2-} MAXIMUM:

Malik and Chand (25) reported that a $2.5 \times 10^{-3} \text{ M CdI}_2$ solution in 0.1 M KI gave a maximum at about -0.70 volts (vs. SCE). They employed LDC (Lauric Acid-Diethanolamine Condensate), a non-ionic soap to suppress the maximum. Since the potential at which this maximum occurs is less negative than that at which the nickel and Se(IV) maxima appear, it was decided to investigate the effect of sodium alkyl sulfates on this presumably "less negative" maximum. The MSP determination was carried out by the usual procedure and the values obtained by extrapolation procedure are listed in table 5.

On comparing the MSP values obtained in case of CdI_4^{2-} maximum with those obtained for Ni^{2+} maximum, it is found that values for decyl and dodecyl sulfates in the present

case are, as expected, lower than their corresponding values for the Ni^{2+} maximum. The extrapolated MSP values for C_8 , C_{14} and C_{16} in the case of CdI_4^{2-} maximum came out higher than the values obtained for nickel maximum. The maximum could not be suppressed at all by sodium octadecyl sulfate. Even for the suppressors for which the MSP values are listed in the table 5, large volumes of the suppressors were needed to cause suppression. Our high experimental MSP values confirm the observation made by Kolthoff and Lingane (26) who reported that iodide-cadmium complex gave a pronounced maximum which was difficult to suppress. Likewise, Malik and Chand (25) reported that large amounts of anionic soaps (sulfonated phenyl, tolyl and xylyl stearic acids) were needed to eliminate the maximum. One reason for the higher MSP values in the case of CdI_4^{2-} maximum as compared to nickel maximum is the fact that the cadmium iodide is a large ion, whereas the nickel ion is very small. And since the MSP values of the surfactants obtained in the present case are close to their CMC values, we can also say that the readiness with which the ionic micelles are formed should play an important role in the suppression of the maximum. The formation of micelles takes place at a certain critical concentration of the soap solution, which in turn is highly influenced by (a) the presence of complex ions (like CdI_4^{2-}) in the solution, (b) possible interaction between the

metal ions and the soap (which leads to turbidity formation in some cases), and (c) on the extent to which the suppressor undergoes ionization.

THALLIUM (or Tl^+) MAXIMUM:

Monovalent thallium ions produce a large and sharp-breaking (break-off potential = $-0.73v.$ vs. SCE) maximum (27) in presence of potassium nitrate as the supporting electrolyte. Sodium decyl, dodecyl and tetradecyl sulfates all of which appear to be fairly strong maximum suppressors eliminated the Tl^+ maximum easily. (See table 5 for MSP values). However in the case of sodium octyl and hexadecyl sulfates, the maximum was hard to suppress. And since addition of sodium octadecyl resulted in turbidity and consequent distortions in the C-V plot, the MSP could not be determined in this case.

Since the break-off potential of the thallium maximum is more negative than that of the lead maximum, the MSP values in the present case came out somewhat higher. This is in line with the arguments presented earlier that due to the anionic nature of sodium alkyl sulfates, the negative maxima are suppressed with difficulty.

VII. EFFECTS OF SODIUM ALKYL SULFATES ON POLAROGRAMS OF COMPLEXES

The M.S.P. data (table 4,5) for sodium alkyl sulfates in case of O_2 , Pb^{2+} and UO_2^{2+} maxima clearly proves that these anionic soaps are very effective for the suppression of positive maxima and are not so efficient for suppressing the negative maxima. In fact, the high M.S.P. values obtained in case of nickel and CdI_4^{2-} maxima indicate that these surfactants cause an inhibiting or distorting effect 1) when the depolarizer has the same charge as the adsorbed layer of the surfactant 2) when the polarographic wave is due to a large complex ion, which penetrates the pores of the adsorbed layer with difficulty.

In order to investigate the distorting effects of sodium alkyl sulfates in detail, work was carried out on the d.c. polarographic waves of the following charged & uncharged complexes: (i) Triethylenetetramine-copper(II) complex ion or $[Cu(Trien)]^{2+}$; (ii) Tetraethylenepentamine-copper(II) complex ion or $[Cu(Tetren)]^{2+}$; (iii) Ethylenediaminetetraacetato-copper(II) complex ion or $[Cu(EDTA)]^{2-}$; (iv) (Tartrato)-copper(II) or $[Cu(Tart)]^0$ complex.

A literature survey showed that similar investigations were carried out on the non-ionic surfactant, Triton X-100 by Meites and Meites (47) and Schmid & Reilley (21). Jacobsen & Kalland (30) did work on sodium dodecyl sulfate

and studied its effects using C-V plots. In the present work, effects of dodecyl sulfate and other homologs have been studied both by current-voltage and current-time plots. The current-time curves are discussed in the next chapter. The results based on C-V plots are presented below. (See discussion on page 99).

RESULTS

EFFECT ON POSITIVELY CHARGED COMPLEXES:

Cu(II) when combined with triethylenetetramine (trien) and tetraethylenepentamine (tetren) forms $[\text{Cu}(\text{trien})]^{2+}$ and $[\text{Cu}(\text{tetren})]^{2+}$ respectively. Both these complexes are reported to be reversibly reduced (48) at the DME. Following the procedure of Jonassen et. al (48), technical grade samples of triethylenetetramine and tetraethylenepentamine were purified by converting them into respective chlorides. The white solid chlorides thus obtained were used to make 10^{-2} M Trien and Tetren solutions. These were mixed with solutions containing Cu^{2+} ions to obtain the complexes.

$[\text{Cu}(\text{tetren})]^{2+}$ COMPLEX:

This positively charged complex is reversibly reduced and the wave has a half-wave potential = -0.17v (vs. SCE). The solution used to run the polarogram had the composition:

$1 \times 10^{-3} \text{ M Cu}^{2+}$, $0.8 \times 10^{-2} \text{ M Tetren}$ in 0.16 M acetate buffer of $\text{pH} = 4.50$. The limiting current resulting from the above solution in the absence of any surfactant has a value of 4.74 ua at -0.60 v (fig. 25). Although not reported by Jonassen et. al (48), the reduction wave of $[\text{Cu}(\text{tetren})]^{2+}$ complex is sometimes accompanied by a slight maximum, which can be easily suppressed by adding small amounts of surfactants. The effects observed with various members of the homologous series are described below:

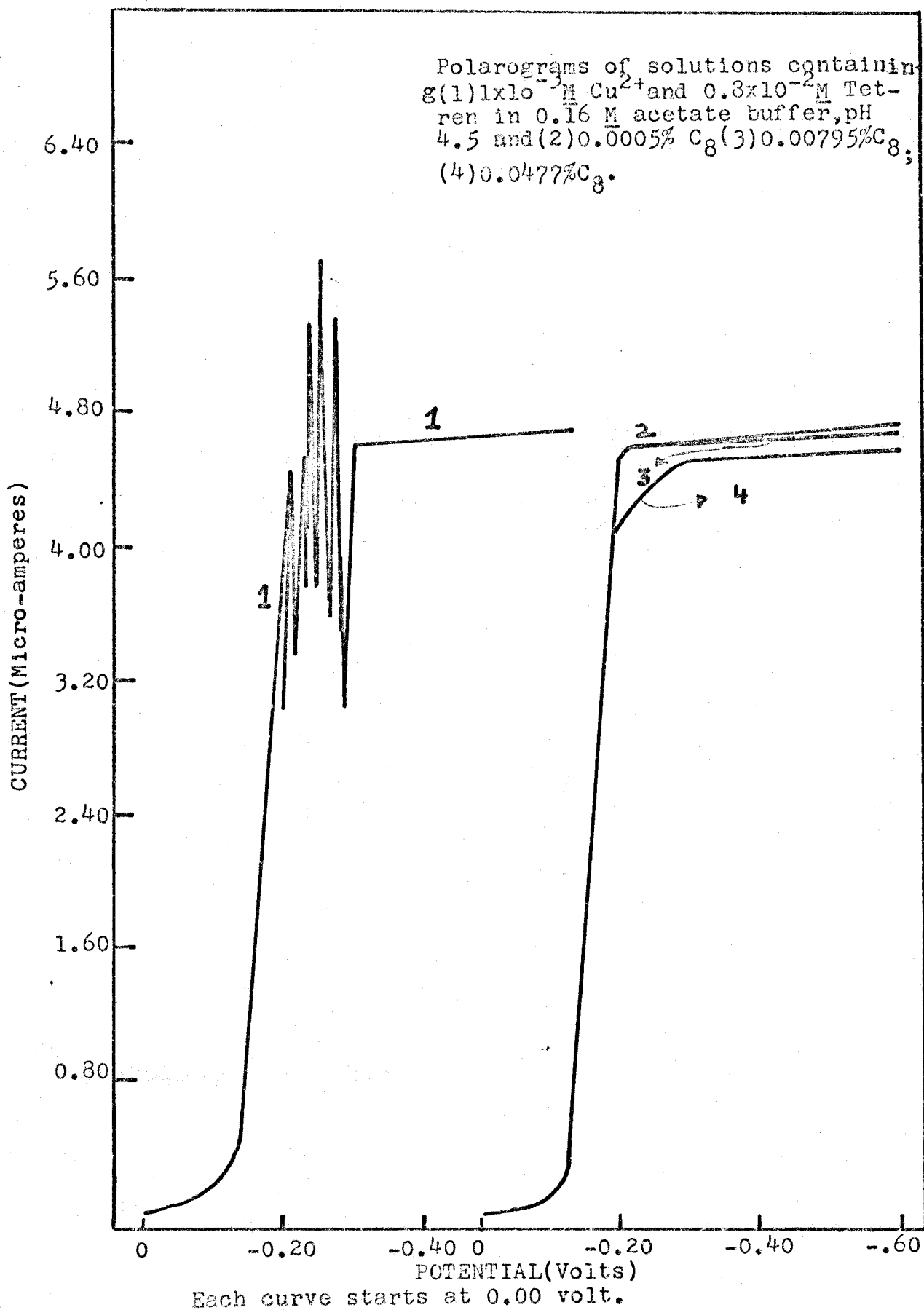
C₈:

The slight maximum obtained was easily suppressed in the presence of 0.0005% sodium octyl sulfate. As the concentration approached 0.00795% , a slight turbidity was noticed in the solution. However, on stirring the solution by bubbling N_2 gas, the turbidity disappeared & the addition of sodium octyl sulfate had practically no influence on the polarogram. When the concentration of the surfactant was raised to 0.0477% , the upper part of the wave was slightly drawn out (fig. 25), indicating that the reaction becomes irreversible at this concentration. The half-wave potential was not affected by the addition of sodium octyl sulfate.

C₁₀:

Here too, the addition of surfactant did not produce

FIGURE 25

Effect of Sod. Octyl Sulfate on $\text{Cu}(\text{tetren})^{2+}$ reduction wave.

any significant change in half-wave potential of the limiting current. Turbidity occurred when the C_{10} concentration was approximately 0.01%.

C_{12} :

On adding 0.0047% sodium dodecyl sulfate, a slight turbidity resulted, but on stirring the solution it disappeared. Again, the presence of the surfactant did not influence the polarogram, except of course, the wave did look slightly drawn out.

C_{14} :

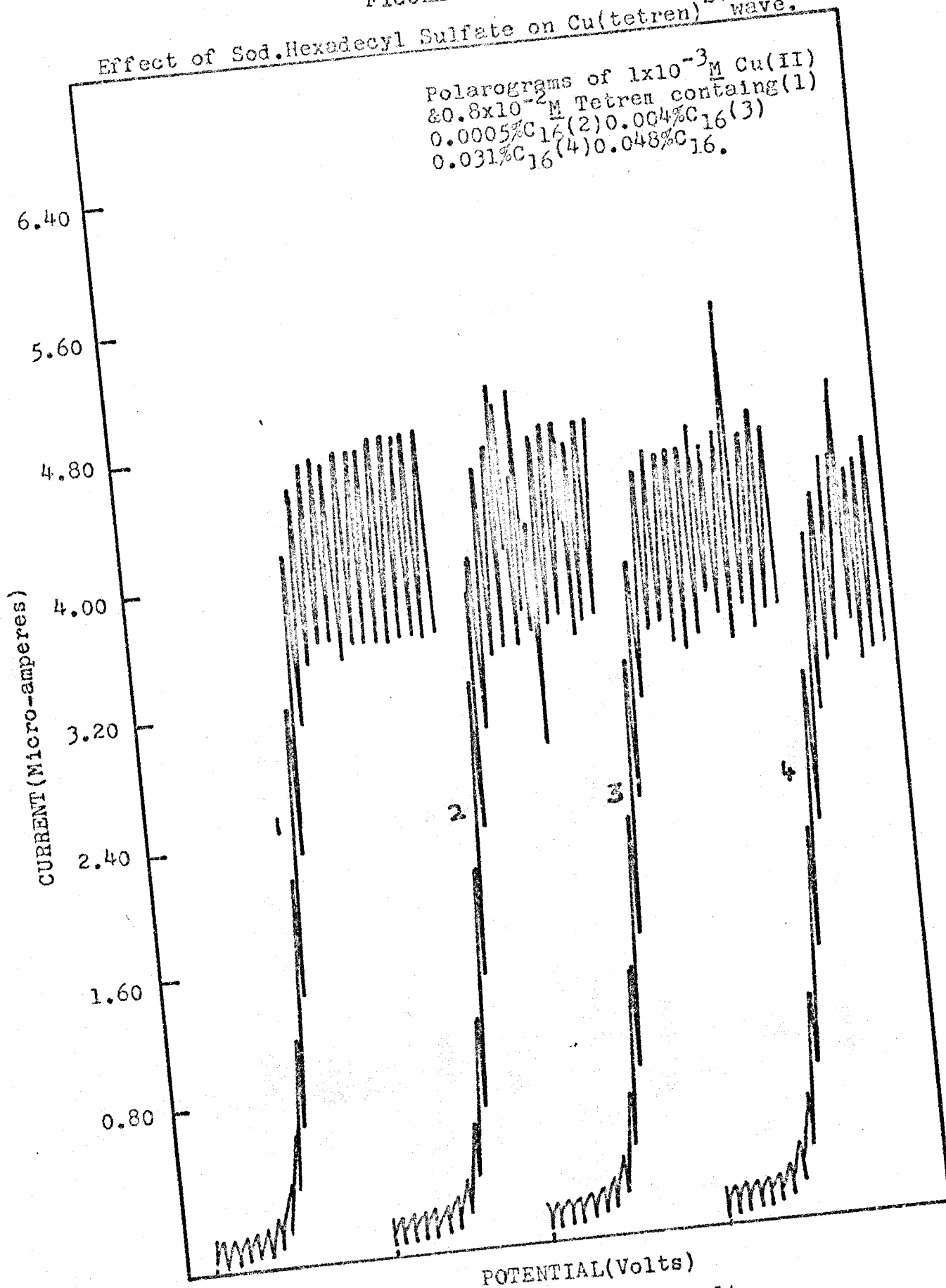
The addition of 0.000696% surfactant produced some cloudiness, but this did not cause any distortion in the region of limiting current plateau. In fact, even upto a suppressor concentration of 0.0477%, the shape of the wave was unaffected.

C_{16} :

The slight maximum in the absence of the suppressor was eliminated by adding 0.0005% sodium hexadecyl sulfate. Further additions of the surfactant caused turbidity and that resulted in distortions (fig. 26). When the suppressor concentration was 0.002%, thick clumps of white precipitate could be seen floating in the solution. However, in spite of the distortions in the C-V plot, the $E_{\frac{1}{2}}$ did not change

FIGURE 26

Effect of Sod. Hexadecyl Sulfate on $\text{Cu}(\text{tetren})^{2+}$ wave.



Each curve starts at 0.00 volt.

Reproduced with permission of the copyright owner. Further reproduction prohibited without permission.

even when the concentration of the suppressor was increased to 0.0477%.

C₁₈:

In this case the maximum on the reduction wave could not be suppressed and like sodium hexadecyl sulfate, addition of octadecyl sulfate produced thick white precipitate and distortion on the limiting current plateau. However, here too, the half-wave potential did not seem to be affected.

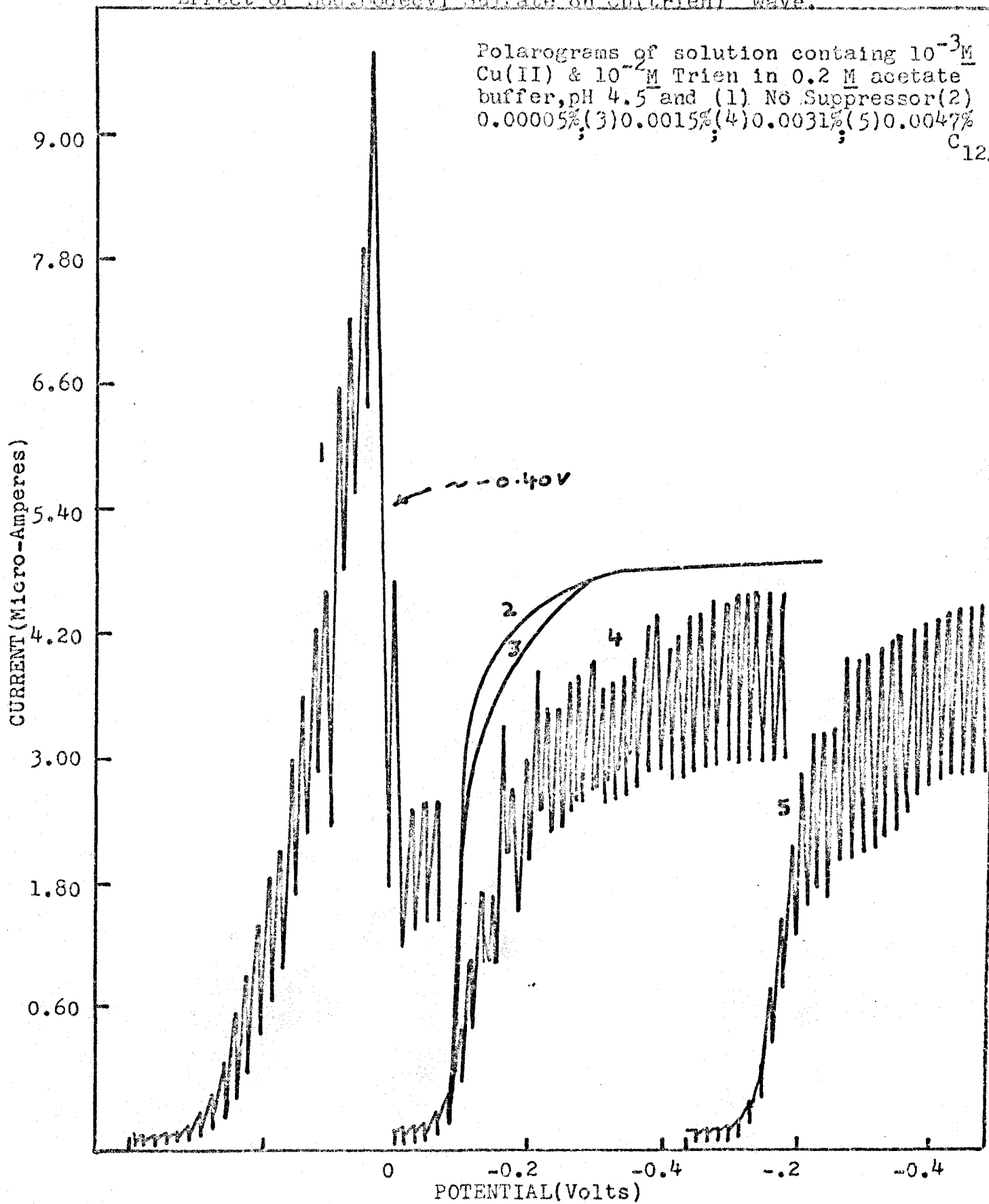
[Cu(trien)]²⁺ COMPLEX:

When a solution containing 10^{-3}M Cu^{2+} and 10^{-2}M Trien in 0.2M acetate buffer of pH 4.5 was employed to obtain a polarogram, the resulting wave was accompanied by a maximum, which had a break-off potential of about -0.40v (fig. 27). Jacobsen & Kalland (30), who studied the effect of sodium dodecyl sulfate on $[\text{Cu}(\text{trien})]^{2+}$ at pH 4.6 did not report the appearance of any maximum. The following effects were noted in the presence of different sodium alkyl sulfates.

C₈:

The maximum, as reported above was eliminated easily by adding 0.00025% surfactant. The addition of sodium octyl sulfate did not change the half-wave potential and also produced no turbidity [unlike in the case of $\text{Cu}(\text{tetr-en})^{2+}$ complex]. In the presence of 0.0477% C₈, the upper

FIGURE 27

Effect of Sod. Dodecyl Sulfate on $\text{Cu}(\text{trien})^{2+}$ wave.

part of the wave began to be drawn out.

C₁₀:

The maximum was suppressed on adding 0.00031% C₁₀. After this, addition of this surfactant up to a concentration of 0.00477% did not influence the polarogram much. No turbidity was noticed.

C₁₂:

The maximum was suppressed on adding 0.00005% sodium dodecyl sulfate. After this, further additions of the surfactant up to a concentration of 0.0015% did not produce any change in the shape of the curve. At this stage, the wave was slightly drawn out (fig. 27). When the concentration of suppressor was raised to 0.0031%, the first signs of white turbidity were noticed and this resulted in erratic droptimes between the potential range -0.10 and -0.40v. (curve 4 of fig. 27). Jacobsen and Kalland (30) did not report any turbidity formation in acidic solutions. Also, they reported the 'drawn-out' behavior of the wave when the surfactant concentration was 0.01%. (vs. 0.0015% as indicated above by the author). As shown in the fig. 27, in the presence of 0.00477% C₁₂, the wave was heavily drawn out.

C₁₄:

The addition of tetradecyl sulfate to the purple-colored $[\text{Cu}(\text{trien})]^{2+}$ solution did produce turbidity, but did not cause any distortions in the C-V plot. Even in the presence of 0.00477% C₁₄, the half-wave potential was unaffected.

C₁₆:

As in the case of $[\text{Cu}(\text{tetren})]^{2+}$ complex, the addition of hexadecyl sulfate to $[\text{Cu}(\text{trien})]^{2+}$ solution produced a heavy amount of white precipitate, and as a result of this, a slight distortion of the wave in the limiting current region was caused. The distortion disappeared at potentials greater than -1.0v. Due to distortion between 0 and -1.0v, the half-wave potential could not be determined precisely. However, it did not seem to be changed even up to a suppressor concentration of 0.0244%.

C₁₈:

The maximum on the reduction wave of Cu-trien complex could not be eliminated. When the suppressor concentration was 0.002%, a thick white precipitate resulted and caused distortions in the C-V plot. However, in spite of the distortion in the limiting current region, the half-wave potential seemed to be unaffected by the addition of sodium octadecyl sulfate.

[Cu(EDTA)]²⁻ COMPLEX:

Schmid & Reilley (21) reported that current-voltage curve in case of Cu - EDTA complex is distorted in the presence of Triton X-100. Jacobsen and Kalland (30) reported a similar behavior in case of sodium dodecyl sulfate (SDS). According to them, when the concentration of dodecyl sulfate was increased above 0.003%, the Cu - EDTA wave in acetate buffer of pH 4.5 was split into two parts and in the presence of 0.005% SDS, only a penetration wave ($E_{\frac{1}{2}} = -0.8v$) appeared on the polarogram. In order to explore the behavior of other homologs, polarograms were obtained by using a solution containing $2.26 \times 10^{-3} M$ $Cu(ClO_4)_2$ and $2 \times 10^{-2} M$ EDTA in $0.1 M$ acetate buffer of pH 4.5. The resulting C-V plot showed a sharp maximum (break-off potential = $-0.48v$). The maximum could be eliminated by adding 0.0002% SDS. In order to avoid the maximum, a tartrate buffer was tried. However, due to the low solubility (0.37 g/100 ml.) of potassium hydrogen tartrate (49) used for making the buffer solution, it was difficult to prevent its slow precipitation and thus even this buffer solution was found to be unsuitable. Finally, following the suggestion of Pecsok (50) it was decided to use EDTA itself as the supporting electrolyte. A solution containing

$1 \times 10^{-3} \text{M}$ $\text{CuSO}_4 \cdot 5\text{H}_2\text{O}$ in 0.25M EDTA was prepared and its pH was measured and was found to be 4.32. When a polarogram of this solution was taken, a reversible-looking wave with a half-wave potential of -0.32v . was obtained (curve fig. 28). On adding 0.1% solutions of the surfactants to this negatively-charged depolarizer solution, the following effects were observed:

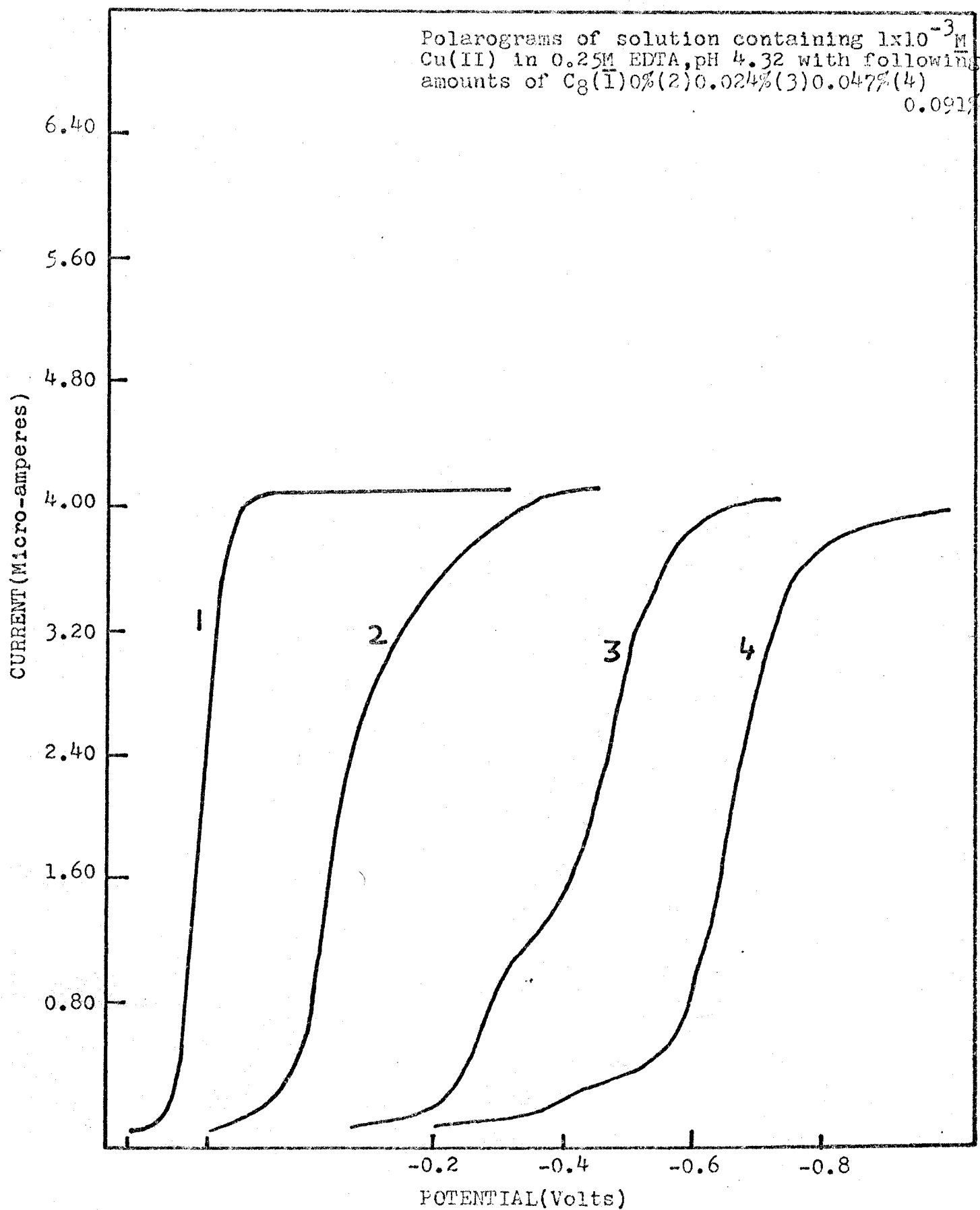
C_8 :

In this case, a 0.1% solution of the surfactant was found to be too dilute. Even on employing a 1% solution of sodium octyl sulfate, the penetration wave (30) with a half-wave potential of -0.66v did not result until a suppressor concentration of 0.091% was reached (fig. 28). This clearly shows that sodium octyl sulfate is not adsorbed on the mercury surface very strongly.

C_{10} :

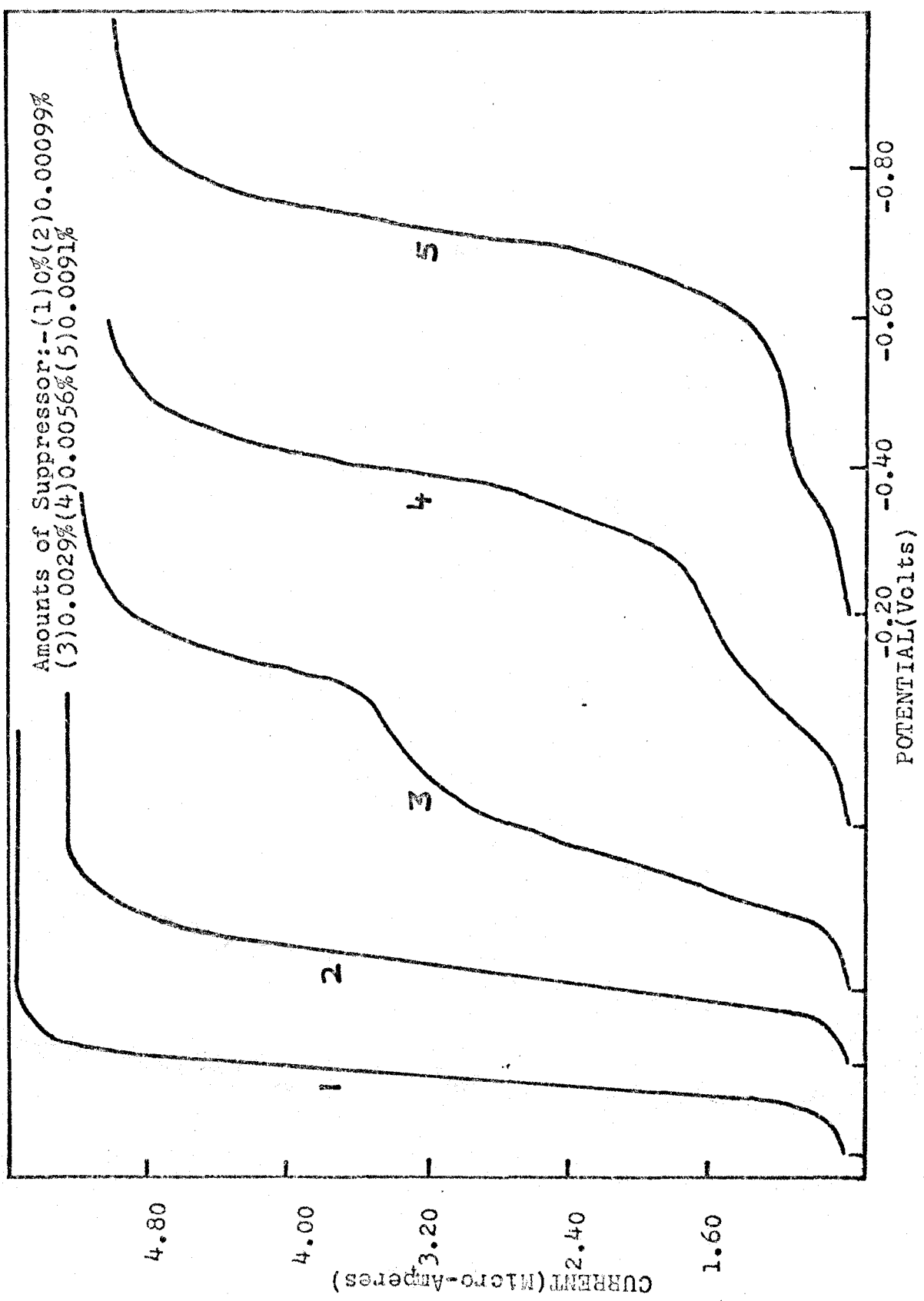
The original Cu-EDTA wave was split when the suppressor concentration was 0.0029% (fig. 29). As more surfactant was added, the half-wave potential was shifted to more negative potentials and in the presence of 0.0029% surfactant, a penetration wave with $E_{\frac{1}{2}} = -0.72 \text{v}$ appeared. This wave was fully developed in the presence of 0.0091% surfactant (curves 3 and 5 in fig. 29).

Effect of sod.octyl sulfate on Cu-EDTA wave.



Each curve starts at -0.20 volt.

FIGURE 29
Effect of Sod. Decyl Sulfate on Cu-EDTA wave.



Each curve starts at -0.20 volt.

C₁₂:

The Cu-EDTA reduction wave was split into two parts (fig.30) in the presence of 0.00196% surfactant (vs. a value of 0.003% SDS reported by Jacobsen and Kalland (30) for Cu-EDTA wave in acetate buffer). By increasing the dodecyl sulfate concentration to 0.0070%, it was possible to shift the half-wave potential to -0.90v (curve 5 in fig.30).

C₁₄, C₁₆, C₁₈:

The addition of tetradecyl, hexadecyl and octadecyl sulfates to Cu-EDTA solutions resulted in turbidity formation in each case and as a result of this the C-V plots in the region of limiting current plateau were greatly distorted (fig.31) and this prevented the exact measurement of half-wave potentials of the penetration waves.

The turbidity formation and the consequent distortion took place at the following approximate surfactant concentrations:

Sodium Tetradecyl Sulfate: 0.0029% ($\cong 9.20 \times 10^{-5} \underline{\underline{M}}$);

Sodium Hexadecyl Sulfate: 0.00196% ($\cong 5.71 \times 10^{-5} \underline{\underline{M}}$);

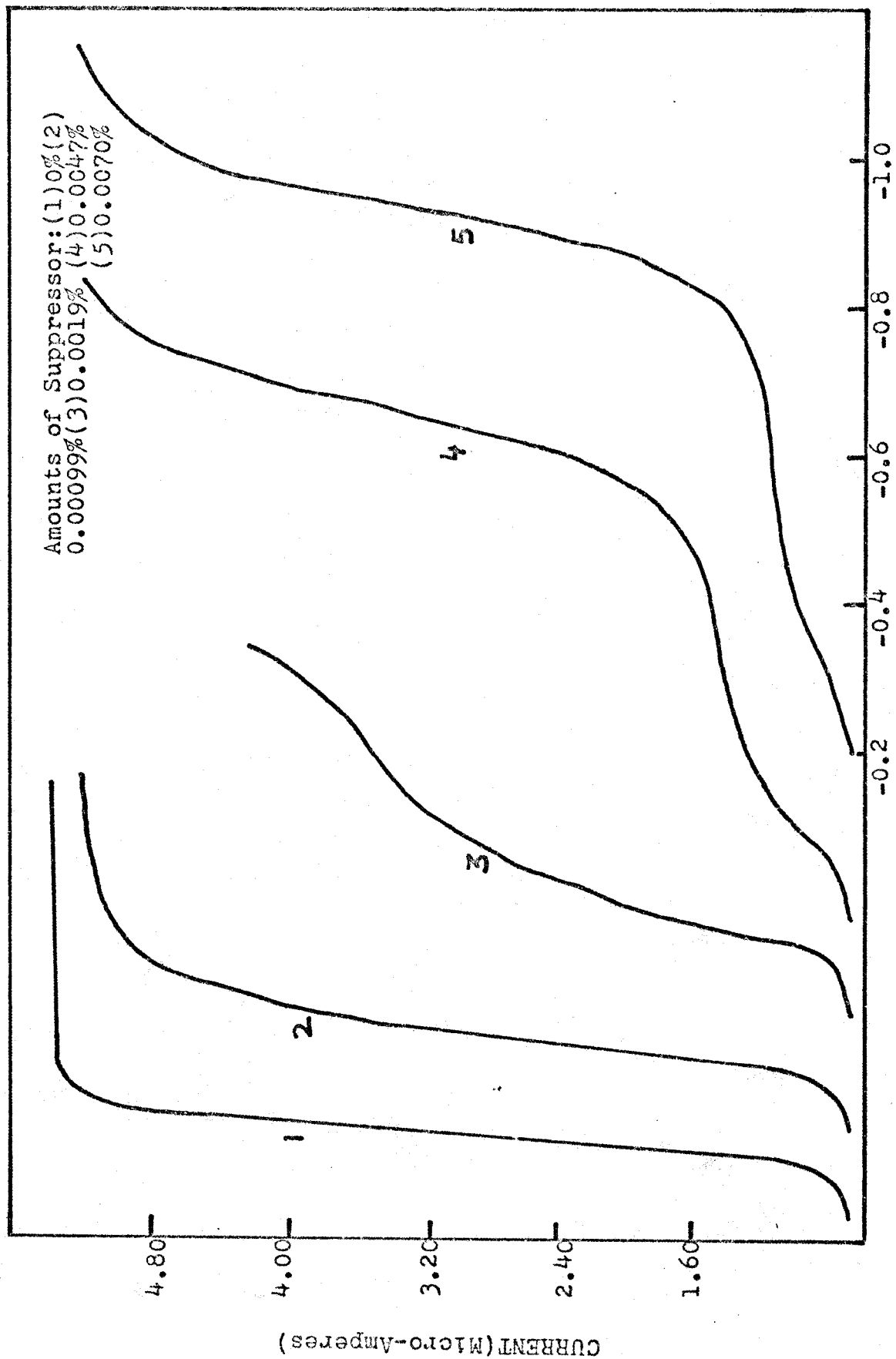
Sodium Octadecyl Sulfate: 0.00148% ($\cong 4.0 \times 10^{-5} \underline{\underline{M}}$).

[Cu(Tart)]⁰ COMPLEX:

Schmid and Reilley (21) described a neutral complex that is formed between Cu²⁺ ions and tartrate buffer at

FIGURE 30

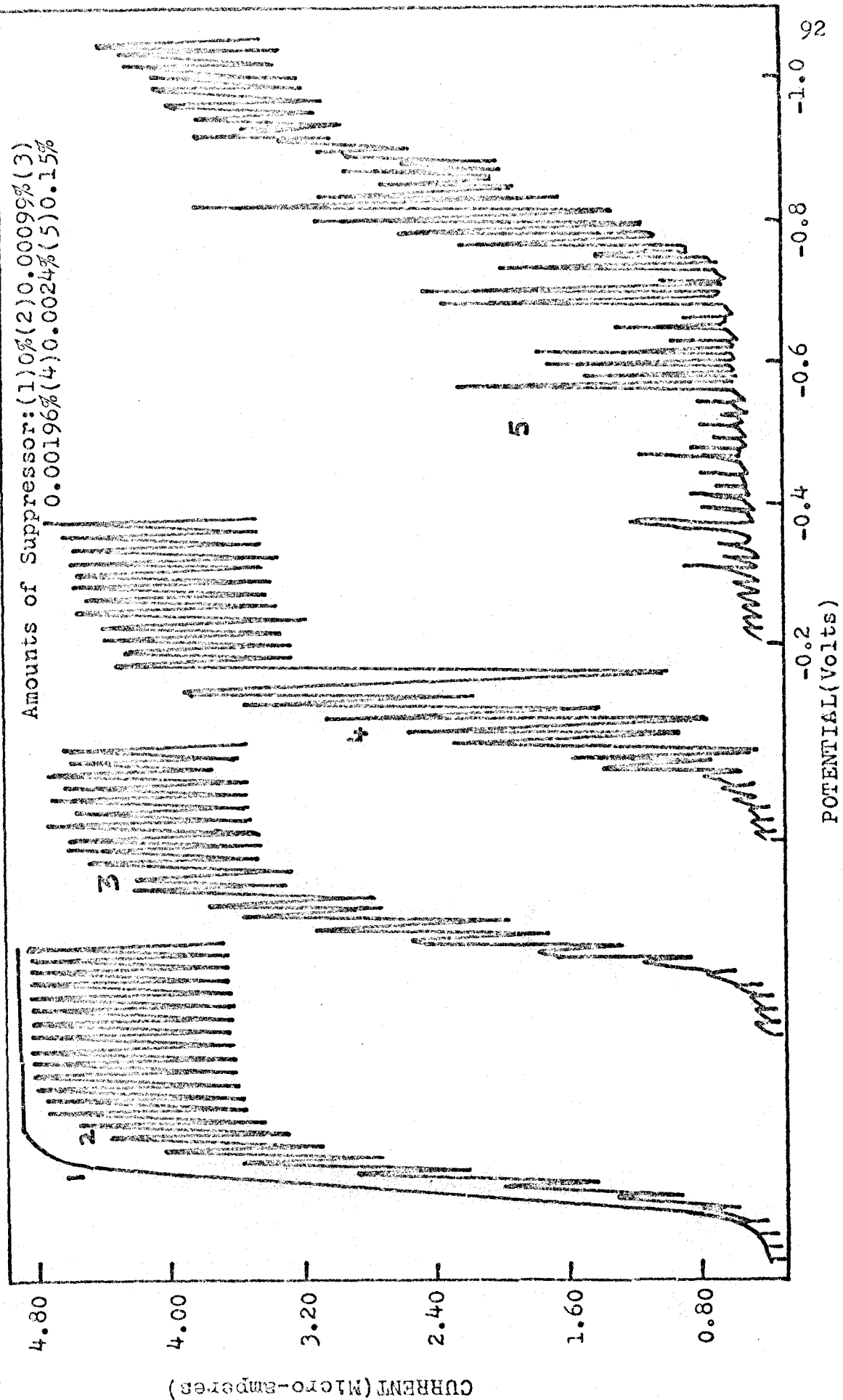
Effect of Sod. Dodecyl Sulfate on Cu-EDTA wave.



Each curve starts at -0.20 volt.

FIGURE 31

Effect of Sod. Tetradecyl Sulfate on Cu-EDTA wave.



pH 4. In order to study the effects of anionic surfactants on this uncharged complex, polarograms were obtained with the following solution: 10 ml. of $2 \times 10^{-3} \text{ M}$ $\text{CuSO}_4 \cdot 5\text{H}_2\text{O}$ + 10 ml. of 0.2 M tartrate buffer of pH 4. (0.0603 moles of disodium tartrate and 0.0396 moles of tartaric acid were mixed to obtain the buffer solution. These number of moles were theoretically calculated). Contrary to expectations, the resulting C-V plot showed a large, sharp-breaking maximum at -0.40v (fig.32). However, the maximum could be suppressed by adding different amounts of the sodium alkyl sulfates. After the suppression of the maximum in each case, increasing amounts of surfactants were added to the depolarizer solution and the following effects were noted:

C₈:

On adding a small amount (0.0005%) of sodium alkyl sulfate, the break-off potential of the maximum shifted to -0.36v . Further additions of the suppressor shifted the break-off potential to still less negative potentials (fig.33). The MSP value came out to be $10.31 \times 10^{-4} \text{ M}$. After the suppression of maximum, more surfactant was added, but $E_{\frac{1}{2}}$ remained unaffected (curves 4 and 5 of fig.33).

C₁₀:

The addition of first increment (0.00005%) of sodium decyl sulfate shifted the break-off potential to more

[Cu(Tart)]⁰ Maximum.

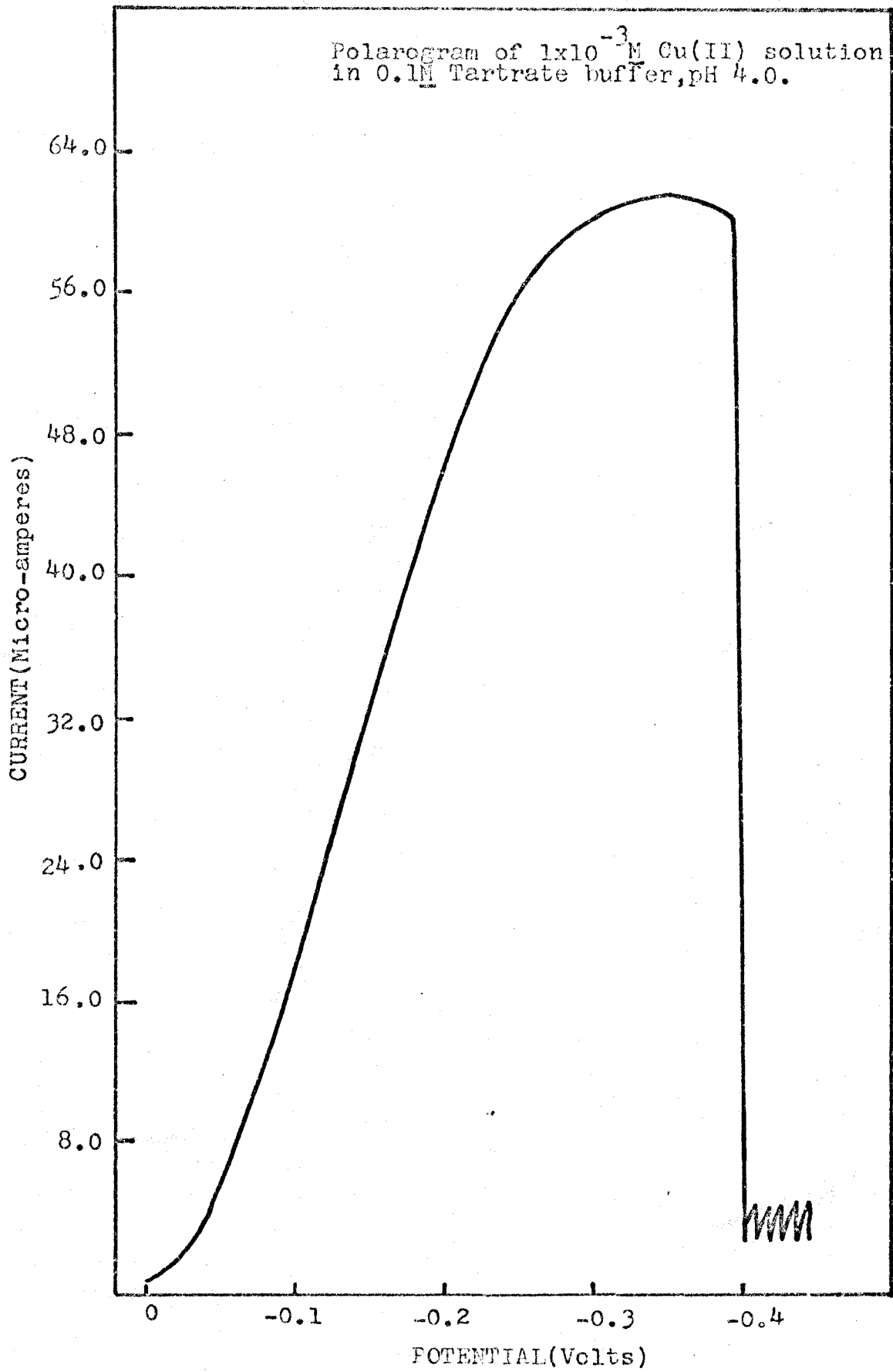
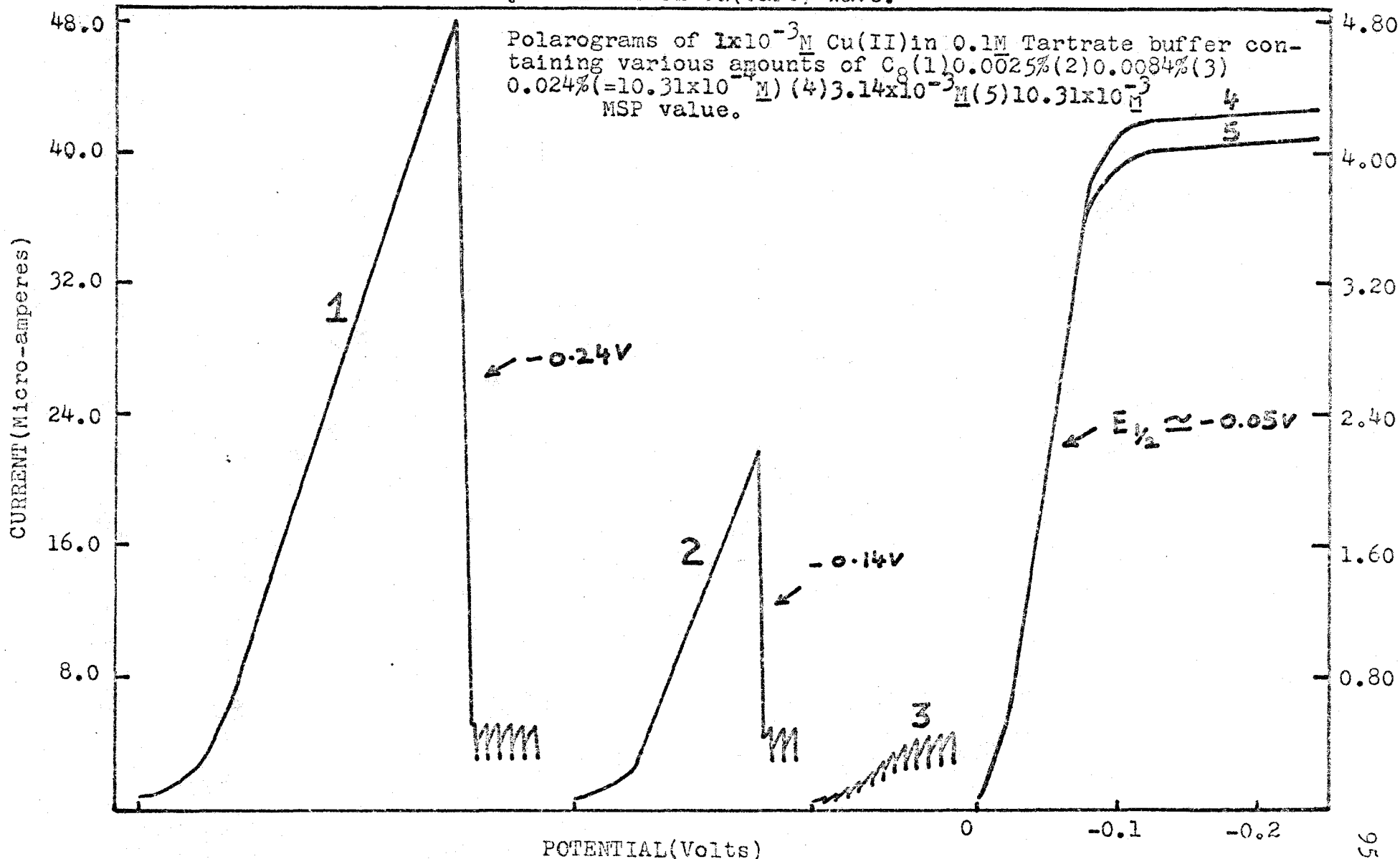


FIGURE 33

Effect of Sod. Octyl Sulfate on $\text{Cu}(\text{tart})^0$ wave.



Each curve starts at 0.00 volt. Curves 4 & 5 are drawn at a different current sensitivity (shown on the right hand side of the plot.)

positive (-0.38v) potential. Likewise, further additions of the suppressor shifted the break-off potential to still more positive potentials. This behavior continued till the maximum was completely suppressed. The MSP value in this case was $= 10.27 \times 10^{-5} \text{M}$. After the maximum was completely suppressed, further increase in the concentration of the surfactant did not produce any change in the half-wave potential. Also, the limiting current was not affected much. The insignificant decrease in the limiting current was caused by dilution.

C₁₂:

The shift of the break-off potential of the maximum in this case was even greater than that observed in case of octyl or decyl sulfates. For example, 0.00005% SDS shifted the break-off potential to -0.34v. The maximum was completely suppressed when concentration of dodecyl sulfate was 0.00099% ($= 3.425 \times 10^{-5} \text{M}$). Even when the concentration of the suppressor was raised to $3.14 \times 10^{-4} \text{M}$, the $E_{\frac{1}{2}}$ was unaffected and the limiting current was very insignificantly reduced.

C₁₄:

The addition of tetradecyl sulfate produced the same effect as observed in case of decyl sulfate. As no turbidity resulted on adding the surfactant to the depolarizer, the

MSP value in this case came out to be lower ($5.13 \times 10^{-5} \text{ M}$) than in the case of decyl sulfate. After the suppression of the maximum, the concentration of the surfactant was raised to $2.87 \times 10^{-4} \text{ M}$, but this did not change the half-wave potential even slightly. It remained constant at -0.050 v (curves 4 and 5 of fig. 34).

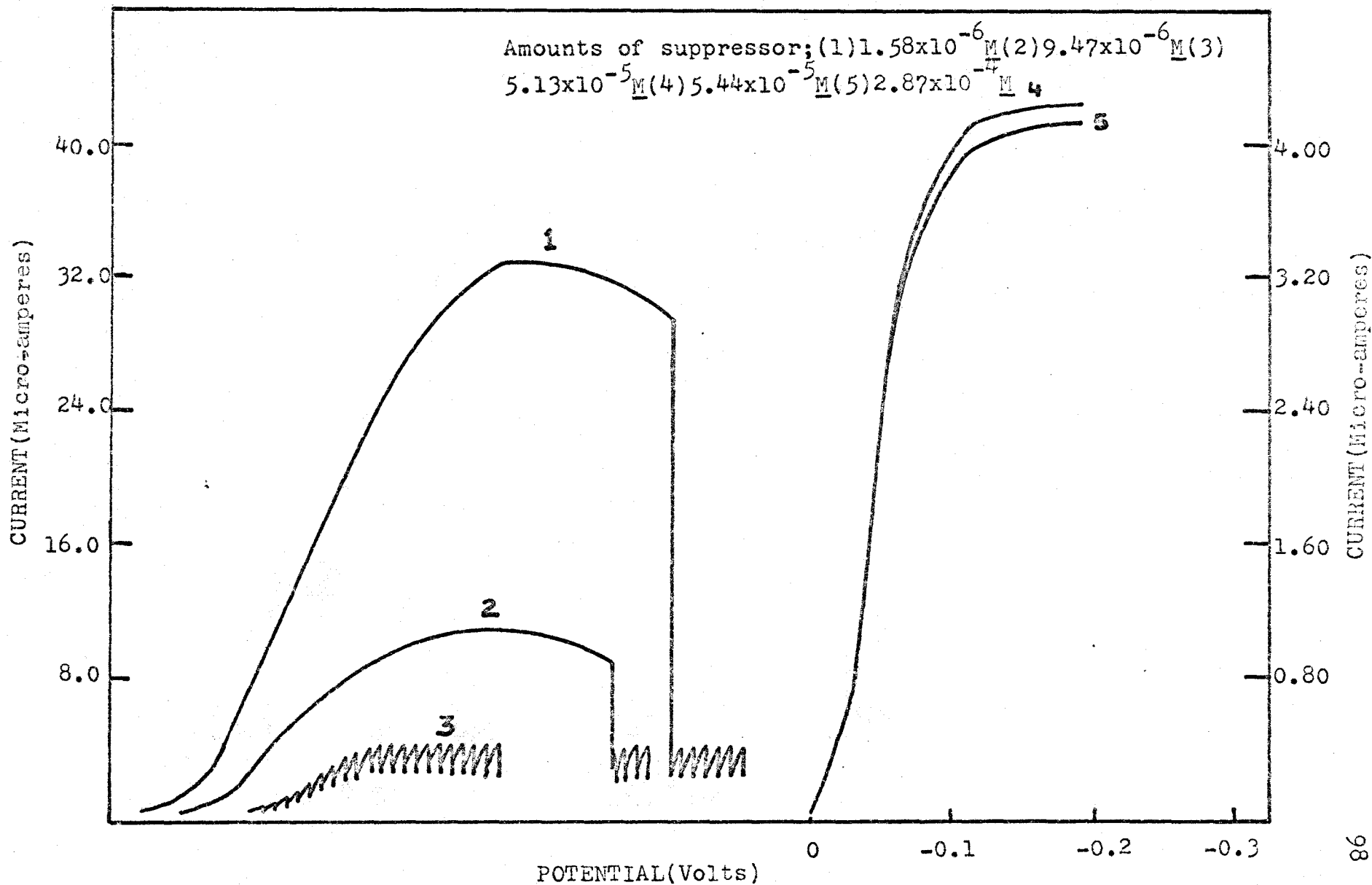
C₁₆:

When hexadecyl sulfate solution was added to the solution containing Cu^{2+} ions in tartrate buffer, a white precipitate was formed when the surfactant concentration was $0.145 \times 10^{-3} \text{ M}$. On raising the suppressor concentration, the amount of precipitate increased. In the presence of $5.71 \times 10^{-4} \text{ M}$ sodium hexadecyl sulfate, a white gelatinous precipitate was obtained. This resulted in very slight distortion on the limiting current plateau. However, $E_{\frac{1}{2}}$ seemed to be unaffected even when the surfactant concentration was raised to $1.385 \times 10^{-3} \text{ M}$.

C₁₈:

As in the case of hexadecyl sulfate, turbidity resulted in this case too. This became apparent when the surfactant concentration was $1.60 \times 10^{-4} \text{ M}$. However, the C-V plot looked distorted even before the turbidity was noticed. Due to distortions, an exact MSP value could not be obtained.

FIGURE 34
Effect of Sod. Tetradecyl Sulfate on $\text{Cu}(\text{tart})^0$ wave.



Each curve starts at 0.00 volt. Curves 4 & 5 are drawn at a different sensitivity (shown on right hand side of the plot).

The approximate MSP value was $5.92 \times 10^{-4} \text{ M}$. Due to distortions in the region of limiting current plateau, $E_{1/2}$ could not be measured accurately.

DISCUSSION

As indicated above the addition of sodium alkyl sulfates to $\text{Cu}(\text{tetren})^{2+}$ and $\text{Cu}(\text{trien})^{2+}$ solutions did not cause any change in the limiting current and half-wave potential. This is easy to understand. Since these depolarizers are positively charged and the adsorbed layer of the surfactants on the mercury drop has a negative charge, the depolarizers can pass through the pores of the adsorbed layer almost without any hindrance and thus the C-V plots are unaffected. However, as was also reported by Schmid and Reilley (21), the presence of adsorbed film of anionic surfactants at the electrode-solution interface decreases the rate of the electron-transfer reaction and this increases the irreversibility of the reaction.

The addition of the surfactants to Cu-EDTA solutions shifts the half-wave potential to more negative potentials. As suggested by Jacobsen and Kalland (30), this is because the depolarizer, $\text{Cu}(\text{EDTA})^{2-}$, in the present case has the same charge as the adsorbed layer and so it is electrostatically repelled by the surface of the mercury drop. or in other words, the depolarizer has to cross a potential

energy barrier before being reduced, and, as a result of this, its wave is shifted to more negative potentials.

The formation of turbidity on mixing the alkyl sulfates with the trien and tetren solutions at pH 4.5 is most likely due to formation of an insoluble salt of the trien and tetren and the paraffin chain ion of the surfactants. At this pH the trien and tetren exist as protonated positively charged ions. The turbidity was produced even in absence of copper.

The turbidity formation in $\text{Cu}(\text{EDTA})^{2-}$ and $\text{Cu}(\text{tart})^0$ systems can be ascribed to formation of insoluble copper salts of alkyl sulfates. As reported on page 96 of this chapter, addition of equivalent amounts of the first three members of the homologous series shifted the half-wave potential of Cu-EDTA wave to increasingly negative potentials. The shift was greatest for dodecyl sulfate and least in case of octyl sulfate. This again clearly shows that with increase in the carbon chain-length, the adsorption of a surfactant increases. Or, in other words, sodium octyl sulfate is mildly adsorbed and sodium dodecyl sulfate is strongly adsorbed.

Since the addition of alkyl sulfates to Cu-Tartrate system did not affect the half-wave potential, it can be said that like the positively charged $\text{Cu}(\text{trien})^{2+}$ and $\text{Cu}(\text{tetren})^{2+}$ complexes, the neutral $\text{Cu}(\text{tart})^0$ complex has

no difficulty in passing through the adsorbed layer of the surfactants and thus, the half-wave potential remains unaffected even in the presence of large amounts of surfactants. And again, as in the case of positively charged complexes, due to the presence of the adsorbed film of the surfactants, deceleration of the electron transfer is caused and this makes the reduction wave look more drawn out or irreversible.

VIII. CURRENT-TIME CURVES

RESULTS AND DISCUSSION

When a dropping mercury electrode is brought into contact with a solution, surface forces at the mercury-solution interface can cause adsorption of dissolved substances. The adsorption is of two kinds 1) The depolarizer or its electrode reaction product is adsorbed. 2) Some other component of the solution is adsorbed. If the other component is a surface active substance, then its adsorption can cause a shift, deformation or split in the polarographic wave. In the present study, the effects resulting from the second kind of adsorption were studied.

In the earlier chapters, the effects of electroinactive substances were explained with the help of electrocapillary and current-voltage curves. In this chapter, the changes in the shape of current-time curves during the life of a single drop are discussed. The oscillographic current-time determinations at a constant potential provide much more information than the conventional polarograms and were thus used to investigate the effect of surfactants on electrode processes.

According to Loshkarev and Kryukova (51), adsorption of surfactants on electrodes leads to the formation of a compact film, the permeability of which toward the depolarizer ions

depends on the charge, ionic radius and chemical nature of the depolarizer. Any repulsion between the ions of the depolarizer and the particles of the adsorbed layer results in inhibition of the electrode process.

Schmid and Reilley (21) studied the inhibitory effects of surface active compounds on complexes with the help of current-time curves and reported that the chemical reaction or the electron-transfer taking place near the electrode surface was retarded by the adsorbed layer. They related the extent of inhibition of a given electrode reaction during the life of a drop to the extent of coverage of the electrode surface. And according to them, the extent of film formation was governed (1) by the rate of diffusion of the surfactant, (2) by the adsorption equilibrium, and (3) by the rate of adsorption and the adsorption equilibrium. Depending upon these factors, three different types of current-time curves were obtained. Schmid and Reilley (21) had used Triton-X-100, camphor, eosin and thymol and investigated their effects on a solution containing 0.001M CuEDTA, 0.009M EDTA and 0.1M Tartrate buffer in the pH range 3.5-4.6.

In order to study the behavior of sodium alkyl sulfates in the case of the Cu-EDTA system, current-time pictures were obtained at a constant potential of -0.60v (vs. SCE). The solution employed had the following composition: $1 \times 10^{-3}\text{M}$ Cu(II)

and 0.25M EDTA. The pH of the solution was 4.32. Since EDTA is a good electrolyte and has a reasonable buffer capacity at this concentration and pH, no auxiliary buffer solution was employed. The following results were obtained:

SODIUM DODECYL SULFATE:

Figure 35 shows the current-time curves with the various amounts of dodecyl sulfate present. Increasing concentrations of the surfactant terminated the electrode reaction (the point where the current drops to zero) at shorter and shorter time intervals. However, as can be noticed, during the initial growth of the drop, the curves always followed the pattern of the normal, diffusion-controlled current-time curves. This behavior can be explained as follows: In the beginning of the droplife, the amount of dodecyl sulfate which reaches the electrode surface by diffusion and adsorbs on it, is not enough to retard the electrode reaction and therefore no deviation from the diffusion-controlled current is observed. However, later in the droplife, enough surfactant is adsorbed on the expanding mercury drop to decrease the reaction rate considerably and cause the current to decrease. When the drop is completely covered with a monolayer of the surfactant, the current falls to zero. As indicated above, the higher the concentration of surfactant, the shorter is the time required

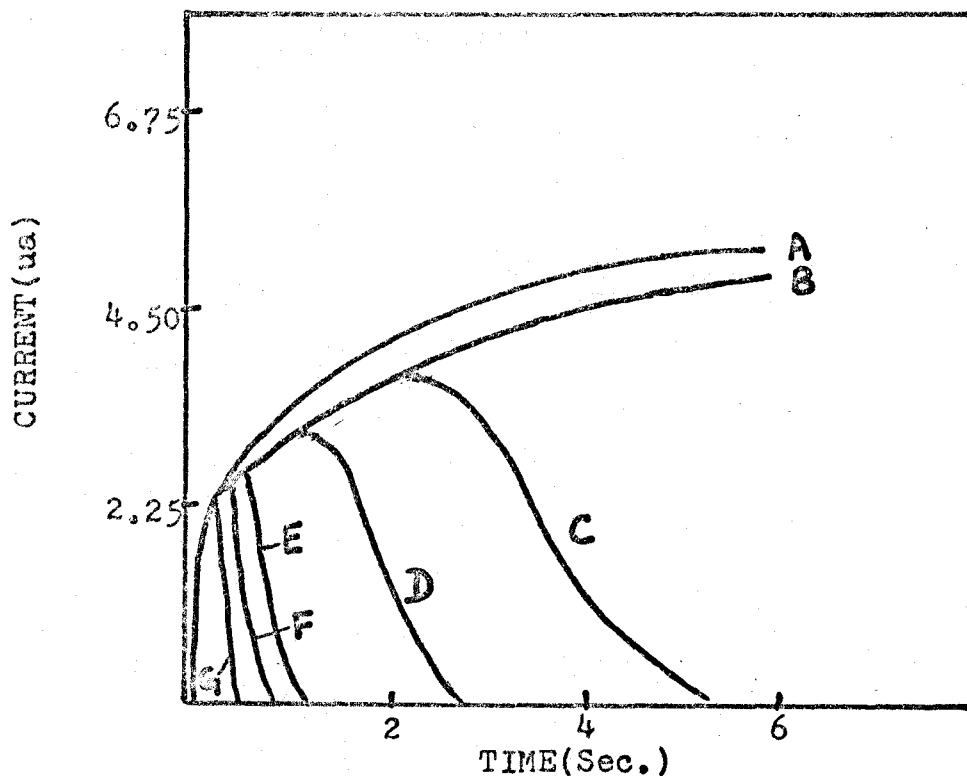


Figure 35: $i-t$ curves for a soln. containing $1 \times 10^{-3} \text{ M}$ Cu(II) and 0.25 M EDTA, pH 4.32. (A) 0; (B) $3.43 \times 10^{-5} \text{ M}$; (C) $6.78 \times 10^{-5} \text{ M}$; (D) $10.06 \times 10^{-5} \text{ M}$; (E) $1.64 \times 10^{-4} \text{ M}$; (F) $1.91 \times 10^{-4} \text{ M}$; (G) $2.41 \times 10^{-4} \text{ M}$ C_{12} .

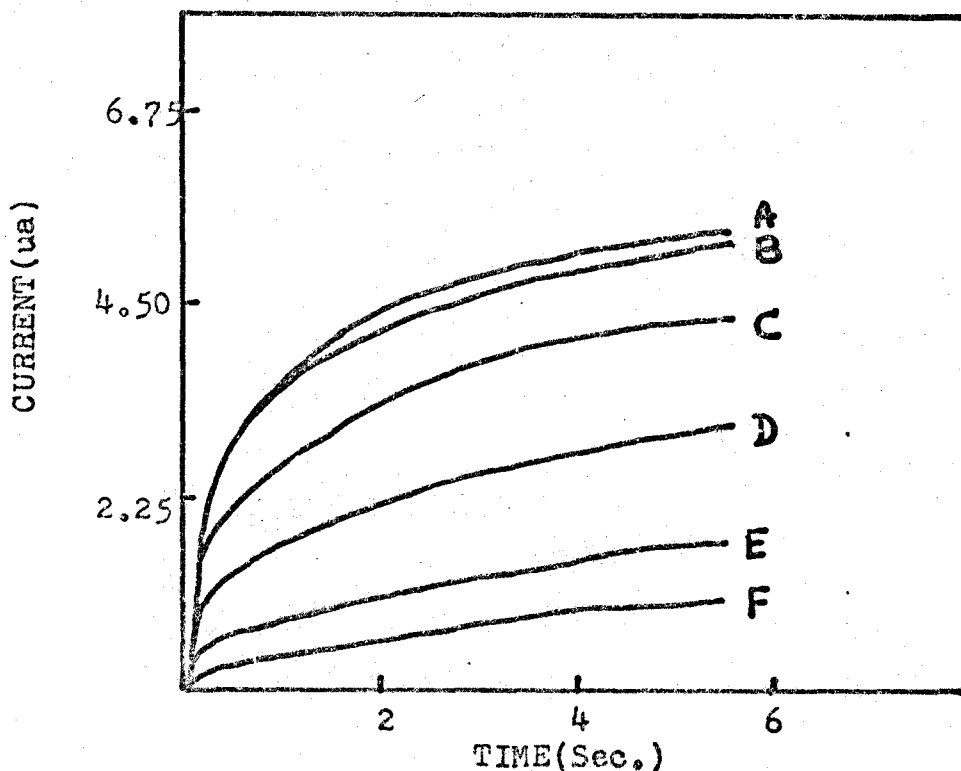


Figure 36: $i-t$ curves for a solution containing $1 \times 10^{-3} \text{ M}$ Cu(II) and 0.25 M EDTA, pH 4.32. (A) 0; (B) $3.92 \times 10^{-4} \text{ M}$; (C) $1.66 \times 10^{-3} \text{ M}$; (D) $2.44 \times 10^{-3} \text{ M}$; (E) $3.92 \times 10^{-3} \text{ M}$; (F) $5.62 \times 10^{-3} \text{ M}$.

to cover the drop. The current-time behavior described above is similar to those obtained by Schmid and Reilley (21) in case of Triton X-100 and eosin under the assumption that the rate of covering the mercury drop with the surfactants was governed by diffusion.

According to Koryta (52), the time required to cover the surface completely with a surfactant on a fresh mercury drop is inversely proportional to the square of the bulk concentration of the surfactant. He derived the following equation, which relates the time ϑ , at which the drop surface is completely covered, to C , the bulk concentration of the surfactant in moles/liter:

$$\vartheta = 1.82 \times 10^6 \times \frac{\Gamma_s^2}{DC^2} \quad \text{-----(I)}$$

Γ_s is the number of moles of surfactant per cm^2 of the mercury surface and D is the diffusion coefficient of the surfactant in $\text{cm}^2 \text{sec}^{-1}$. The "1.82" is a constant geometrical factor. In deriving the equation he assumed 1) that the adsorption equilibrium is reached very rapidly and that the adsorption coefficient is very large, and 2) that the current suddenly vanishes at the instant when the surface is completely covered.

As suggested by Schmid and Reilley (21), the validity of equation (I) can be tested by assuming ϑ , the time when the surface of the drop is completely covered, is equal to

the time t^0 , the time when the current reaches zero in the current-time curves. To find t^0 , the descending branch of the current-time curves is extrapolated linearly to zero. A plot of t^0 versus $1/C^2$ should, according to equation (1), yield a straight line passing through the origin. On plotting t^0 vs. $1/C^2$, (see table 6 for data) in the case of dodecyl sulfate, a straight line was actually obtained (fig. 41) with the slope of $2.04 \times 10^{-8} \text{ mole}^2 \text{ sec. liter}^{-2}$. According to equation (I), this slope is equal to the coefficient $1.82 \times 10^6 \times \bar{V}^2 / D$.

In order to calculate \bar{V} for sodium dodecyl sulfate, its diffusion coefficient D is needed. A search of the literature yielded the following two values of D_m , the diffusion coefficient of dodecyl sulfate micelles (72,73): (i) $D_m = 0.914 \times 10^{-6} \text{ cm}^2 / \text{sec.}$ at 25° in presence of $0.1M$ NaCl (72); (ii) $D_m = 1.17 \times 10^{-6} \text{ cm}^2 / \text{sec.}$ at 30° in presence of $0.2M$ NaCl (73). Since the current-time studies in case of dodecyl sulfate were carried out at concentrations below its CMC (that is, in the absence of micelles), it was necessary to know D_o , the diffusion coefficient of the unmicellized (monomeric) dodecyl sulfate.

According to Courchene (73), D_o and D_m are related as follows:

$$D = D_m + \frac{C}{C_o} (D_o - D_m)$$

where D is the apparent diffusion coefficient; C is the bulk concentration of the surfactant and C_0 is the concentration of the unmicellized form. Since (73) "below the CMC, $C = C_0$, and $D_m = 0$, so $D = D_0$. Above the CMC, C_0 is nearly a constant ($C_0 \cong \text{CMC}$). Thus a plot of the observed D vs $1/C$ will consist of two straight lines: one intersects the ordinate at D_m , the micellar self-diffusion coefficient, and one is parallel to the abscissa at $D = D_0$, the monomer self-diffusion coefficient. From the D vs $1/C$ plot of Courchene (73), a value of 6.2×10^{-6} cm^2/sec . for D_0 was obtained. Since this value of D_0 is at 30°C , a value of D_0 at 25° was estimated as shown below:

$$\frac{D_m \text{ at } 25^\circ}{D_0 \text{ at } 25^\circ} = \frac{D_m \text{ at } 30^\circ}{D_0 \text{ at } 30^\circ}$$

On substituting the D_m and D_0 (at 30°) values, the D_0 at 25° was calculated to be 4.8×10^{-6} cm^2/sec . Using this value of D_0 , the \bar{F} was calculated from the following relation:

$$2.04 \times 10^{-8} (\text{slope of line in figure 41}) = 1.82 \times 10^6 \bar{F}^2/D.$$

The value of \bar{F} , thus obtained was equal to 2.32×10^{-10} mole cm^{-2} .

SODIUM OCTYL SULFATE:

The current-time curves showing the effect of octyl sulfate on Cu-EDTA system (fig. 36) were similar to those obtained by Schmid and Reilley (21) for thymol. Both sodium octyl sulfate and thymol are weak surface active agents and

decrease the diffusion current only when present in large molar concentrations. For example, the limiting current in the absence of suppressor (fig. 36A) is 4.83ua and in the presence of 0.0384% (= $1.66 \times 10^{-3} \text{M}$), it is decreased to 3.57ua (fig. 36C). Likewise, a $1.7 \times 10^{-3} \text{M}$ solution of thymol decreased (21) the limiting current by approximately 2.5uA. And unlike in the case of sodium dodecyl sulfate, the deviation from the normal diffusion-controlled current-time curve occurred almost from the start of drop formation i.e; early in the drop life. As the concentration of octyl sulfate was increased further, the shape of the current-time curves deviated from a sixth-order parabola. In other words, it can be said that in the presence of large concentrations of the surfactant (e.g. 0.056% or $2.44 \times 10^{-3} \text{M}$ C_8 --- curve D in fig. 36) the current behaves as a kind of kinetic current. A similar behavior for thymol was reported by Schmid and Reilley (21). According to them, surface active agents (like thymol) with small adsorption coefficients never cover the drop surface completely, but do so only partially right from the beginning of the drop life.

SODIUM DECYL SULFATE;

As was shown earlier by means of electrocapillary curves and MSP studies, decyl sulfate is a stronger suppressor

than octyl sulfate, but is weaker than dodecyl sulfate. Thus, as expected, the current-time curves (fig. 37) at smaller concentrations of decyl sulfate resembled those of octyl sulfate and at larger concentrations approached the shape of current-time curves due to dodecyl sulfate. However, as in the case of dodecyl sulfate, at smaller concentrations of decyl sulfate, the current did not fall to zero, but only decreased a little. (see curves C and D in fig. 37a). The decrease in current was fairly sharp and the time period in which the current fell, decreased as the concentration of the surfactant was raised further. This can be explained by saying that up to a concentration of $2.17 \times 10^{-4} \text{ M}$ (curve D in fig. 37a), decyl sulfate decreases the reaction rate only slightly. And when its concentration is increased further (curves E and F in fig. 37b), the behavior of decyl sulfate closely resembles that of dodecyl sulfate and now the current drops to zero in shorter and shorter time intervals. The curves E and F in fig. 37b were taken at a higher sensitivity setting on the oscilloscope panel.

SODIUM TETRADECYL, HEXADECYL AND OCTADECYL SULFATES:

As pointed out earlier in chapter 7, addition of these three surfactants to Cu-EDTA solutions causes turbidity, which leads to distortions in the region of the limiting

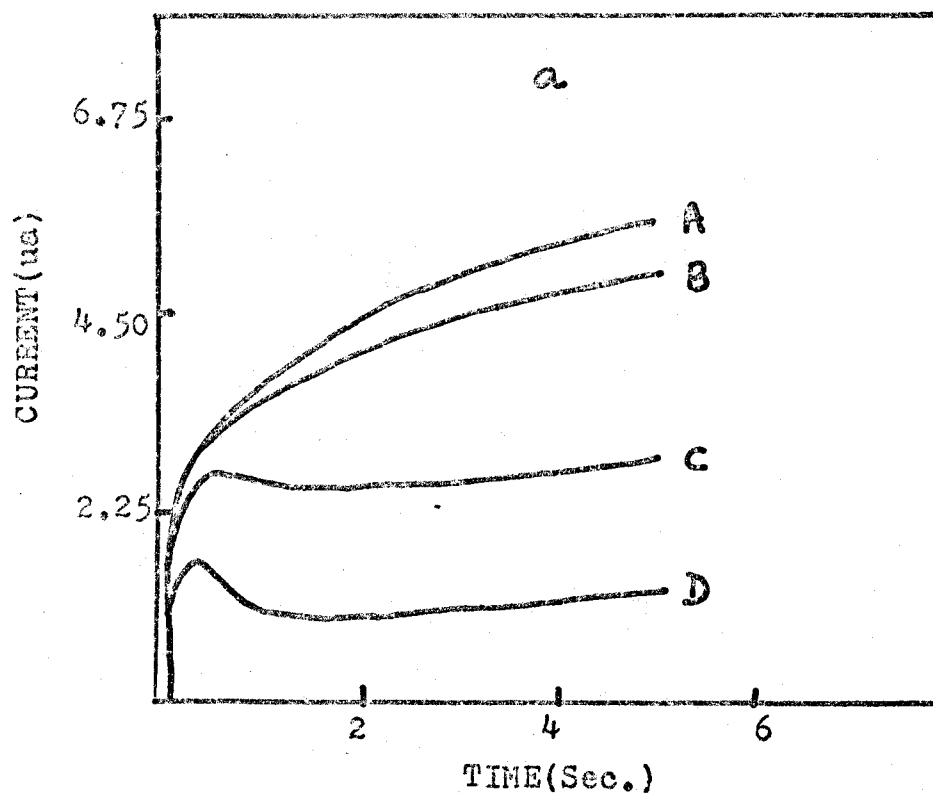


FIGURE 37: $i-t$ curves for a solution containing $1 \times 10^{-3} \text{ M}$ Cu(II), 0.25 M EDTA, pH 4.32. (A) $3.80 \times 10^{-5} \text{ M}$; (B) $7.53 \times 10^{-5} \text{ M}$; (C) $1.48 \times 10^{-4} \text{ M}$; (D) $2.17 \times 10^{-4} \text{ M}$ sodium decyl sulfate.

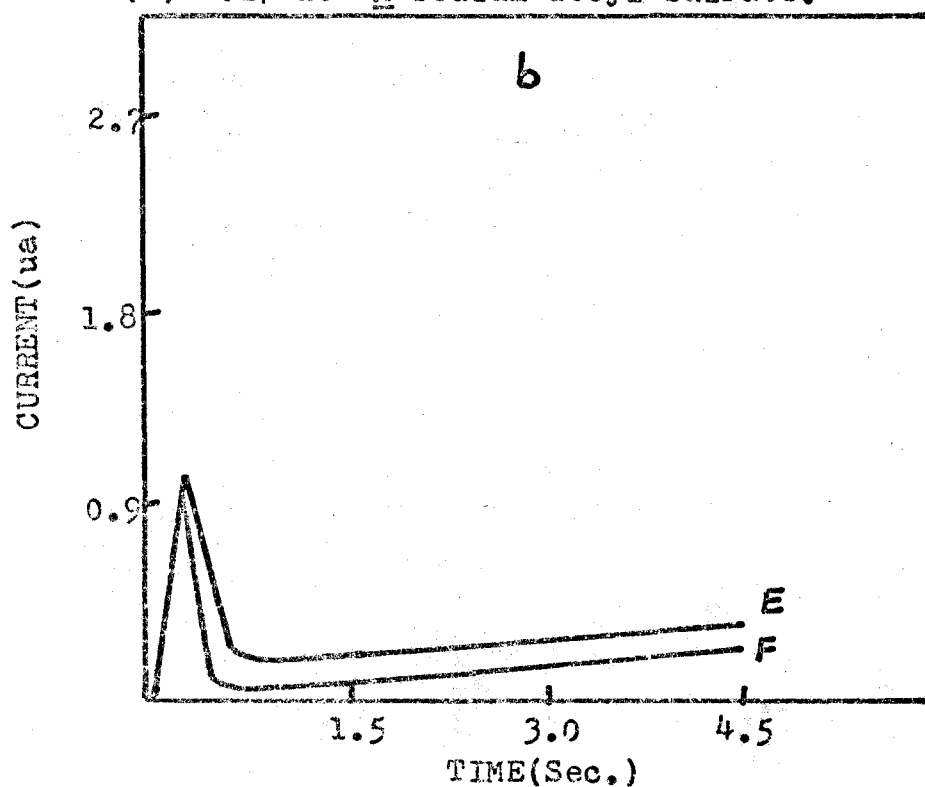


FIGURE 37 (Contd.): (E) $2.68 \times 10^{-4} \text{ M}$; (F) $3.49 \times 10^{-4} \text{ M}$ C_{10} .

current plateau. The current-time curves (figures 38-40) show the concentrations at which the distortions begin in each case. The distortions in the case of tetradecyl sulfate were the least and but for these, the overall behavior of tetradecyl sulfate resembled that of dodecyl sulfate. The plot of t^0 vs. $1/C^2$ data (table 6) yielded a straight line passing through the origin (fig. 41). The slope of the line was 7.50×10^{-8} mole²sec.liter⁻². Since Koryta's equation is followed even in this case, it can be safely said that in spite of the distortions resulting from turbidity formation, diffusion governs the rate of covering the mercury drop surface with the tetradecyl sulfate.

Since a value of D_0 in the case of sodium tetradecyl sulfate was not available from the literature, it was decided to calculate \bar{t} in the present case by using the estimated D_0 value of dodecyl sulfate. This approximation should not introduce too much error because the chain length in sodium dodecyl and tetradecyl sulfate differs by only two carbon atoms and thus the D_0 values for the two surfactants should not be too much different from each other. The \bar{t} value for sodium tetradecyl sulfate was thus calculated to be 4.45×10^{-10} mole,cm⁻². \bar{t} values for dodecyl and tetradecyl sulfates thus determined, are comparable with those of eosin (21) and Tritons X-45, X-100 and X-305 (53).

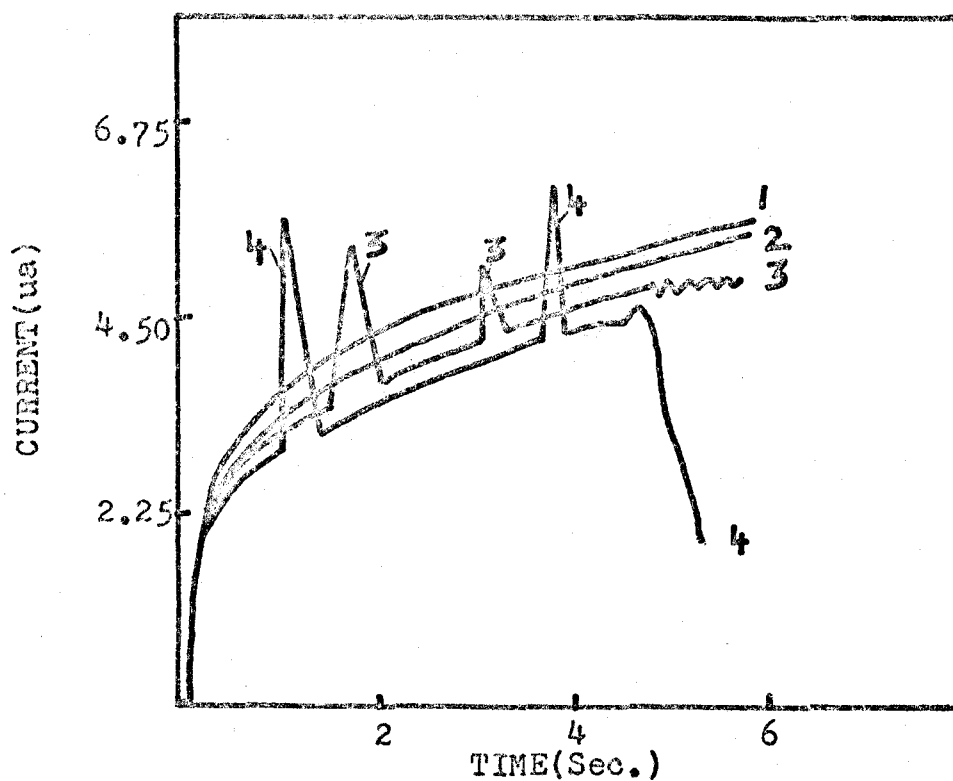


FIGURE 38: $i-t$ curves for a soln. containing $1 \times 10^{-3} \text{ M}$ Cu(II) , 0.25 M EDTA, pH 4.32. (1) 0; (2) $3.13 \times 10^{-5} \text{ M}$; (3) $9.21 \times 10^{-5} \text{ M}$; (4) $1.50 \times 10^{-4} \text{ M}$ Sodium tetradecyl sulfate.

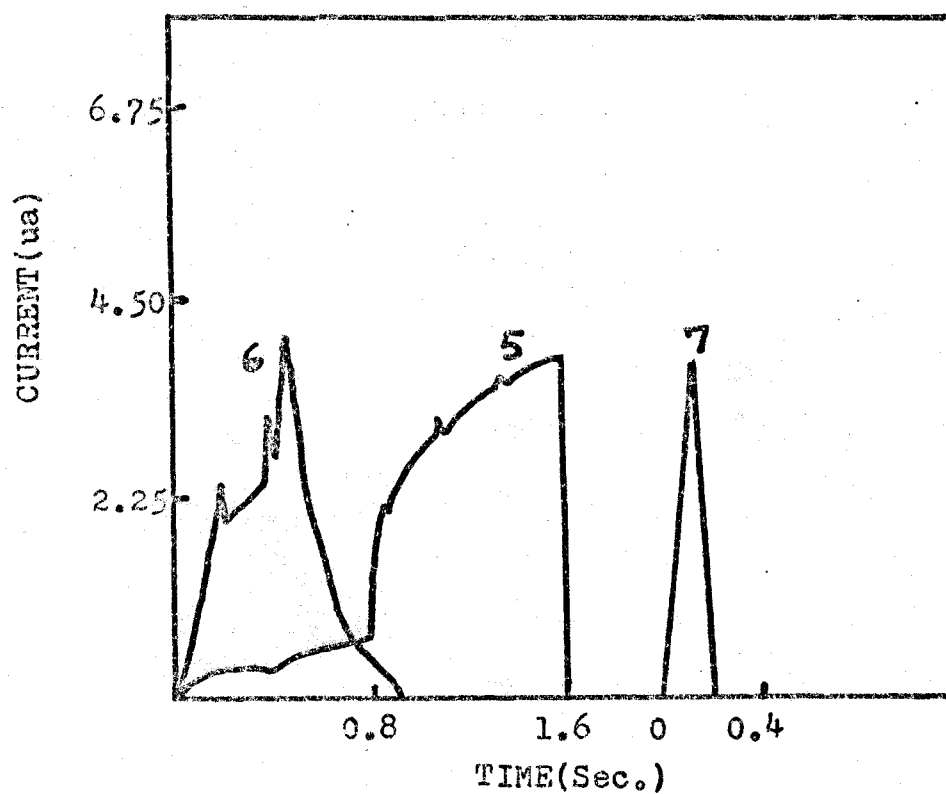


FIGURE 38(Contd.): (5) $2.14 \times 10^{-4} \text{ M}$; (6) $2.88 \times 10^{-4} \text{ M}$; (7) $4.70 \times 10^{-4} \text{ M}$ Sodium tetradecyl sulfate.

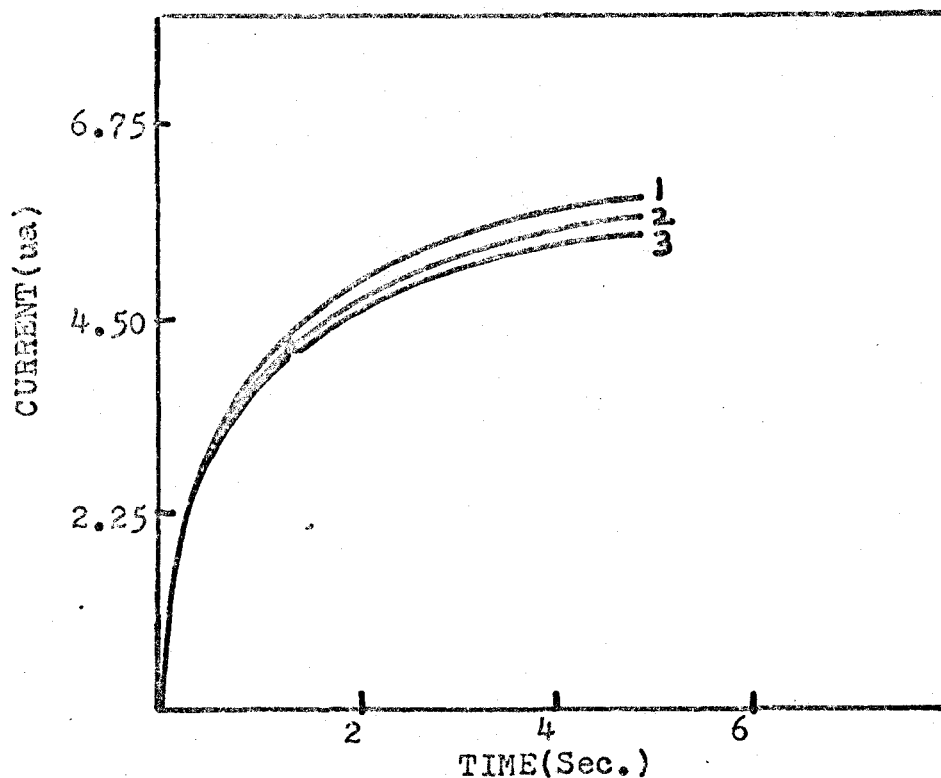


FIGURE 39: $i-t$ curves for a solution containing $1 \times 10^{-3} \text{ M}$ Cu(II), 0.25 M EDTA, pH 4.32. (1) 0; (2) $2.88 \times 10^{-5} \text{ M}$; (3) $4.30 \times 10^{-5} \text{ M}$ Sodium hexadecyl sulfate.

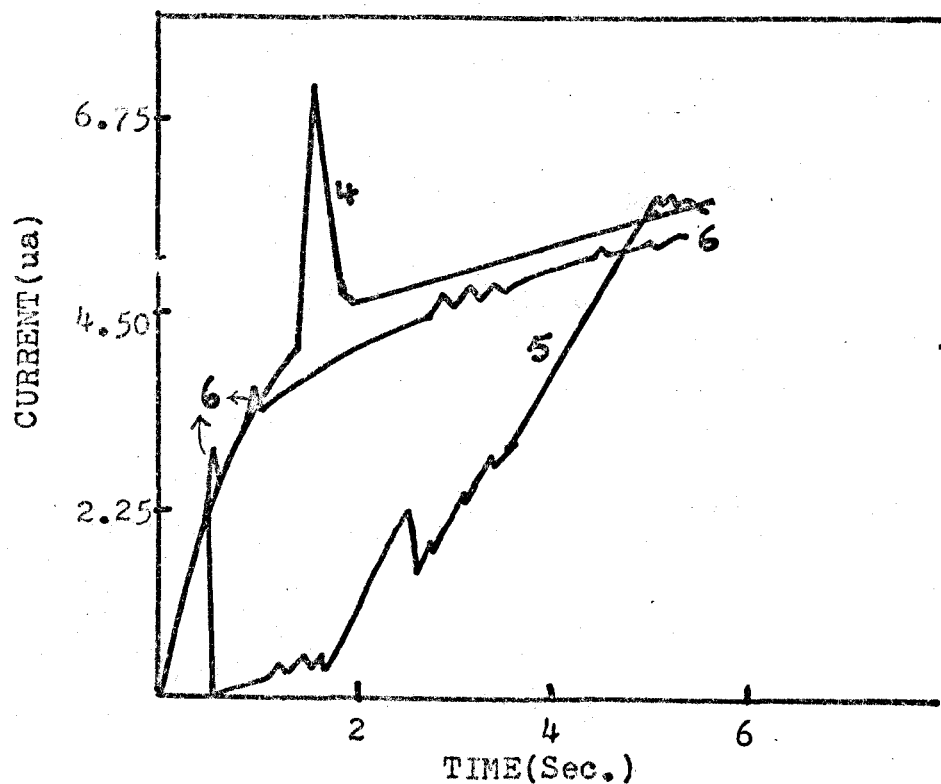


FIGURE 39(Contd.): (4) $5.71 \times 10^{-5} \text{ M}$; (5) $8.47 \times 10^{-5} \text{ M}$; (6) $2.64 \times 10^{-4} \text{ M}$ Sodium hexadecyl sulfate.

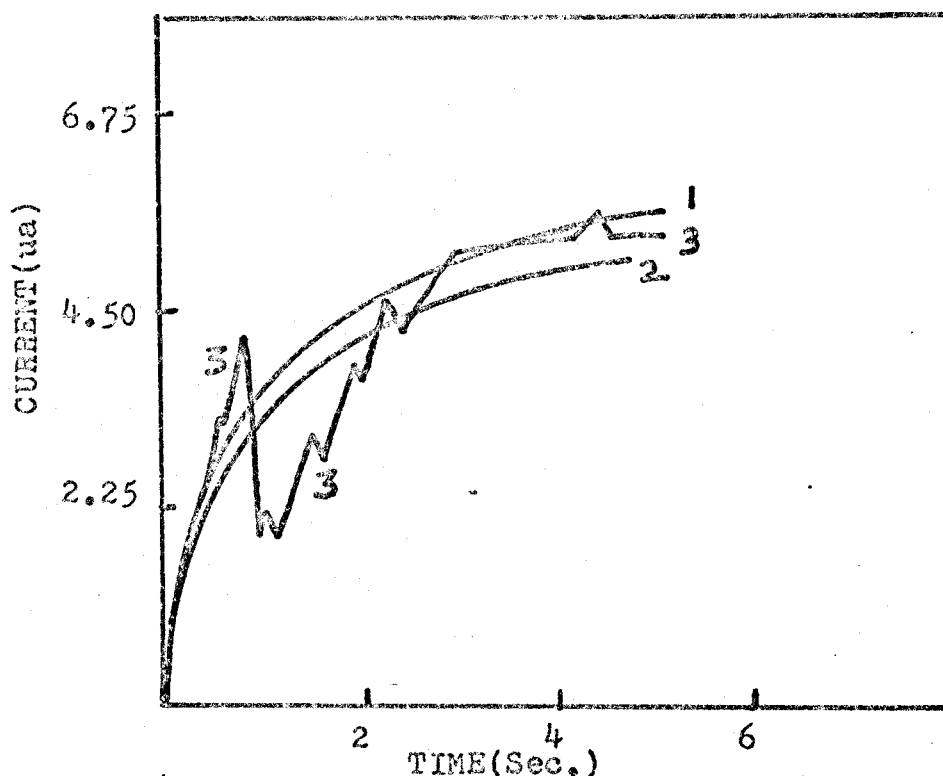


FIGURE 40: $i-t$ curves for a solution containing $1 \times 10^{-3} \text{ M}$ Cu(II), 0.25 M EDTA, pH 4.32. (1) 0; (2) $9.1 \times 10^{-5} \text{ M}$; (3) $1.03 \times 10^{-4} \text{ M}$ Sodium octadecyl sulfate.

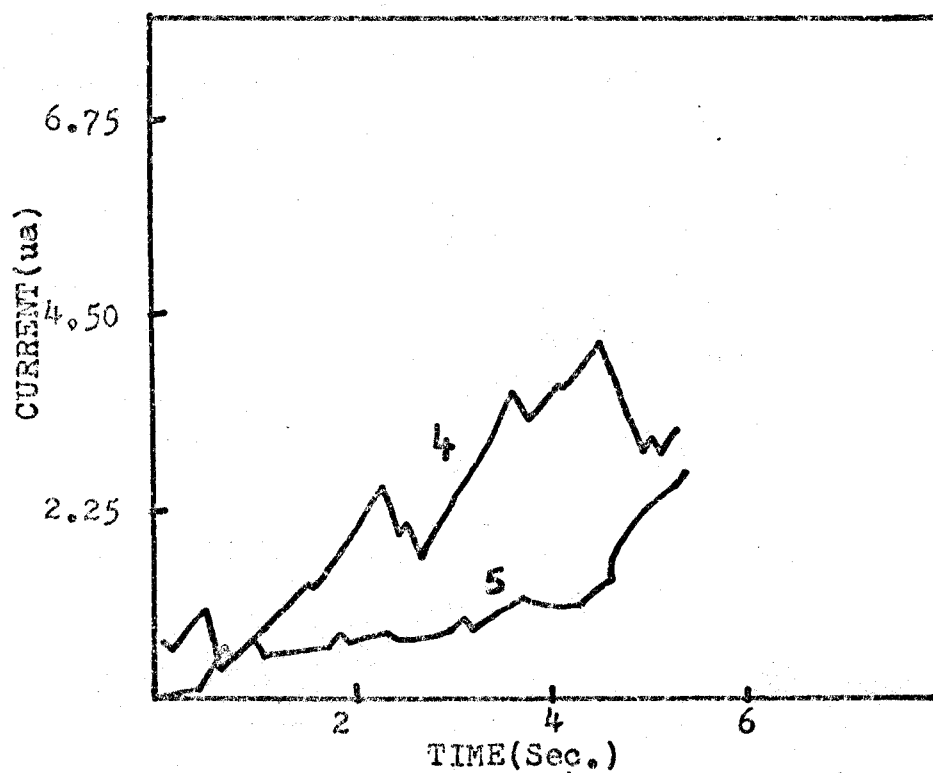
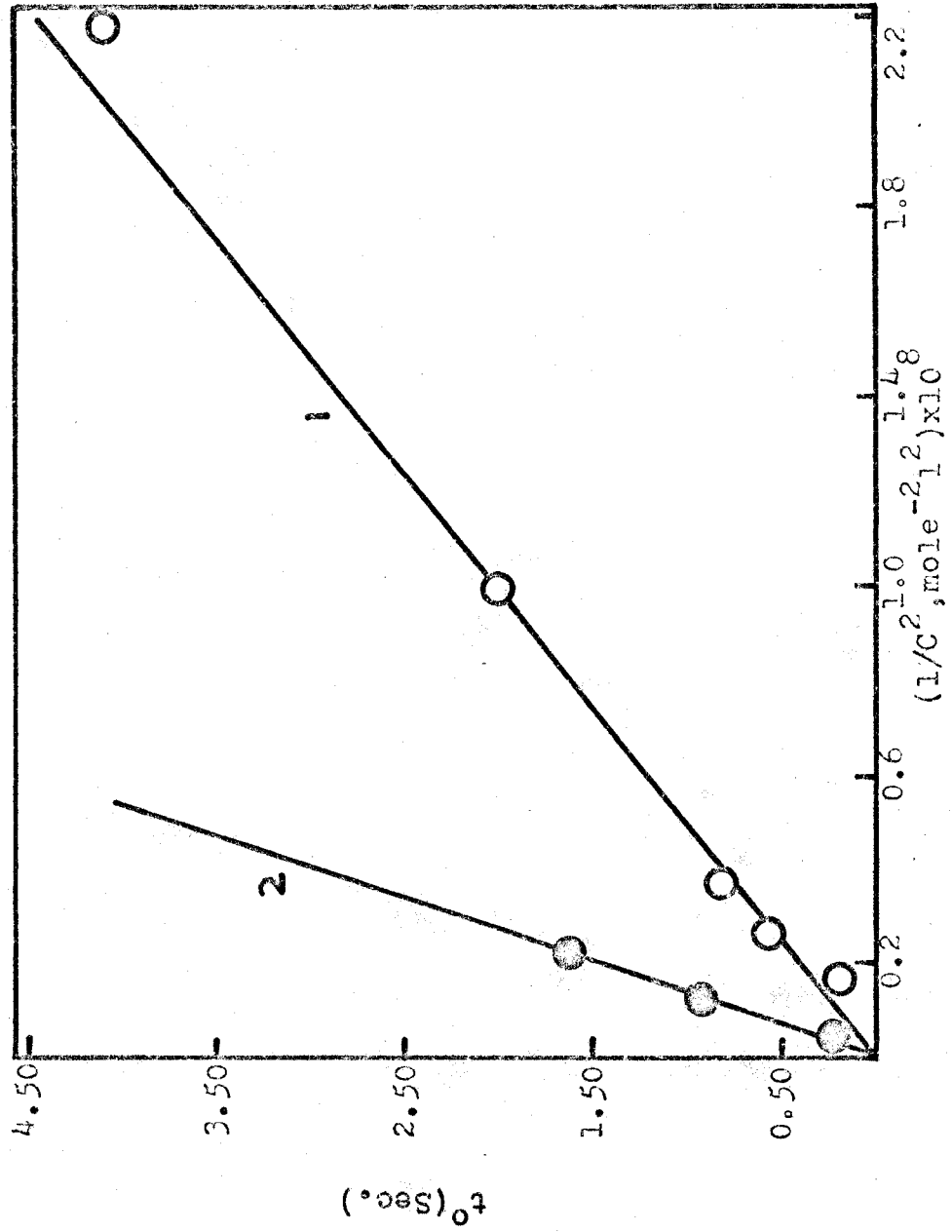


FIGURE 40 (Contd.): (4) $1.16 \times 10^{-4} \text{ M}$; (5) $1.88 \times 10^{-4} \text{ M}$ Sodium octadecyl sulfate.

TABLE 6

<u>Surfactant</u>	<u>t^0 (sec.)</u>	<u>C (moles/l) $\times 10^{+4}$</u>	<u>$10^{-8}/C^2$</u>
Sod. dodecyl sulfate:			
	5.20	0.343	8.55
	4.10	0.678	2.18
	2.00	1.01	0.99
	0.80	1.65	0.37
	0.55	1.96	0.26
	0.30	2.42	0.17
Sod. tetradecyl sulfate:			
	5.20	1.50	0.444
	1.60	2.14	0.22
	0.90	2.88	0.121
	0.20	4.70	0.045

FIGURE 41



Plot of data in table 6: Curve (1) Sod. dodecyl sulfate
 (2) Sod. tetradecyl sulfate.

Too much distortions in case of hexadecyl and octadecyl sulfates prevented an accurate measurement of t° and hence t° vs. $1/C^2$ plot could not be obtained.

CURRENT-TIME CURVES IN CASE OF $\text{Cu}(\text{tetren})^{2+}$ COMPLEX :

It was shown in chapter 7 that sodium alkyl sulfates do not effect the $E_{\frac{1}{2}}$ or the limiting current in the case of the positively charged $\text{Cu}(\text{tetren})^{2+}$ and $\text{Cu}(\text{trien})^{2+}$ complexes. To check this behavior further, current-time measurements were carried out using the same solutions as employed earlier for current-voltage studies. The figures (42-46) show the current-time curves in the case of sodium octyl, decyl, tetradecyl, hexadecyl and octadecyl sulfates. Except for slight distortions due to turbidity formation in case of hexadecyl and octadecyl sulfates, the presence of surfactants did not seem to affect the shape of the current-time curves. Very slight decrease in limiting current is probably due to dilution effects.

CURRENT-TIME CURVES SHOWING POLAROGRAPHIC MAXIMA

The experimental data for the current-time curves in the case of Cu-EDTA and Cu-Tetren systems were obtained in the potential regions corresponding to diffusional transfer of the surfactants from the bulk of the solution

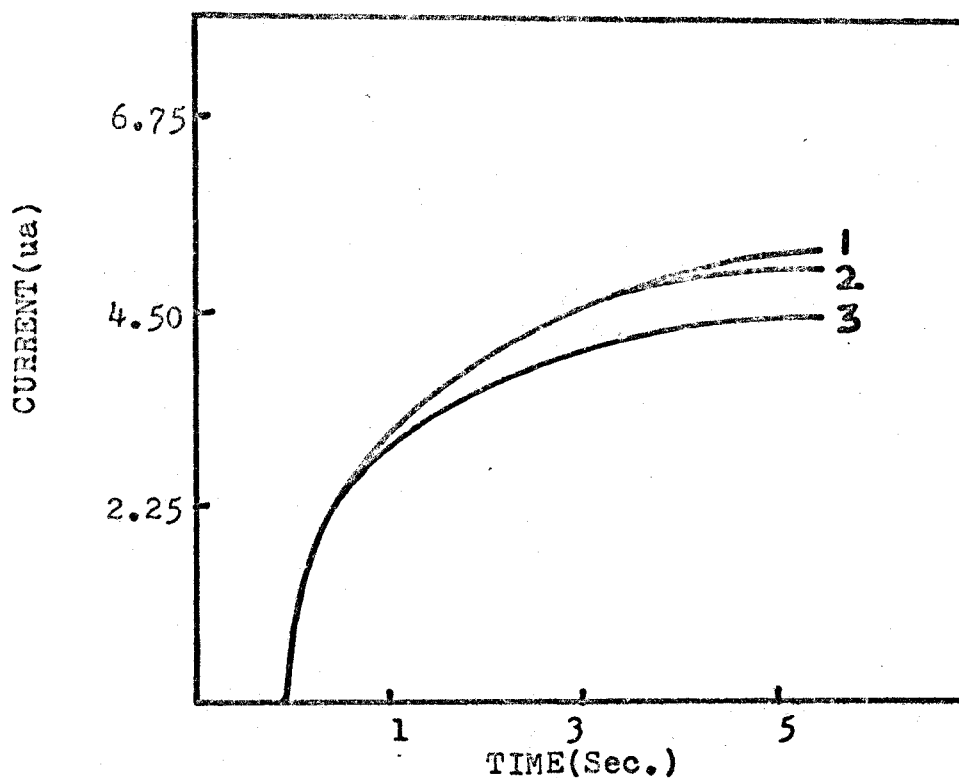


FIGURE 42: $i-t$ curves in case of Cu-Tetren system containing (1) 0; (2) $3.42 \times 10^{-4} \text{ M}$; (3) $2.05 \times 10^{-3} \text{ M}$ Sodium octyl sulfate.

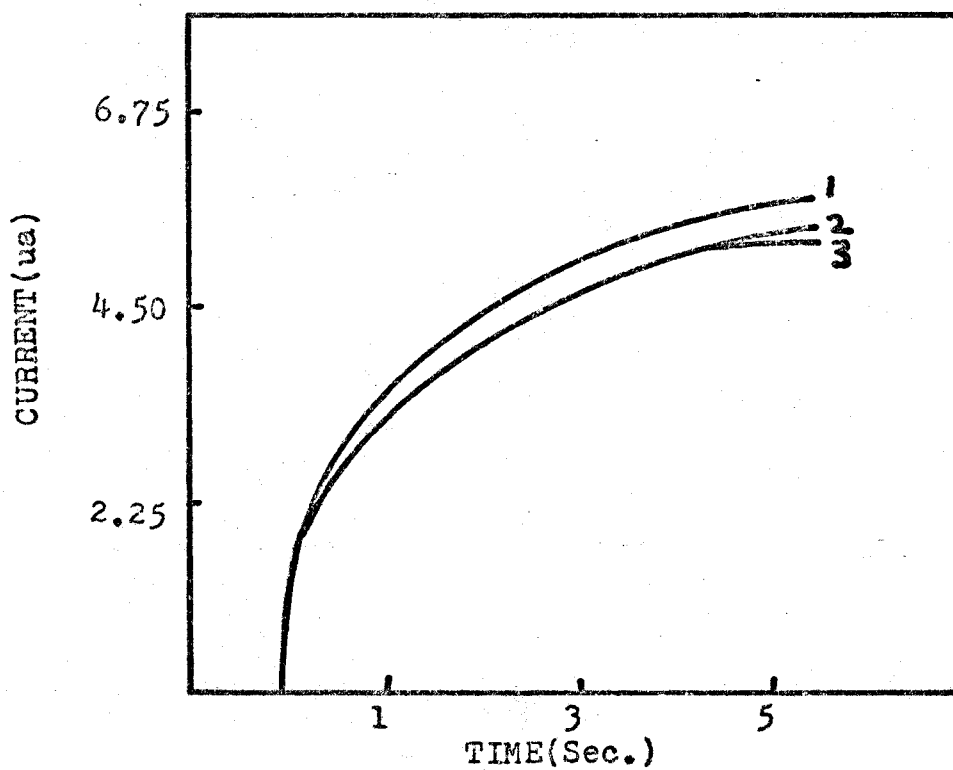


FIGURE 43: $i-t$ curves in case of Cu-Tetren system containing (1) 0; (2) $5.68 \times 10^{-5} \text{ M}$; (3) $1.83 \times 10^{-4} \text{ M}$ Sodium decyl sulfate.

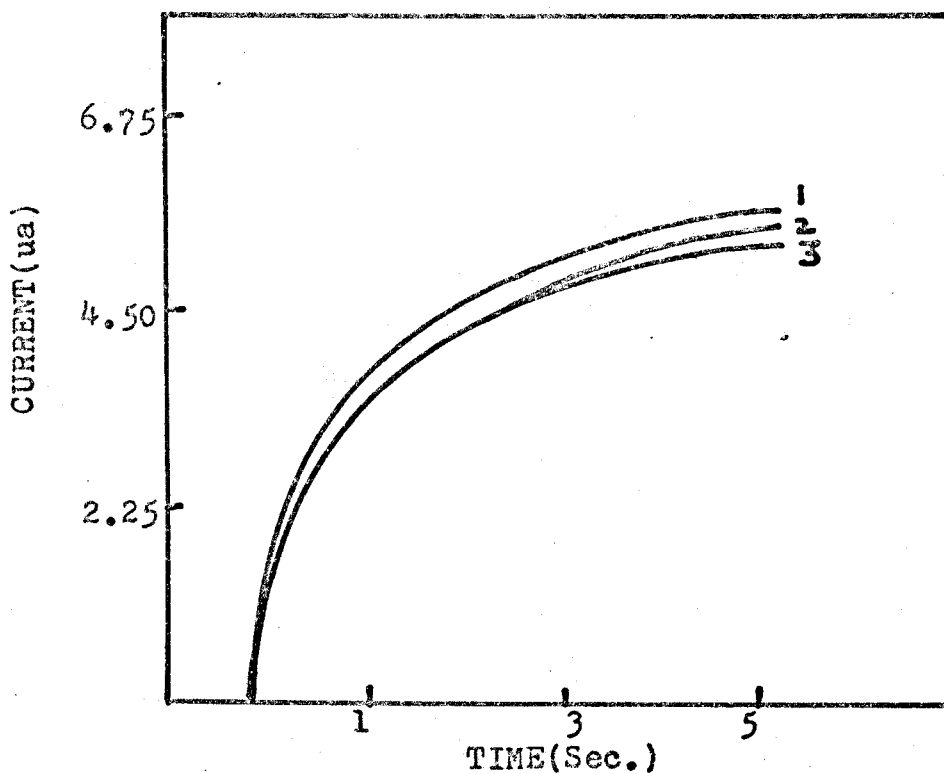


FIGURE 44: $i-t$ curves for a soln. containing $1 \times 10^{-3} \text{ M}$ Cu(II); $1 \times 10^{-2} \text{ M}$ Tetren in 0.16 M acetate buffer, pH 4.5 in presence of (1) 0; (2) $4.36 \times 10^{-5} \text{ M}$; (3) $1.50 \times 10^{-4} \text{ M}$ Sodium tetradecyl sulfate.

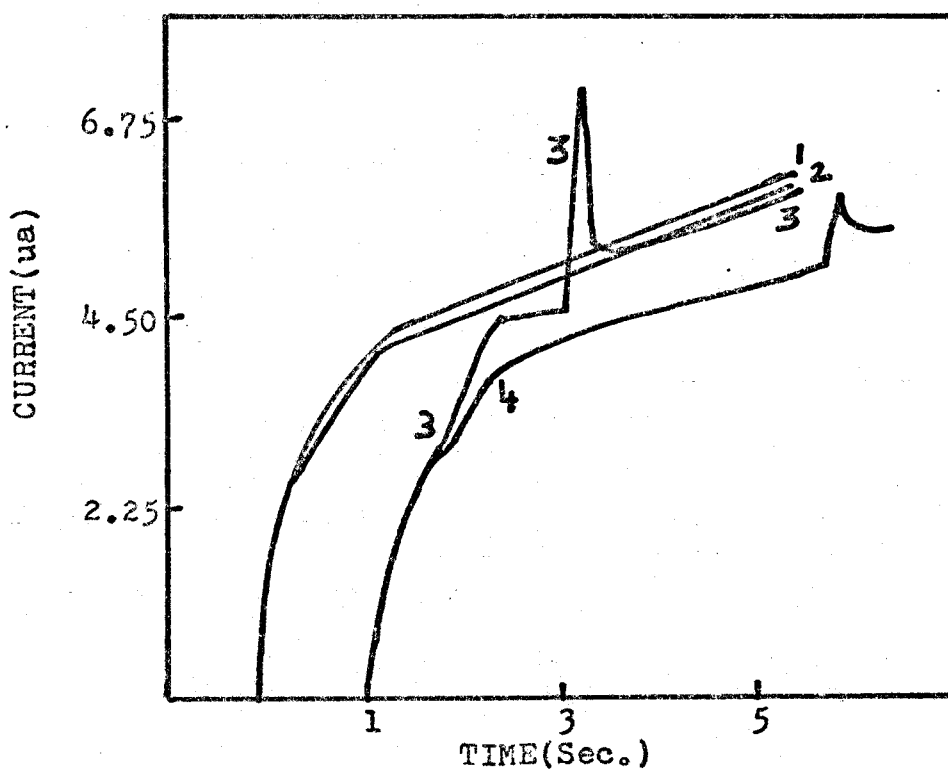


FIGURE 45: $i-t$ curves in the case of Cu-Tetren system containing (1) $1.45 \times 10^{-5} \text{ M}$; (2) $1.16 \times 10^{-4} \text{ M}$; (3) $2.31 \times 10^{-4} \text{ M}$; (4) $1.38 \times 10^{-3} \text{ M}$ Sodium hexadecyl SO_4 .

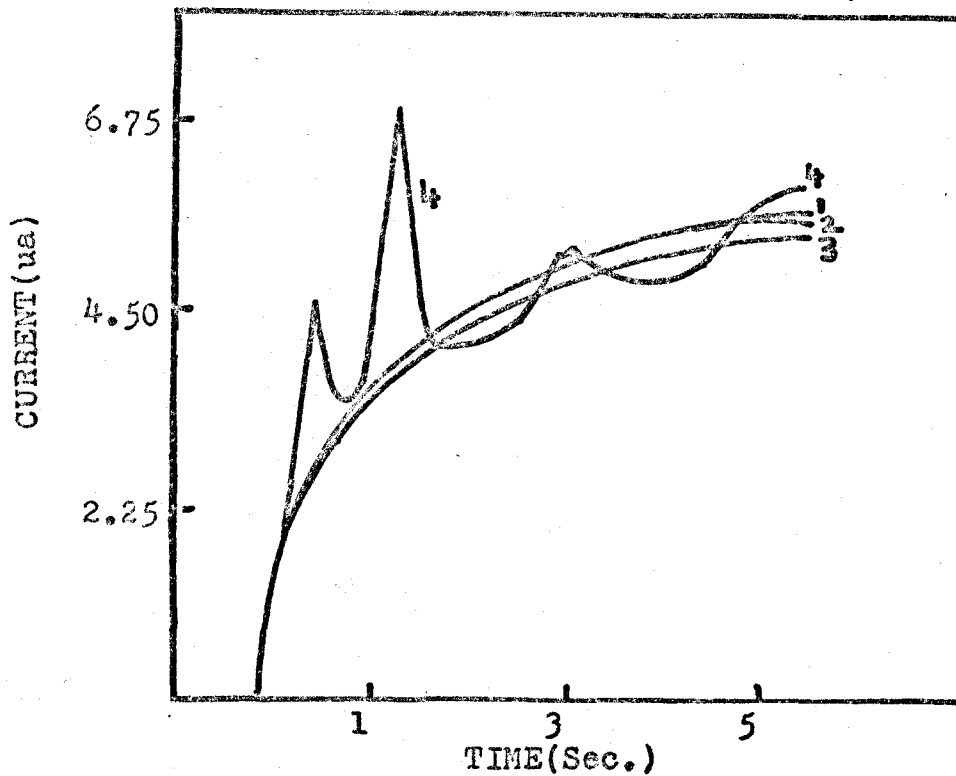


FIGURE 46: $i-t$ curves in the case of Cu-Tetren system containing (1) $2.68 \times 10^{-5} \text{ M}$; (2) $1.07 \times 10^{-4} \text{ M}$; (3) $4.24 \times 10^{-4} \text{ M}$; (4) $8.34 \times 10^{-4} \text{ M}$ Sodium octadecyl sulfate.

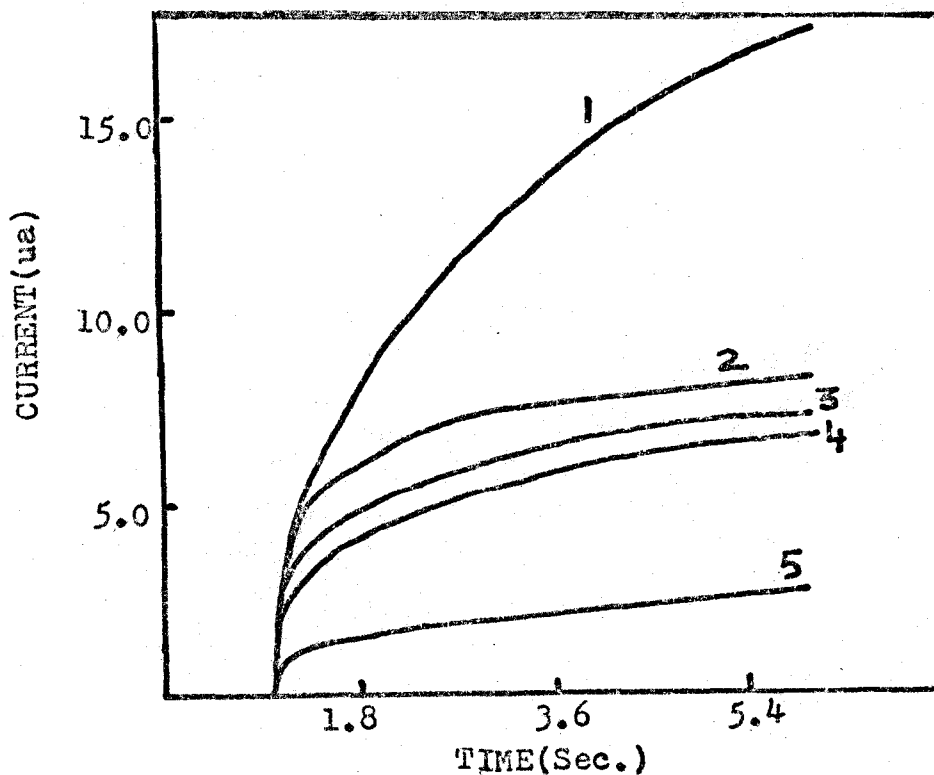


FIGURE 47: $i-t$ curves in the case of oxygen (in 0.01M KCl) maximum. (1) 0; (2) 2.15; (3) 4.27; (4) 4.33; (5) $5.94 \times 10^{-5} \text{ M}$ Sodium octyl sulfate.

to the electrode surface. Under these conditions (in the absence of polarographic maxima), the time at which the current fell to zero was related to the surface coverage by Koryta's equation (1). However, Koryta's equation does not apply in the region of polarographic maxima, because here the mass transfer is not diffusion-controlled, but, instead, takes place under hydrodynamic or streaming conditions. In other words, in the presence of maxima, the mass transfer is convection-controlled. Due to the turbulent streaming motion of the solution, the depolarizer and the surfactant are transported to the electrode surface by convection. To obtain an estimate of the amount of adsorption of surfactant during streaming in case of oxygen maximum, Barradas and Kimmerle (53) had derived an equation which related the surface coverage, diffusion coefficients of the depolarizer and the surfactant, total charge passed, and the concentrations of the depolarizer and the surfactant. Later, Phillips (54) modified the complicated equation of Barradas and Kimmerle and derived the following simplified equation:

$$\Gamma_s = D^{\frac{1}{2}} C \mathcal{U} / \delta' \quad \text{----- (II)}$$

In equation II, the terms Γ_s , D , C and \mathcal{U} have the same significance as in equation I. δ' is a constant (53). Phillips tested the validity of equation II in the case of the oxygen

maximum obtained by using 0.002M KCl solution. He used cysteine as the surfactant. On plotting \mathcal{V} (or t°) against $1/C$, he obtained a straight line passing through the origin and thus concluded that equation (II) which was derived to predict adsorption under streaming conditions, was adequate enough to describe the physicochemical situation corresponding to the oxygen maximum.

OXYGEN MAXIMUM

In order to check the behavior of sodium alkyl sulfates with regard to equation (II), current-time measurements were made. However as in the case of C-V plots, instead of using 0.002M KCl, an air-saturated 0.01M KCl solution was employed and current-time data was obtained at -0.30v (vs. SCE), a potential on the rising part of the polarographic maximum. The resulting current-time curves depicting the effect of various alkyl sulfates are shown in figures 47-52. Except in the case of sodium octyl sulfate, the current-time curves observed were similar to those obtained by Phillips (54). In all cases, in the early part of drop life the curves followed the same paths as those in the absence of surfactant, but as the surfactant concentration was increased gradually, the current fell to a constant value in shorter and shorter intervals. This behavior is easy to

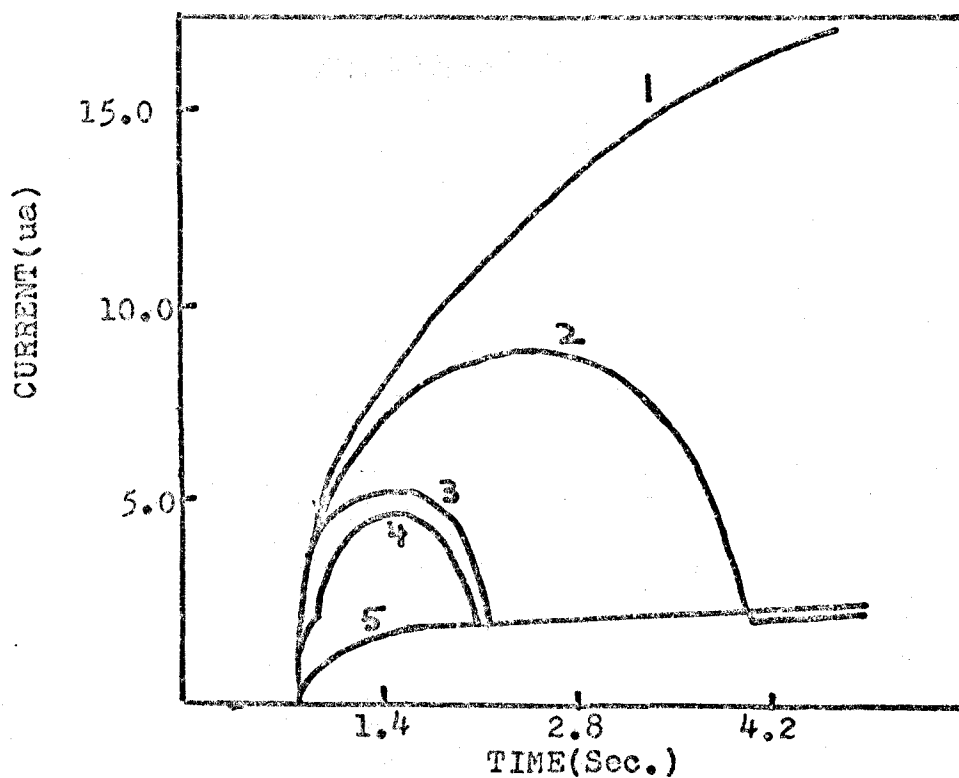


FIGURE 48: $i-t$ curves in the case of oxygen (in 0.01M KCl) maximum. (1) 0; (2) 1.92; (3) 3.83; (4) 4.84; (5) 9.58×10^{-6} M Sodium decyl sulfate.

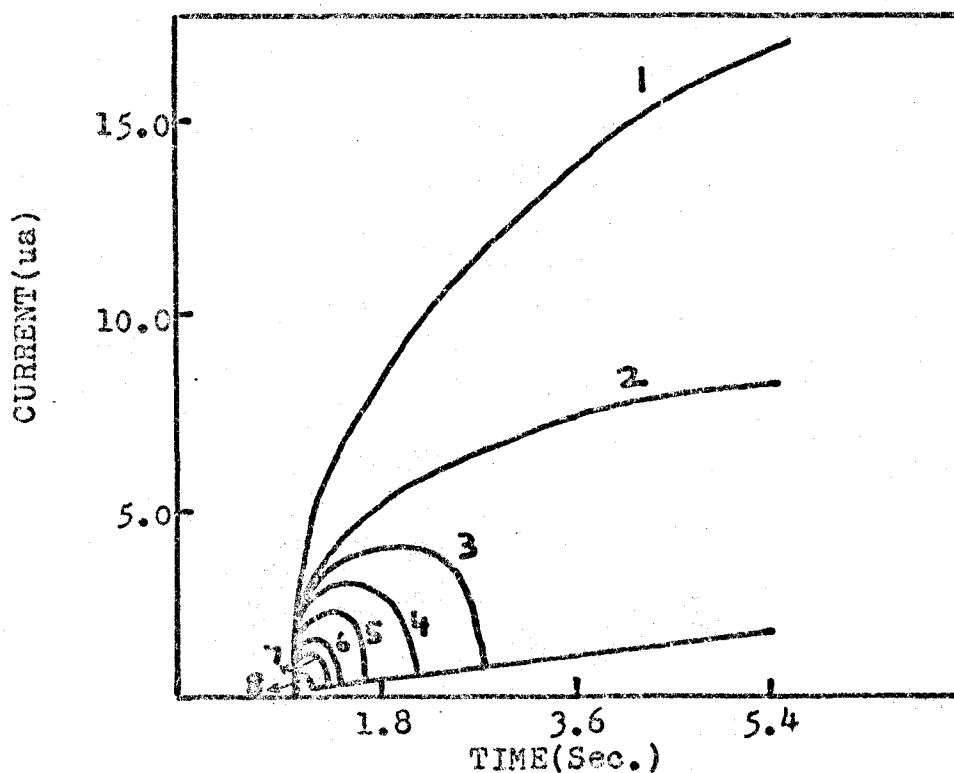


FIGURE 49: $i-t$ curves in the case of oxygen (in 0.01M KCl) maximum. (1) 0; (2) 1.73; (3) 3.45; (4) 5.18; (5) 6.90; (6) 8.65; (7) 10.37; (8) 17.2×10^{-6} M C_{12} .

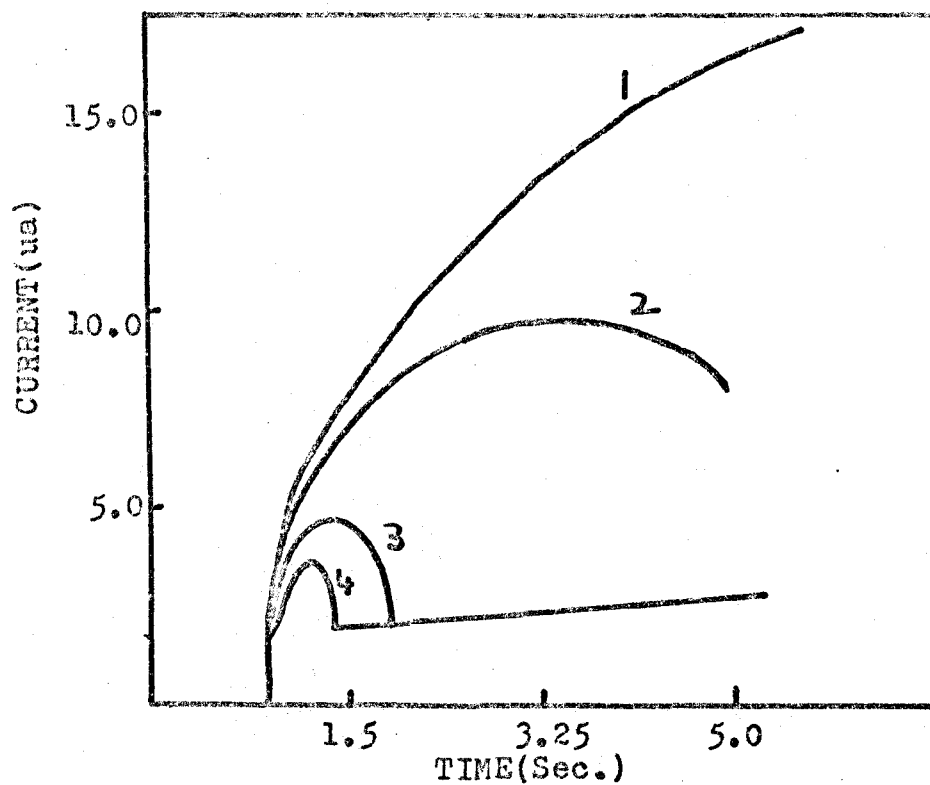


FIGURE 50: $i-t$ curves in the case of oxygen (in $0.01M$ KCl) maximum. (1) 0; (2) 2.21; (3) 6.30; (4) $9.45 \times 10^{-6} M$ Sodium tetradecyl sulfate.

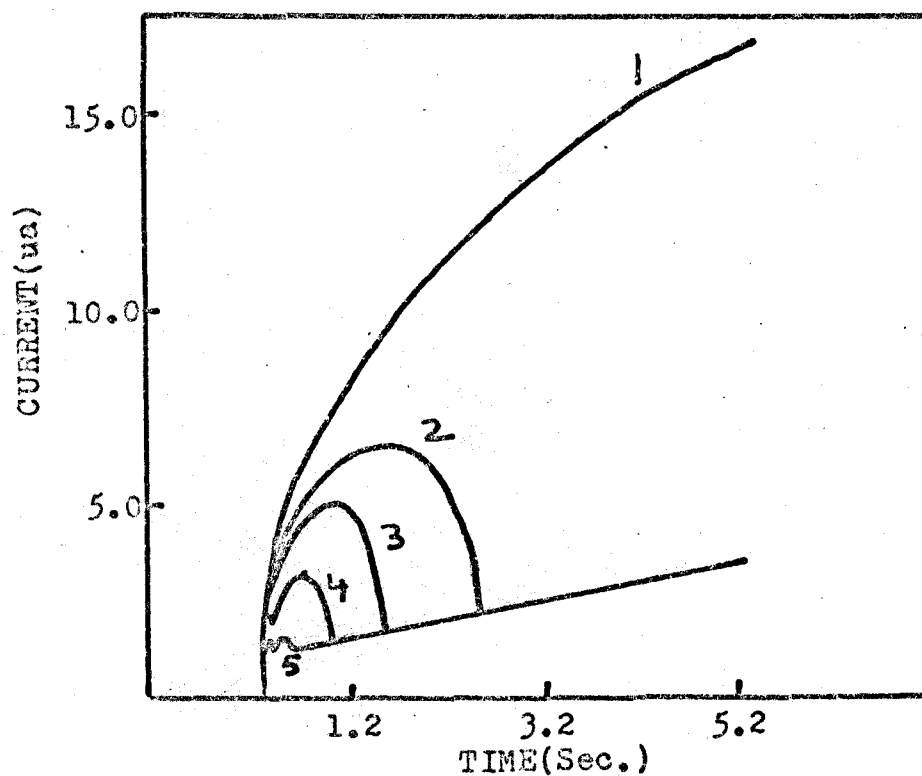


FIGURE 51: $i-t$ curves in the case of oxygen (in $0.01M$ KCl) maximum. (1) 0; (2) 0.73; (3) 1.45; (4) 2.33; (5) $8.73 \times 10^{-5} M$ Sodium hexadecyl sulfate.

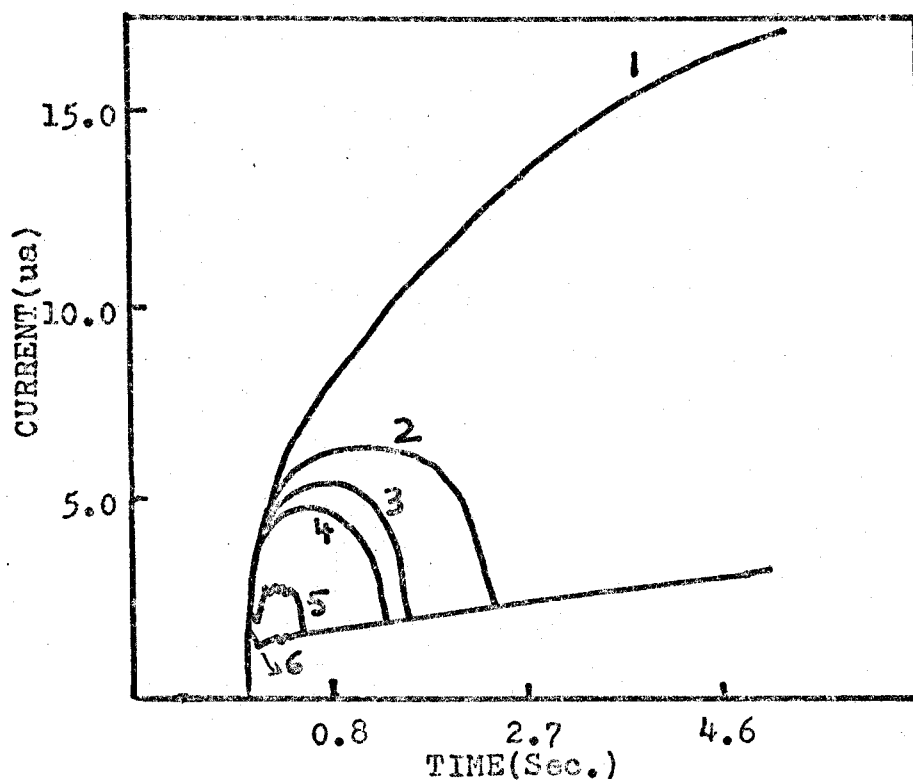


FIGURE 52: $i-t$ curves in the case of oxygen (in 0.01M KCl) maximum. (1) 0; (2) 1.35; (3) 2.68; (4) 4.03; (5) 8.06×10^{-5} M Sodium octadecyl sulfate.

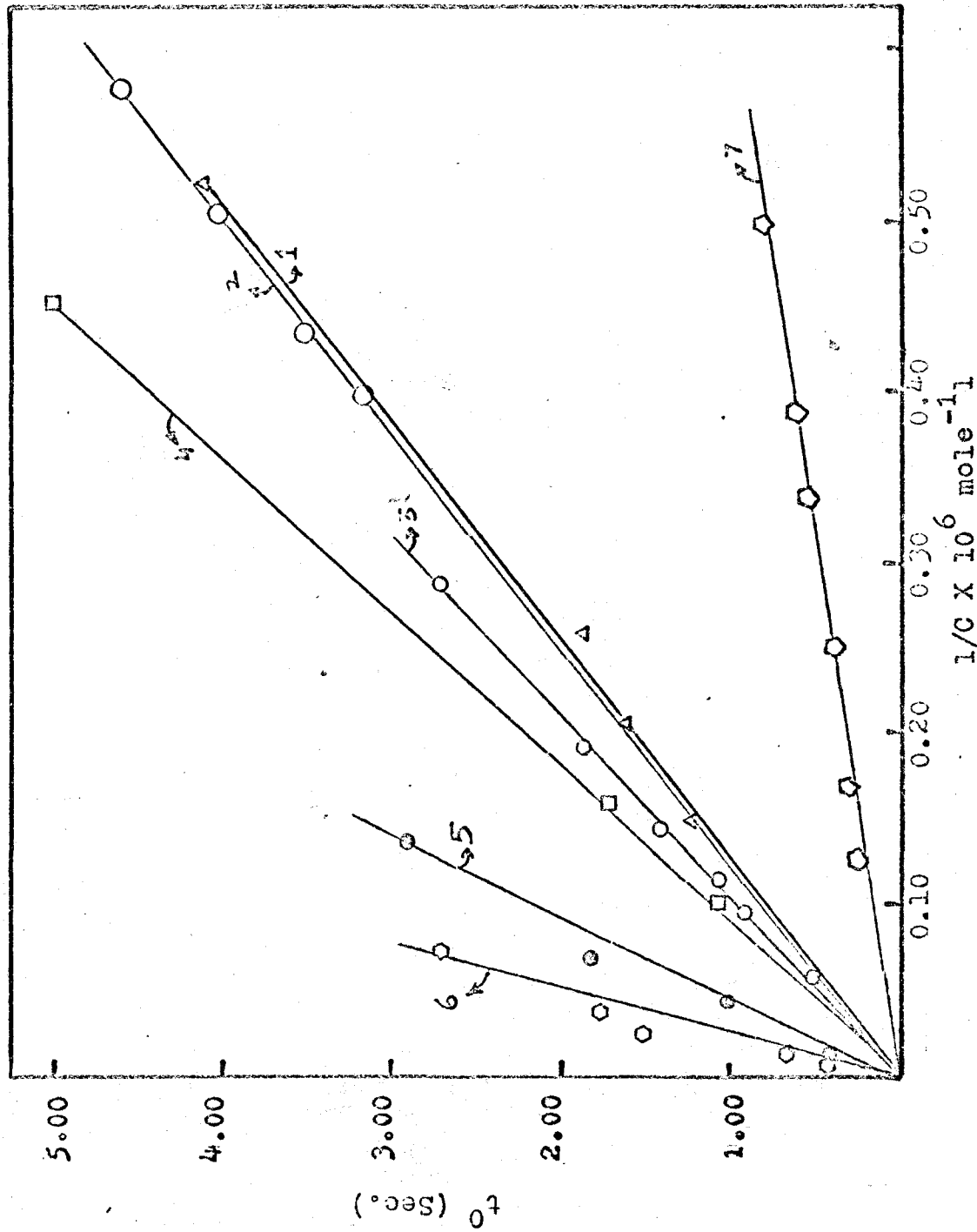
understand, because during the early part of the drop life, very little surfactant is adsorbed on the drop surface and this does not alter the streaming process or the shape of the $i-t$ curve. However, as the drop grows, enough surfactant reaches the electrode surface and it gradually suppresses the streaming motion and eventually stops it altogether.

In the case of sodium hexadecyl and octadecyl sulfates, at higher concentrations some distortion was caused in the $i-t$ curves. As explained earlier during the discussion of C-V plots. This behavior is caused by the turbidity which results on adding these long-chained paraffin salts to electrolyte solutions.

In order to obtain t° vs. $1/C$ plots, in every case, the time at which the current fell to the constant plateau was taken as a measure of t° . As shown in figure 53, straight lines passing through the origin were obtained in the case of decyl, dodecyl, tetradecyl, hexadecyl and octadecyl sulfates. As a further test of equation (II), the products of C and t° were calculated in each case and as can be seen in table 7, were found to be reasonably constant in case of decyl, dodecyl and tetradecyl sulfates. The quantity Ct° was not constant in case of hexadecyl and octadecyl sulfates and this could be due to the distortions as reported above. Due to the different nature of $i-t$ curves of sodium octyl sulfate, the product Ct° could not be obtained. In the case of

FIGURE 53

Plot of data in table 7



Curve (1) Sod. decyl sulfate; (2) Sod. dodecyl sulfate (0.002M KCl); (3) Sod. dodecyl sulfate (0.01M KCl); (4) Sod. tetradecyl sulfate; (5) Sod. hexadecyl sulfate; (6) Sod. octadecyl sulfate

TABLE 7

<u>Surfactant</u>	$\frac{CX10^{+6}M}{(\text{moles/l})}$	$\frac{t^0}{(\text{Sec.})}$	$\frac{Cxt^0 \times 10^{+6}}{(\text{moles-sec./l})}$	$\frac{10^{-6}/C}{(\text{mole}^{-1}l)}$
1. Sod. decyl sulfate:	1.92	4.10	7.87	0.522
	3.83	1.85	7.10	0.261
	4.85	1.60	9.20	0.207
	6.66	1.22	9.20	0.151
	3.45	2.70	9.35	0.290
	5.18	1.85	9.59	0.193
	6.90	1.40	9.66	0.145
	8.64	1.05	9.07	0.116
	10.37	0.90	9.34	0.097
	17.22	0.50	8.62	0.058
(Data with 0.002M KCl)	1.73	4.60	7.96	0.578
	1.98	4.00	7.92	0.506
	2.30	3.50	8.05	0.435
	2.50	3.15	7.87	0.40
2. Sod. dodecyl sulfate: (Data with 0.01M KCl)				

continued on next page

TABLE 7 (Contd.)

3. Sod. tetradecyl sulfate:	2.21	5.00	11.05	0.453
	6.30	1.70	10.70	0.159
	9.47	1.05	9.95	0.106
4. Sod. hexadecyl sulfate: (Data with 0.01M KCl)	14.55	1.80	26.2	0.069
	7.27	2.90	21.1	0.137
	23.30	1.00	43.6	0.043
	87.30	0.40	34.92	0.012
(Data with 0.002M KCl)	19.90	0.80	15.92	0.050
	25.83	0.60	15.52	0.039
	29.80	0.55	16.38	0.034
	39.60	0.45	17.82	0.025
	59.20	0.32	18.94	0.017
	78.40	0.25	19.60	0.013
5. Sod. octadecyl sulfate:	13.46	2.70	36.35	0.074
	26.8	1.75	47.0	0.037
	40.3	1.50	60.5	0.025
	80.6	0.65	52.4	0.012
	152.0	0.40	60.8	0.007

sodium dodecyl and hexadecyl sulfates, $i-t$ data was obtained using air-saturated $0.002M$ KCl and t° vs $1/C$ plot in these cases also gave linear relationships.

Cu[(Tart)]^o MAXIMUM:

As reported in chapter (7), the reduction wave of Cu[(Tart)]^o complex is accompanied by a large maximum, which breaks off at -0.40 v (vs. SCE). To check the validity of equation(II) in case of this maximum due to the reduction of a complex ion, current-time measurements were made (at a constant potential of -0.25 v) using a $1 \times 10^{-3}M$ Cu(II) solution in $0.1M$ Tartrate buffer of pH, 4.0 both in the absence and presence of sodium alkyl sulfates. As expected, the shape of the $i-t$ curves (fig. 54-55) resembled those obtained earlier in case of oxygen maximum and t° vs $1/C$ plots (fig. 56) yielded straight lines passing through the origin. The experimental data is shown in table 8. The constancy of the product term (CXt°) and the linear relationship in the t° vs $1/C$ plot not only lend support to the validity of equation II, but also confirm the author's observation that the reduction of Cu[(Tart)]^o complex is accompanied by a maximum. As mentioned earlier, Schmid and Reilley (21) did not report the occurrence of such a maximum.

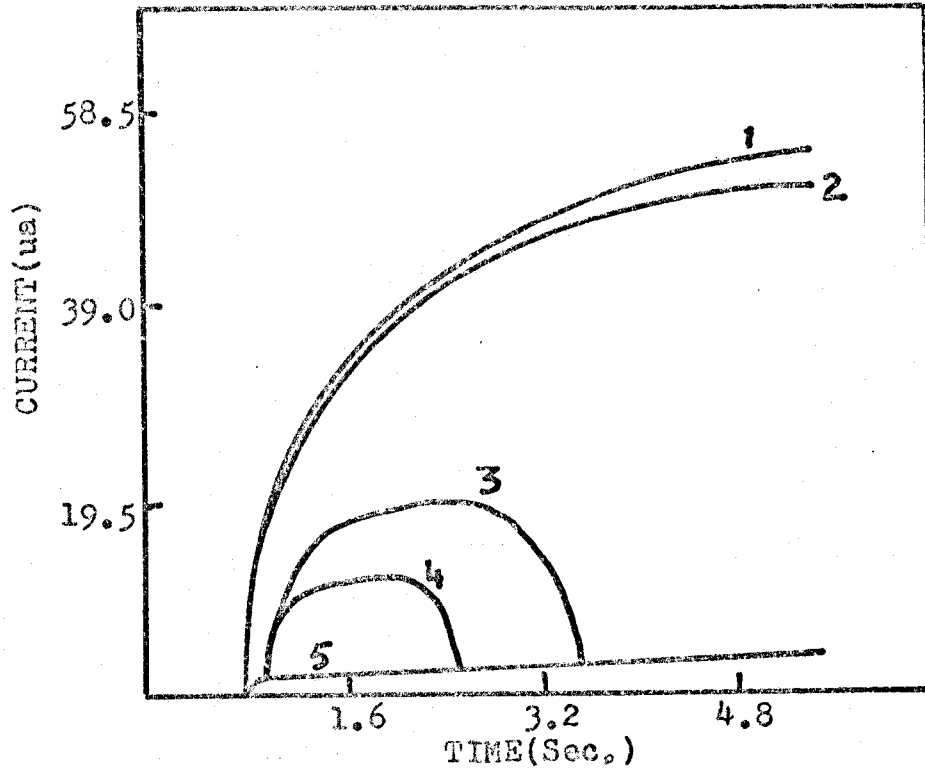


FIGURE 54A: $i-t$ curves at -0.25 v. for a solution containing 1×10^{-3} M Cu(II) in 0.1 M tartrate buffer, $\text{pH}=4$ (1) 0; (2) 1.92×10^{-6} M; (3) 9.58×10^{-6} M; (4) 1.34×10^{-5} M; (5) 1.91×10^{-5} M C_{10} .

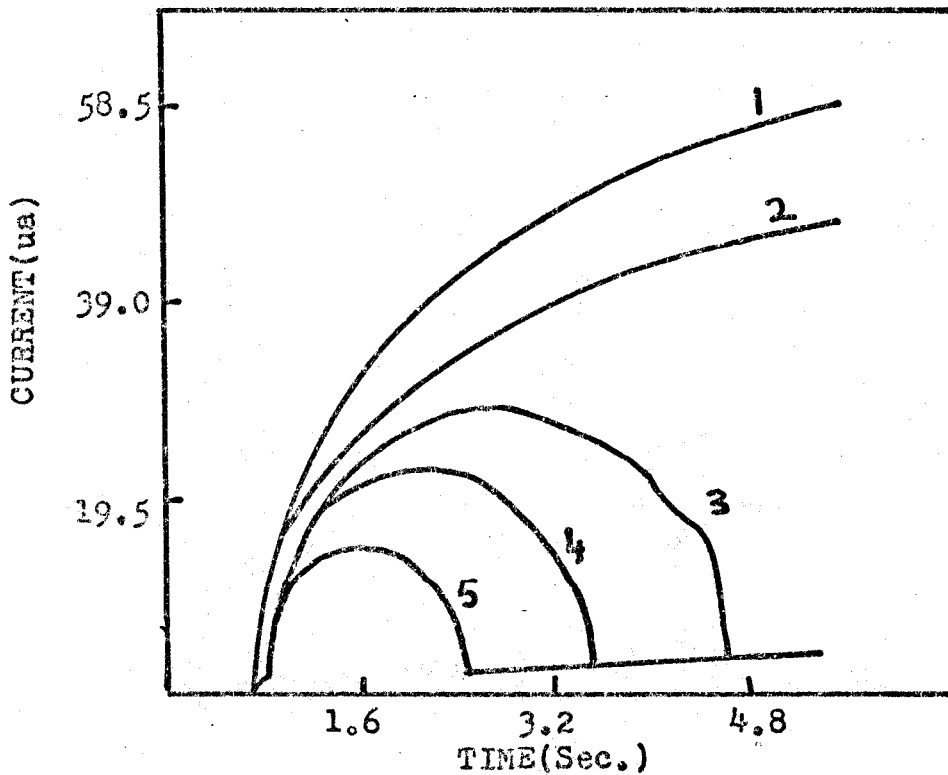


FIGURE 54B: $i-t$ curves at -0.25 v. for a solution containing 1×10^{-3} M Cu(II) in 0.1 M tartrate buffer, $\text{pH} = 4$ in presence of (1) 0; (2) 1.73×10^{-6} M; (3) 3.45×10^{-6} M; (4) 5.18×10^{-6} M; (5) 8.65×10^{-6} M Sodium dodecyl sulfate.

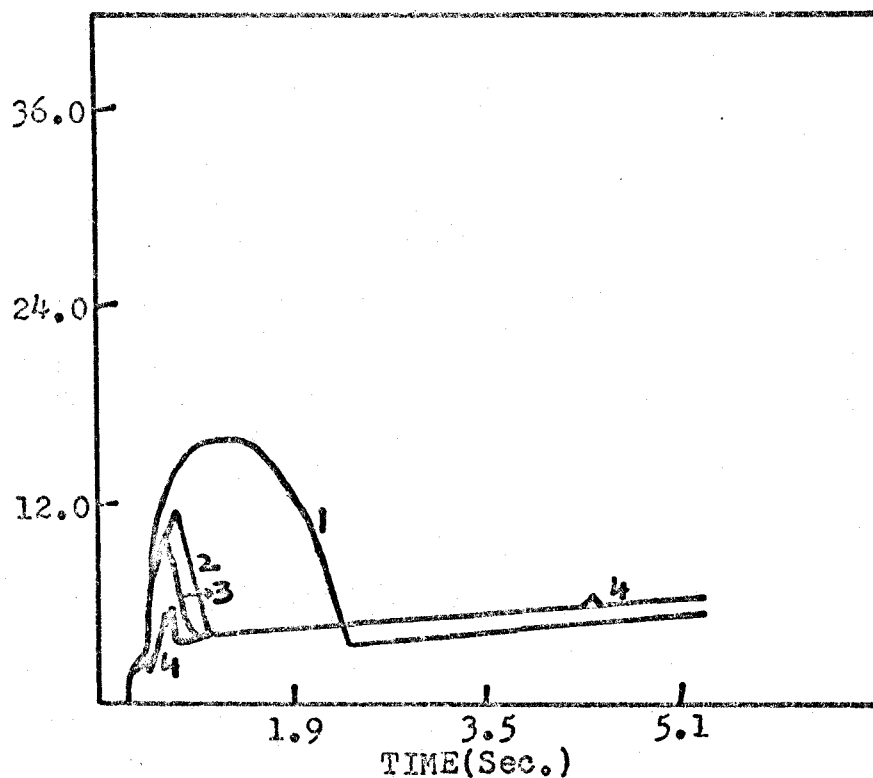


FIGURE 55A: $i-t$ curve at -0.25 v. for a solution containing $1 \times 10^{-3} \text{ M}$ Cu(II) in 0.1 M tartrate buffer, $\text{pH} = 4$ in presence of (1) $2.90 \times 10^{-5} \text{ M}$; (2) $5.81 \times 10^{-5} \text{ M}$; (3) $8.65 \times 10^{-5} \text{ M}$; (4) $1.45 \times 10^{-3} \text{ M}$ Sodium hexadecyl sulfate.

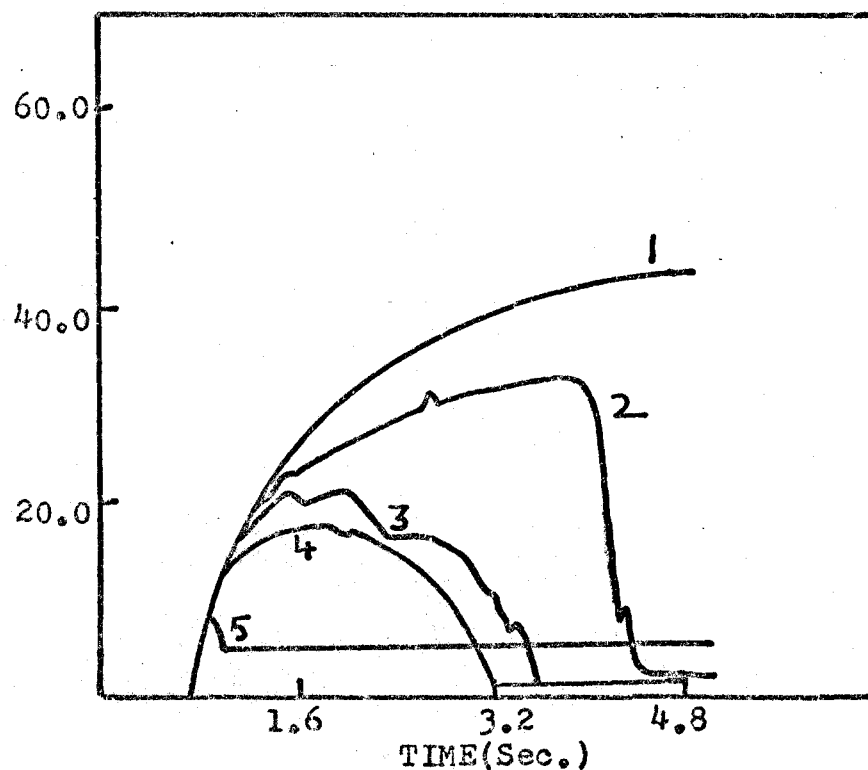
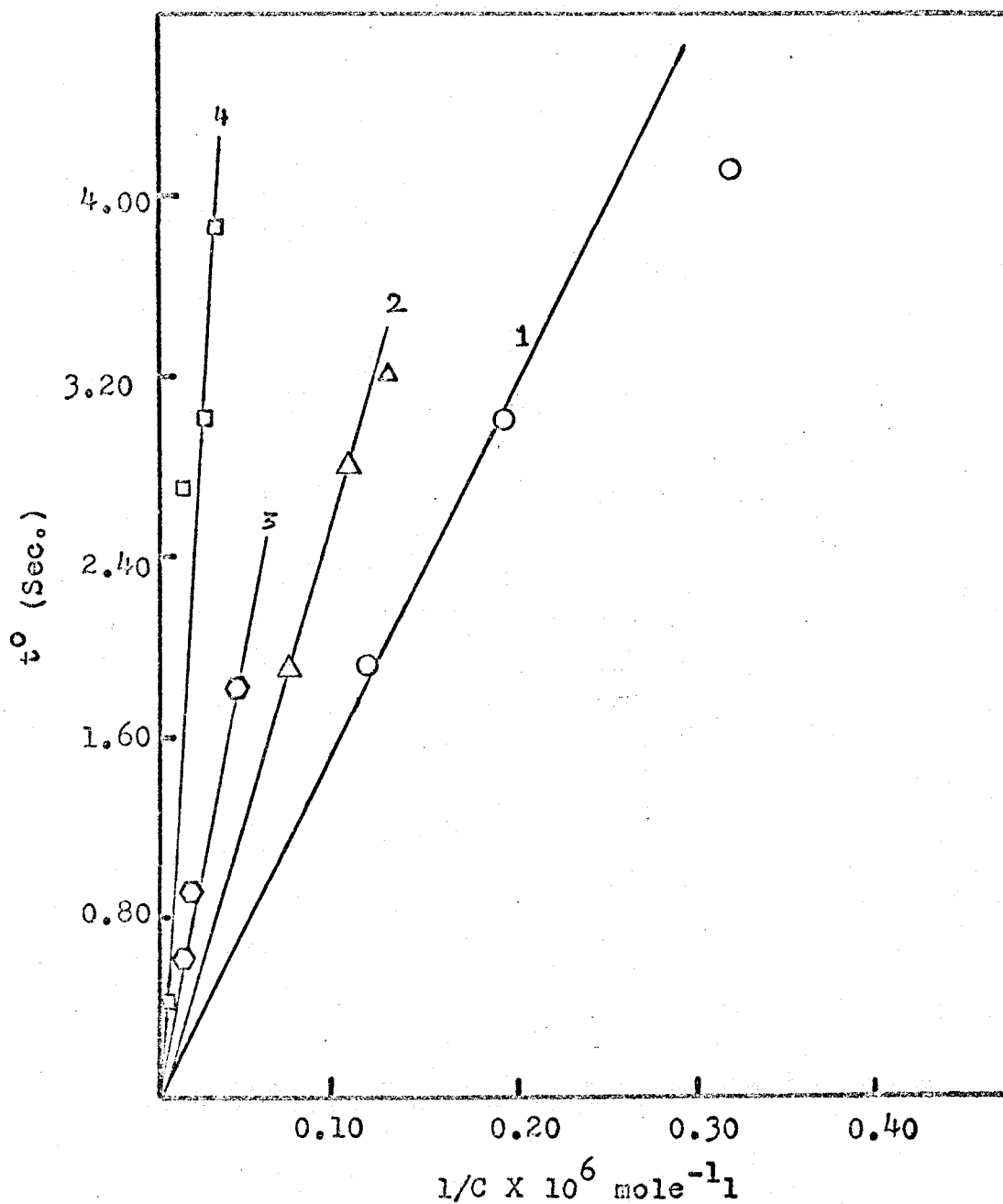


FIGURE 55B: $i-t$ curve at -0.25 v. for a solution containing $1 \times 10^{-6} \text{ M}$ Cu(II) in 0.1 M tartrate buffer, $\text{pH} = 4$. (1) $6.72 \times 10^{-6} \text{ M}$; (2) $1.35 \times 10^{-5} \text{ M}$; (3) $4.03 \times 10^{-5} \text{ M}$; (4) $8.06 \times 10^{-5} \text{ M}$; (5) $2.66 \times 10^{-4} \text{ M}$ Sodium octadecyl sulfate.

Plot of data in table 8



Curve(1)Sod. dodecyl sulfate (2)Sod. decyl sulfate (3)Sod. hexadecyl sulfate (4)Sod. octadecyl sulfate.

TABLE 8

<u>Surfactant</u>	$CX10^{+6} M$	$t^{\circ}(\text{sec.})$	$CXt^{\circ} \times 10^{+6}$	$\frac{-\delta}{c}$
1. Sod. decyl sulfate:				
	7.32	3.20	25.10	0.13
	9.58	2.80	26.8	0.105
	13.40	1.90	25.5	0.075
	3.45	4.10	14.30	0.319
	5.18	3.0	15.5	0.193
	8.63	1.90	16.4	0.116
	29.05	1.80	52.30	0.0416
	58.10	0.90	52.30	0.0172
	86.50	0.60	51.90	0.0116
	33.45	3.85	12.88	0.030
	40.30	3.00	12.09	0.025
	80.60	2.70	21.8	0.0124
	266.0	0.40	106.4	0.038
2. Sod. dodecyl sulfate:				
3. Sod. hexadecyl sulfate:				
4. Sod. octadecyl sulfate:				

LEAD MAXIMUM:

The lead maximum was studied in the presence of sodium decyl, dodecyl and tetradecyl sulfates. The shape of the current-time curves in all the three cases was somewhat similar to that obtained in the case of the oxygen maximum and the sodium decyl sulfate (fig. 37a). Since due to the presence of surfactants the current did not drop to zero, Phillips' equation could not be applied rigorously. However, using the values of time at the inflection points of the curves, t vs. $1/C$ plots were obtained. In the case of decyl and tetradecyl sulfates reasonably good straight lines passing through the origin were obtained. The data in the case of dodecyl sulfate yielded points and few of these were widely scattered.

IX. CONCLUSIONS AND SUMMARY

Sodium alkyl sulfates, which are anionic surfactants, contain polar and non-polar groups. As a result, they show surface active behavior and adsorb at electrode-solution interfaces. This property of sodium octyl, decyl, dodecyl, tetradecyl, hexadecyl and octadecyl sulfates was utilized to suppress polarographic maxima due to oxygen and Pb(II), Ni(II), UO_2^{2+} , Tl^+ , Se(IV) and CdI_4^{2-} ions. In order to compare their behavior and to investigate their physico-chemical properties as a group, their effect on polarographic waves both in the presence and absence of maxima was studied. To understand the mechanism by which the anionic surfactants suppress various kinds of maxima, both current-voltage plots and current-time curves were studied. The adsorption behavior was further compared by carrying out electrocapillary measurements. On the basis of the data obtained, the following conclusions are made:

Sodium octyl sulfate is very weakly adsorbed on the mercury surface. This is evident from its high maximum suppression point (MSP) values and its very small effect on electrocapillary (EC) and current-time curves. Sodium decyl and dodecyl sulfates are strongly adsorbed and tend to flatten the E-C curve. The addition of tetradecyl, hexadecyl and octadecyl sulfates to potassium chloride solution

resulted in turbidity, which sharply reduced the adsorbability of these three surfactants. By carrying out electrocapillary measurements in 0.2M acetate buffer, the turbidity was avoided in case of tetradecyl sulfate. As a result of this, the latter was very strongly adsorbed on the mercury surface and decreased the interfacial tension (droptime) even more than the dodecyl sulfate. The appearance of turbidity is due to the formation of micelles in the presence of the relatively high concentration of supporting electrolytes. During MSP determinations, the presence of this turbidity resulted in such erratic droptimes that reproducible polarographic waves could not be obtained. The turbidity formation also resulted in high MSP values in the case of tetradecyl, hexadecyl and octadecyl sulfates. When sodium and lithium chlorides were employed as supporting electrolytes, no turbidity formation was observed in the case of tetradecyl sulfate and the amount of turbidity in the case of hexadecyl and octadecyl sulfates was considerably reduced. On the basis of this observation, it is clear that turbidity is caused by 1) formation of an insoluble potassium salt of the alkyl sulfates 2) formation of micelles.

Contrary to what was reported by Colichman, namely, that MSP values and values of the critical micelle concentration (CMC) for surfactants are essentially identical, the MSP values of the alkyl sulfates were found to depend

strongly on the potential at which the maximum occurs. Since the anionic surfactants are strongly adsorbed in the vicinity of the electrocapillary maximum, the MSP values for the positive maxima of oxygen, lead and UO_2^{2+} ions were far below the experimentally determined CMC values for the same alkyl sulfates under the same conditions. When the alkyl sulfates were used to suppress the maxima on the reduction waves of increasingly negative half-wave potential, larger and larger amounts of surfactants were required for suppression and as a result, the MSP values in case of Ni^{2+} , Se(IV) and CdI_4^{2-} maxima came out to be very high. The high MSP values in case of negative maxima are ascribed to the following two reasons: (a) At high negative potentials, due to similarity of charges on mercury drop and the surfactants, the adsorption of the suppressor on the mercury drop is hindered, or in other words, the surfactants are desorbed when the potential is sufficiently negative; (b) the negative charge and the large size of the depolarizer in the case of CdI_4^{2-} ion, hinders its penetration into the adsorbed layer of the surfactants.

The addition of surfactants to solutions containing positively charged copper-Trien and Tetren complexes did not cause any appreciable change in the diffusion current and also it did not effect the half-wave potentials. However,

at higher surfactant concentrations, the upper part of the reduction wave was slightly drawn out indicating that the electrode reaction becomes irreversible. The turbidity which resulted on adding sodium alkyl sulfates to Cu-Tetren and Cu-Trien solutions, is due to the formation of an insoluble salt between the tetren or trien and the paraffin chain ion of the surfactants. The reduction waves of $\text{Cu}[(\text{trien})]^{2+}$ and $\text{Cu}[(\text{tetren})]^{2+}$ complexes were accompanied by maxima, which, except in the case of octadecyl sulfate were easily suppressed. Likewise, the reduction wave of $\text{Cu}(\text{tart})^{\circ}$ complex was accompanied by a large maximum. As in other cases the addition of surfactants shifted the break-off potential of the maxima to more positive potentials. In each case, after the maximum was completely suppressed, addition of more surfactant did not effect the half-wave potential or the limiting current. The shift in the break-off potential for the same concentration of surfactant followed the following order: $\text{C}_{12} > \text{C}_{10} > \text{C}_8$. This proves that with increase in the carbon chain-length, adsorption of surfactant increases.

The addition of sodium alkyl sulfates to Cu-EDTA solution caused a split in the reduction wave and on increasing the surfactant concentration further, the $E_{1/2}$ was shifted to more negative potentials. In the presence of large surfactant concentrations, a penetration wave was obtained. This is because the depolarizer and the adsorbed

layer of surfactant have the same charge. Thus, the negative Cu-EDTA complex has to cross a potential energy barrier before being reduced at the DME.

Unlike the other surfactants, a very high concentration (0.091%) of sodium octyl sulfate was required to produce the penetration wave, which again shows that this surfactant is not adsorbed on the mercury surface very strongly.

The critical micelle concentrations of sodium alkyl sulfates were determined both in water and in the presence of electrolytes. The CMC determinations were carried out using two methods: (1) The spectral dye method using Pinacyanol chloride and Rhodamine 6G (2) Electrocapillary curve method. The two methods yielded nearly identical results.

The distorting effects of sodium alkyl sulfates on reduction waves of complexes were studied with the help of current-time ($i-t$) curves. The data in case of Cu-EDTA complex and sodium dodecyl and tetradecyl sulfates was obtained under diffusion controlled conditions and was found to correspond to Koryta's equation. Using an estimated value for the diffusion coefficient D values for dodecyl and tetradecyl sulfates were calculated. These D values were found to be comparable to those of eosin

and Tritons X-45, X-100 and X-305. Sodium octyl sulfate and sodium decyl sulfate did not cause any appreciable change in the shape of $i-t$ curves in the case of Cu-EDTA system. And erratic droptimes due to turbidity formation in the case of hexadecyl and octadecyl sulfates prevented accurate measurement of t^0 , the time in which the current falls to zero.

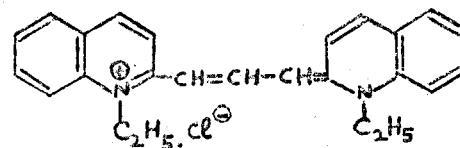
The current-time curves in the case of positively charged Cu-Tetren and Cu-Trien complexes were not affected much by the addition of sodium alkyl sulfates.

The current-time studies were also carried out under streaming conditions in the case of oxygen maximum and the maximum on the reduction wave of $\text{Cu}(\text{Tart})^0$ complex. In both cases, the data was found to correspond to Phillips' equation.

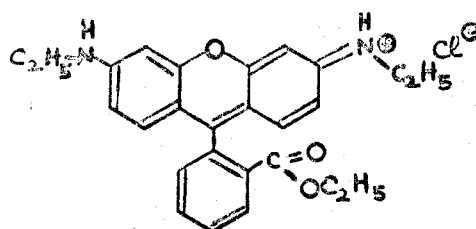
In the case of the lead maximum even in the presence of surfactants, the current did not drop to zero and so the Phillips' equation could not be applied too rigorously.

APPENDIX I

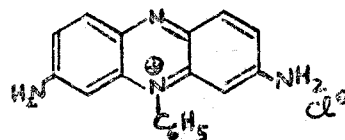
1) Pinacyanol chloride



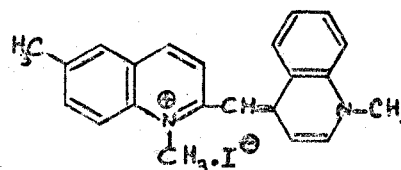
2) Rhodamine 6G



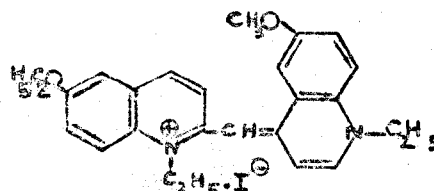
3) Phenosafranin



4) Pinaverdol



5) Pinachrom



APPENDIX II

Procedure and conditions used for taking current-time pictures.*

1) Key 1 was kept pressed during the entire experiment.

2) Before each experiment the manual polarograph (set-up enclosed in dotted lines) was standardized by setting the potentiometer at 1.019 v. --- potential of the standard Cd cell.

3) The following settings were employed for taking the pictures:

(A) On Camera: (i) Position "T"; Sensitivity equal to 1 mv/cm. "f" setting = 16. Exposure time = 10 sec. For taking picture at setting "T", the shutter is pressed and then released immediately for the length of time for which the exposure is needed (in the present case, this was 10 seconds). At the end 10 seconds, shutter is pressed once more and then again released instantly. After this, the white and yellow tabs in the film cartridge are pulled straight out one after the other. After pulling the yellow tab, a developing time of approximately 20 seconds is given and then the picture is separated from the chemical-coated disposable paper. (ii) Position "B"; for taking pictures at this setting the shutter is kept depressed for

*See schematic diagram after two pages.

the length of time the exposure is needed and then released at the end of that period (10 seconds).

(B) On Oscilloscope panel:

Upper focus = 4.5

Intensity = 4.5

Intensity balance = 5.0 or 5.5

Power & Scale illumination = 5.0 or 6.0

Trigger selector = "-"

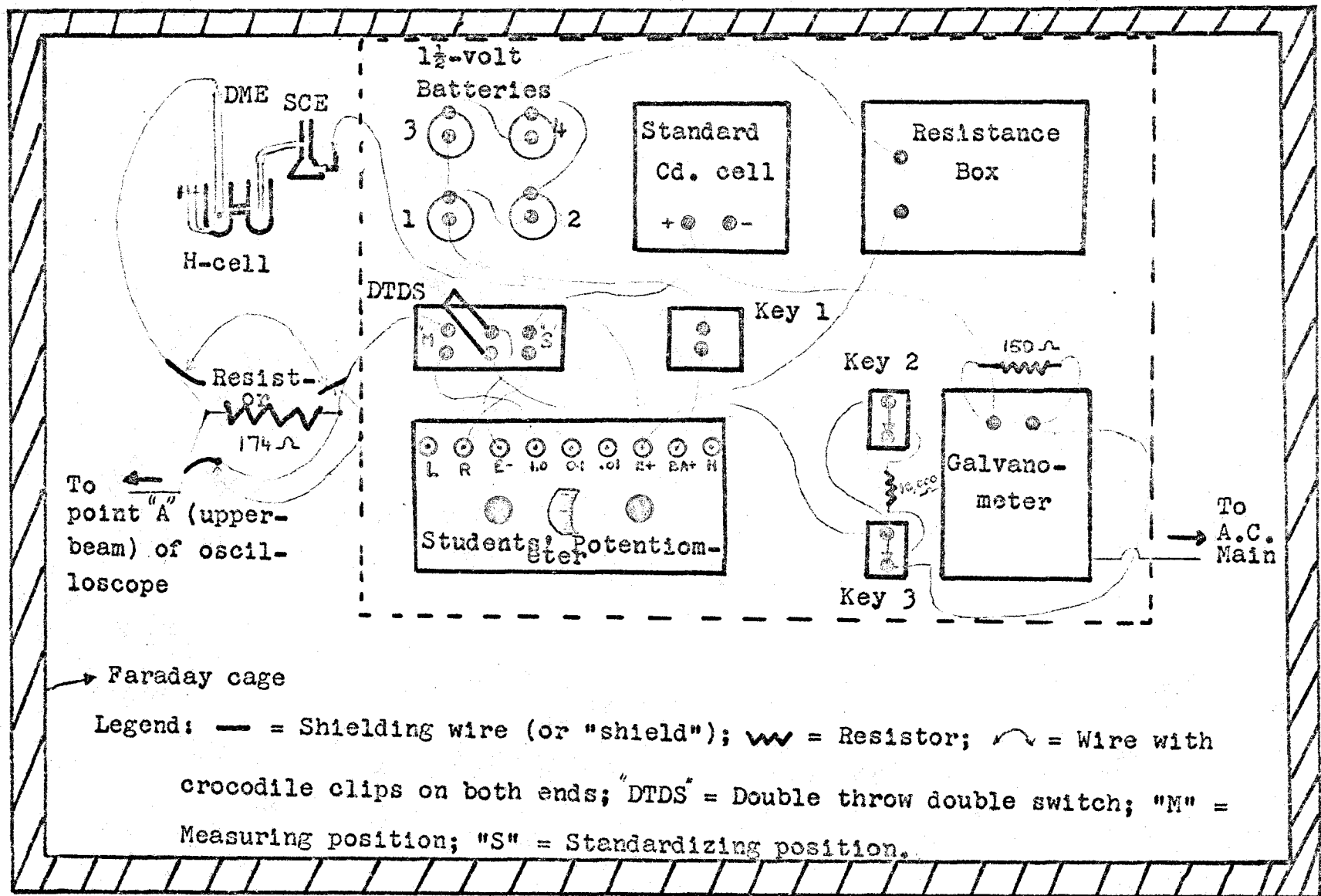
Line switch (knob) = at upper AC

Triggering level = at "Automatic"

Upper beam = at "A" on "DC" half side

Beam sweep rate = 1 cm/sec.

Note: For schematic diagram showing the circuit, see the next page.



Schematic diagram showing the set-up used for obtaining current-time curves.

BIBLIOGRAPHY

1. E. L. Collichman; J. Am. Chem. Soc. 72, 4036 (1950).
2. M. L. Nichols and B. H. Kindt; Anal. Chem. 22, 785 (1950).
3. E. K. Goette; J. Colloid Sci. 4, 459 (1949).
4. R. Tamamushi and T. Yamanaka; Bull. Chem. Soc. Japan. 28, 673 (1955).
5. W. U. Malik, P. Chand and S. M. Saleem; Talanta 15, 133 (1968).
6. David C. Grahame; Chem. Rev. 41, 441 (1947).
7. Jaroslav Heyrovsky and J. Kuta; Principles of polarography, Academic Press, New York, N. Y. 1966 (P 20).
8. J. Heyrovsky and M. Dillinger; Coll. Czech. Chem. Comm. 20, 626 (1930).
9. J. Heyrovsky; Actualities Scientifiques et Industrielles, No. 90, Paris, (1934).
10. A. N. Frumkin, B. Burns; Acta Physicochim; U.R.S.S; 1, 232 (1934).
11. T. A. Kryukova and B. N. Kabanov; J. Gen. Chem. U.S.S.R; 21, 953, 1335 (1947); Cf Chem. Abstr. 40, 3345 (1946).
12. T. A. Kryukova; J. Phys. Chem. U.S.S.R; 21, 365 (1947); Cf. Chem. Abstr. 41, 6160e (1947).
13. L. Meites; Polarographic Techniques; 2nd Ed., Inter-

Science Publishers, New York, N. Y. (P305).

14. A. N. Frumkin and Levich; Zhur. Fiz. Khim 21, 689, 1335 (1947).
15. A. N. Frumkin; Zhur. Fiz. Khim; 29, 1318 (1955).
16. V. Stackelberg and R. Doppelfeld; Advances in Polarography, Vol. 3, Pergamon Press, London 1960 (P8).
17. M. Von Stackelberg; H. J. Antweiler and L. Kieselback, Z. Elektrochem. 44, 663 (1938).
18. J. Heyrovský; Chem. Zvesti; 10, 477, 483 (1956).
19. D. Ilkovic; Coll. Czech. Chem. Comm. 6, 498 (1934).
20. I. M. Kolthoff and J. J. Lingane; Polarography, 2nd ed; Vol. 1, Interscience Publishers, New York, London, 1952 (chap. x).
21. R. W. Schmid and C. N. Reilley, J. Am. Chem. Soc. 80, 2087 (1958).
22. J. Powney and C. C. Addison; Trans. Far. Soc. 33, 1243 (1937).
23. Ref. 20, Page 565.
24. J. J. Lingane and L. W. Niedrach; J. Am. Chem. Soc. 71, 196 (1949).
25. W. U. Malik and Puran Chand; Anal. Chem. 37, 1592 (1965).
26. Ref. 20, Page 509.
27. Ref. 20, Page 157.

28. Hans. B. Jonassen & J. A. Bertrand et. al; J. Am. Chem. Soc. 79, 4279 (1957).
29. C. P. Roe & P. D. Brass; J. Am. Chem. Soc. 76, 4703 (1954).
30. E. Jacobsen & G. Kalland; Anal. Chim Acta. 30, 240 (1964).
31. J. W. McBain, Trans. Far. Soc. 9, 99 (1913).
32. R. S. Stearns, H. Cppenheimer, E. Simon & W. D. Harkins; J. Chem. Phys. 15, 496 (1947).
33. M. L. Corrin & W. D. Harkins; J. Am. Chem. Soc. 69, 679 (1947).
34. G. S. Hartley and D. F. Runnicles; Proc. Roy. Soc. A168, 420 (1938).
35. J. W. McBain & A. P. Brady; J. Am. Chem. Soc. 65, 2072 (1943).
36. R. J. Williams, J. N. Phillips & K. J. Mysels; Trans. Far. Soc. 51, 728 (1954).
37. K. A. Wright & H. V. Tartar; J. Am. Chem. Soc. 61, 544 (1939).
38. K. Hess, W. Phillippoff and H. Kiessig; Kolloid-Z 88, 40 (1939).
39. A. E. Alexander; Trans. Far. Soc. 38, 248 (1942).
40. R. W. Mattoon, R. S. Stearns and W. D. Harkins; J. Chem. Phys. 16, 644 (1948).
41. C. W. Carr, W. F. Johnston and I. M. Kolthoff; J. Phys.

- Colloid. Chem. 51, 636 (1947).
42. H. A. Scheraga & J. K. Backus; J. Am. Chem. Soc. 73, 5108 (1951).
43. O. R. Howell & H. G. B. Robinson; Proc. Roy. Soc.; A155, 386 (1936).
44. G. S. Hartley; J. Chem. Soc. 1968 (1938).
45. E. D. Goddard, O. Harva and T. G. Jones; Trans. Far. Soc. 49, 980 (1953).
46. M. L. Corrin, & W. D. Harkins; J. Am. Chem. Soc. 69, 683 (1947).
47. L. Meites and T. Meites; J. Am. Chem. Soc. 73, 177 (1951).
48. H. B. Jonassen, J. A. Bertrand, F. R. Groves & R. I. Stearns; J. Am. Chem. Soc. 79, 4279 (1957).
49. Handbook of Chemistry & Physics, 49th Ed. (1968-69) Page B-236.
50. R. L. Pecsok; Anal. Chem. 25, 561 (1953).
51. Ref. 7, Page 301.
52. J. Koryta; Collection Czech. Chem. Commun. 18, 206 (1953).
53. R. G. Barradas and F. M. Kimmerle; J. Electro Anal. Chem. 11, 163 (1966).
54. Sidney L. Phillips; Anal. Chem. 39, 679 (1967).
55. I. M. Kolthoff and Y. Okinaka; J. Am. Chem. Soc. 81, 2296 (1959).

56. N. Gunderson and E. Jacobsen; J. Electro Anal. Chem. 20, 13 (1969).
57. E. E. Dreger, G. I. Keim, G. D. Miles, Leo Shedlovsky and John Boss; Ind. Eng. Chem. 36, 610 (1944).
58. V. G. Levich; Physicochemical Hydrodynamics; Prentice-Hall, Inc, Englewood Cliffs, N. J. (1962), P532.
59. H. J. Antweiler, Z. Elektrochem. 43, 596 (1937), 44, 719, 831 and 888 (1938).
60. Ref. 7, Page 441.
61. D. R. Crow and J. V. Westwood; Polarography; Methuen and Co. Ltd; London, Page 41 (1968).
62. Ref. 7, Page 443.
63. C. S. Smith; Chemistry and Industry; September 3, 1949, Page 619.
64. D. Ilkovic; Coll. Czech. Chem. Comm. 8, 13 (1936).
65. Ref. 7, Page 451.
66. Ref. 58, Page 562.
67. H. B. Klevens; J. Phys. Chem. 51, 1143 (1947).
68. E. C. Lingafelter, O. L. Wheeler and H. V. Tartar, J. Am. Chem. Soc. 68, 1490 (1946).
69. B. D. Flockhart and A. R. Ubbelohde; J. Colloid. Sci 8, 428 (1953).
70. Ref. 13, Page 205.
71. D. Stigter and K. J. Mysels; J. Phys. Chem. 59, 45 (1955).

72. D. Stigter, R. J. Williams and K. J. Mysels; J. Phys. Chem. 59, 330 (1955).
73. W. L. Courchene; J. Phys. Chem. 68, 1870 (1964).